MODELLING PARTICLE TRANSPORT IN GAS-OIL-SAND MULTIPHASE FLOWS AND ITS APPLICATIONS TO PRODUCTION OPERATIONS

Doctoral Thesis
(Dissertation)

to be awarded the degree of
Doctor of Engineering (Dr.-lng.)

submitted by
M. Sc. Oladele O. Bello
from Ibadan, Nigeria

approved by the
Faculty of Energy and Economic Sciences
Clausthal University of Technology

July 18th, 2008

Chairperson of the Board of Examiners
Prof. Dr.-lng. Oliver Langefeld

Chief Reviewer
Prof. Dr. Kurt M. Reinicke

Reviewer
Dr.-lng. Catalin Teodoriu

DEDICATION

To my parents, Tade Olayinka Bello and Adenike Agnes Bello for all their myriad sacrifices since my mortal existence.

To the memory of my teacher, Prof. Victor Adesegun Adewusi (PhD, Bath) who always inspired me with his knowledge depth and sense of possibility.

ABSTRACT

Sand particle transport in gas-oil multiphase production and well systems poses special flow assurance challenges and requires accurate multiphase flow prediction tools for efficient design and performance assessment. This thesis presents mechanistic models for predicting optimal transport velocity, system performance, critical velocity, particle velocity and holdup in three-phase wells and pipelines. Predictions of optimal transport velocity, system performance, particle velocity, particle holdup and critical velocity in three-phase wells and pipelines have the potential to solve problems of sand management equipment seizing, sand deposition and bed formation, sand erosion, excessive pressure loss and low well productivity leading to economic benefits. Conventional models for particle transport in gas-oil-sand multiphase production and well systems are generally based on empiricism with many limitations.

This study attempts to overcome these limitations by developing a phenomenological model and computational algorithm for estimating optimal transport velocity, system performance, particle velocity, particle holdup and critical velocity in three-phase wells and pipelines. The model involves balance equations formulated from macroscopic mass and momentum conservation laws and constitutive equations. Governing equations are implemented into a Microsoft visual basic computer program and numerically solved using fourth order Runge-Kutta method on a discretized wellbore and pipeline systems. An experimental study is also conducted to investigate in-situ local particle transport behaviour in gas-liquid-solid three-phase mixture flowing through pipeline systems. A non-invasive high speed charged couple device measuring technique (particle image velocimetry and particle tracking velocimtery) is used in this work, which allowed visualization and investigation of sand particle behaviour in the air-water-sand multiphase pipe flow systems. Processing of the air-water-sand multiphase flow imaging data gave in-situ local and global phase velocity and volumetric fraction (holdup) of sand particle under various flow conditions (system, operating and geometric conditions) in the pipeline systems.

The experimental results show that the flow behaviour of the particles through the three-phase air-water-sand pipe flow systems is changing with variations of operating conditions. The proposed model is validated with experimental data obtained from open literature and present study. The model predictions show good agreement with the experimental data and a better accuracy than the available state-of-the art sand transport modeling methods. A number of problems of engineering importance in gas-oil-sand multiphase production operations are studied with the validated model.

The new computational tool developed in this study may be used to help production engineers and asset managers perform assessment and make cost-effective decision related to the efficiency and integrity of three-phase gas-oil-sand wellbore, flowline, trunkline, production riser and pipeline system design options. The mechanistic model is applicable to three-phase gas-oil-sand production, gas-assisted artificial lift and aerated fluid sand unloading problems.

ABSTRACT (DEUTSCH)

Sandteilchen in Gas-Öl-Produktions- und Mehrphasen-Systemen stellt eine besondere Herausforderung dar und erfordert genaue Mehrphasen-Fluss-Prognose-Werkzeuge für die effiziente Gestaltung und Bewertung der Leistung. Diese These behandelt mechanistische Modelle zur Vorhersage der optimalen Transportgeschwindigkeit, Performance, kritische Geschwindigkeit, Partikelgeschwindigkeit und Partikelverzögerung in Bohrungen und Rohrleitungen mit Drei-Phasen-Fluss. Voraussagen der optimalen Transportgeschwindigkeit, Leistung, Teilchengeschwindigkeit, Teilchenverzögerung und kritischen Geschwindigkeit haben das Potential zur Lösung von Problemen bei der Auswahl von Sand Control Equipment, Sand Deposition und Bettbildung, Sand Erosion, übermäßigem Druckverlust und geringer Produktivität und führen zu wirtschaftlichen Vorteilen. Herkömmliche Modelle der Teilchenphysik basieren in der Regel auf empirischen Grundlagen und beinhalten viele Einschränkungen.

Die Vorliegende Studie versucht diese Einschränkungen durch die Entwicklung eines phänomenologischen Modells und Berechnungsalgorithmus zur Bestimmung der optimalen Transportgeschwindigkeit, Leistung, Teilchengeschwindigkeit, Teilchenverzögerung und kritischen Geschwindigkeit in Bohrungen und Rohrleitungen mit Drei-Phasen-Fluss zu überwinden. Das Modell beinhaltet Gleichgewichtsgleichungen hergeleitet aus makroskopischen Gesetzen zur Massen- und Dynamikerhaltung sowie konstitutiven Gleichungen. Die EZB-Gleichungen werden in Microsoft Visual Basic Computersoftware umgesetzt und numerisch mit der Runge-Kutta-Methode vierter Ordnung auf einem diskreten Bohrloch-Pipelinesystem gelöst. Zusätzlich wurde eine experimentelle Studie durchgeführt zur Untersuchung des lokalen Partikeltransportverhaltens in einem Gas-Flüssigkeit-Feststoff Drei-Phasen-System in Rohrleitungen. In dieser Arbeit wird eine nicht invasive, auf der Verwendung einer Hochgeschwindigkeitskamera basierende, Messtechnik (Particle Image Velocimetry und Particle Tracking Velocimetry) verwendet, die eine Visualisierung und Untersuchung des Sandteilchenverhaltens in Luft-Wasser-Sand-Mehrphasen-Rohrleitungsflusssystemen erlaubt. Die Verarbeitung der Luft-Wasser-Sand-Mehrphasen-Imaging-Daten lieferte in-situ lokale und globale Phasengeschwindigkeiten sowie volumetrische Anteile (Verzögerung) von Sandpartikel unter verschiedenen Fließbedingungen (System-, Betriebs- und geometrischen Bedingungen) im Rohrsystem. Die experimentellen Ergebnisse zeigen, dass sich das Fließverhalten der Partikel im Drei-Phasen-Luft-Wasser-Sand-Rohrsystem mit variierenden Betriebsbedingungen ändert. Das vorgeschlagene Modell wird durch experimentell gewonnene Daten aus der verfügbaren Literatur und dieser Studie bestätigt. Die Modellvorhersagen zeigen eine gute Übereinstimmung mit den experimentellen Daten und eine bessere Genauigkeit als die verfügbaren State-of-the-art Methoden zur Sandtransportmodellierung. Eine Reihe von Problemen die bei der Gas-Öl-Sand Multiphasenproduktion von Bedeutung sind wurden mit dem bestätigten Model überprüft. Das in dieser Studie neu entwickelte Berechnungswerkzeug kann verwendet werden um Produktionsingenieuren und Asset-Managern bei Bewertung der Effektivität und Integrität von Drei-Phasen Gas-Öl-Sand Produktionsbohrungen sowie bei der Auswahl von, Flowline-, Trunkline, Produktions-Riser und Pipeline Systemen zu helfen und so wirtschaftlichere Entscheidungen ermöglichen. Das mechanistische Modell kann für Drei-Phasen Gas-Öl-Sand Produktion, Künstliche Förderung mit Gas-Lift und für Sand Endladungsproblemen in mit Luft durchsetzten Fluiden verwendet werden.

TABLE OF CONTENTS

LIST OF FIGURES

LIST OF TABLES

ACKNOWLEDGEMENTS

The author would like to gratefully acknowledge Professor Kurt M. Reinicke, for his advice, guidance and support throughout the course of this study. Professor Reinicke´s emphasis in being a better person in a whole rather than solely be an intelligent person has made the life in doctoral research more meaningful than pure research.

The author expresses his gratitude to Dr. Catalin Teodoriu for his encouragement, ideas, continuous supervision and intense discussions.

Many thanks to Professor Peter Reichetseder and Professor Mohammed Rahaman for their assistance in facilitating scholarship awards. Dr. Theodore Onyeche immeasurable assistance and support on many fronts is specially noted and appreciated.

The support provided by LaVision GmbH with respect to the particle image velocimetry (PIV) system and commercial DaVis image analysis software is greatly appreciated. Prof. Liu is also particularly thanked for the generosity in allowing the use of his Chemical 2.0 software (particle tracking velocimetry algorithms) and many useful discussions.

The practical help and support of the staff members of the Drilling, Production and Gas Engineering Department, Institute of Petroleum Engineering, Clausthal University of Technology is highly appreciated.

The financial support received from DAAD, Max-Buckner and Petroleum Technology Development Fund is thankfully acknowledged.

Thanks are due to Ibrahim Ajala, Eric Lando, Nicholas Ndamb, Mohammed Namic, Mohammed Saleh, Arron Singhe, Obi Ifeacho, Hillary Okeke, Kingsley Imo, and Bolaji Olayiwola for their interest and assistance.

Thanks also go to Adetutu Bello-Finni, Opeyemi Bello and Bukky Bello for their encouragement and support.

The remarkable tolerance of Folasade Bello and Adebisi Bello to share so many hours that were rightfully theirs is deeply appreciated. Without their amazing patience and love this work could not have been completed.

NOMENCLATURES

D	Pipe diameter	m
D_H	Hydraulic diameter of pipe	m
dp	Equivalent solid particle diameter	m
d_B	Equivalent bubble diameter	m
V_{MTV}	Minimum transport velocity	m/s
V_{TV}	Taylor bubble Minimum velocity	m/s
V_{SGC}	Critical vapour velocity	m/s
V_{SL}	Superficial liquid velocity	m/s
V_{SG}	Superficial gas velocity	m/s
V_{SS}	Superficial solid velocity	m/s
V_S	In-situ mean velocity of particles in three-phase pipe flow	m/s
V_C	Critical (slip) velocity	m/s
V'	Eddy (turbulent) velocity	m/s
$V_0^{\bullet}$	Friction shear velocity	m/s
V_{PL}	Free settling velocity of particle in clear water	m/s
V_d	Drag velocity in sand bed	m/s
V	Mean velocity of flow above sand bed	m/s
V_{LF}	Slug film velocity	m/s
V_T	Transitional mixing zone velocity	m/s
V_{S1}	Particle velocity in liquid film zone	m/s
V_{S2}	Particle velocity in mixing zone	m/s
A_P	Cross-sectional area of pipe	m^2
Ao	Contact flow area	m^2
S_{PL}	Specific gravity of particles in clear water	-
$\dot{m}_S$	Input solid mass rate	Kg/s
$\dot{m}_L$	Input liquid mass rate	Kg/s
$\dot{m}_G$	Input gas mass rate	Kg/s
M_P	Solid mass	Kg
t	Time	s
X	Length in axial direction	m
ρ_S	Solid density	Kg/m^3
ρ_L	Liquid density	Kg/m^3
ρ_G	Gas density	Kg/m^3
ρ_M	Mixture density	Kg/m^3
ρ_A	Apparent mixture density	Kg/m^3
C_{DS}	Solid particle drag coefficient	-
C_{DB}	Bubble drag coefficient	-
H_G	Void fraction	-
H_L	Liquid holdup	-
H_S	Solid holdup	-
ψ_S	Solid shape factor	-

f_{SS}	Solid friction factor	-
f_T	Gas-liquid mixture wall friction factor	-
Z	Gas compressibility factor	-
F_{IS}	Interfacial drag force	N (Kg.m/s^2)
F_{PS}	Particle-particle force	N (Kg.m/s^2)
F_{WS}	Particle-wall force	N (Kg.m/s^2)
F_{TS}	Turbulent-particle force	N (Kg.m/s^2)
F_{BS}	Buoyancy force	N (Kg.m/s^2)
F_{GS}	Gravity force	N (Kg.m/s^2)
F_{LS}	Saffman lift force	N (Kg.m/s^2)
F_{VS}	Virtual mass force	N (Kg.m/s^2)
F_V	Force per volume	N/m^3
N_{Rep}	Particle Reynolds Number	-
N_{Reb}	Bubble Reynolds Number	-
N_{Fr}	Froude Number	-
N_{Bo}	Bond Number	-
L	Length of pipeline	m
μ_G	Gas dynamic viscosity	Pa.s
μ_L	Liquid dynamic viscosity	Pa.s
σ_L	Gas-liquid surface tension	N/m
¢	Input sand particle volumetric fraction	%
F	Transport rate in grain volume of sand bed width compressibility	-
ψ	Dimensionless fluid flow rate	-
ϕ_S	Dimensionless sand transport rate	-
ϕ_d	Dimensionless particle flux	-
ϕ_P	Sand bed porosity	-
τ_d	Dimensionless shear stress	-
g	Gravitational acceleration	m/s^2
P_1	Pressure at inner boundary of a computational cell	Pa
P_2	Pressure at outer boundary of a computational cell	Pa
P_{atm}	Atmospheric pressure	Pa
P_{sys}	System pressure	Pa
Q_S	Solid particle flux	kg/s.m^2
h_{EFF}	Effective slug film height	m
f_{SLUG}	Slug frequency	s^{-1}
t_{AVG}	Average time for one slug unit	s
t_{SF}	Time for one slug film	s
t_{SM}	Time for one slug mixing zone	s
t_{AVG}	Average time for one slug unit	s
LMZ	Average length of mixing zone	m
l_F	Length of the liquid film zone	m
l_S	Length of the liquid slug zone	m
θ	Pipe inclination angle	deg.
R_P	Radius of hemispherical particle	m

1 INTRODUCTION

1.1 Background of the Problem

A large proportion of the worldwide petroleum production comes from regions such as Gulf of Mexico, North Sea, Middle East and Gulf of Guinea with unconsolidated formations and high sand production potential during well life. In such a case, the operator has three options: complete wells with downhole sand exclusion systems, re-complete the well by installing sand exclusion systems at a later date when sand production begins or do not install downhole sand exclusion systems but manage sand production by designing the facilities to handle sand if it is produced (Dusseault, Geilikman and Spanos, 1998; Dusseault and El-Sayed, 2001). The conventional downhole sand completions (such as slotted liners, expandable sand screens, gravel packs, resin consolidation, frac- and pack) strongly affect the overall well performance due to additional pressure drop (skin effect) and several other drawbacks (installation and operation costs). As a result, sand management technology is largely gaining attention and maximum sand free rate objectives are being superseded by maximum acceptable sand rates. This change in philosophy is principally driven by production optimization, minimization of problems associated with formation damage and impaired productivity, and the ever increasing demand for oil and gas production (Geilikman and Dusseault, 1997; Tronvoll, Dusseault, Sanfilippo and Santarelli, 2001). The economic benefits are especially pronounced in offshore environment where sand management technology can effectively increase reserve recovery and eliminate the use of downhole sand exclusion systems generating significant profits and cost savings.

The majority of the newly discovered fields with high recoverable reserves are situated in harsher and less accessible environment. For example remote onshore, deepwater and ultra-deep water where conventional exploitation approaches are no longer suitable. Economic development of these new discoveries in frontier environments require cost-cutting measures to be adopted in order to take advantage of existing infrastructures and new technology to reduce capital investment in facilities and maximize value creation. Alternatives for deepwater and ultra-deep water field developments include subsea wells with floating process facilities or total subsea development with long-distance multiphase export line, tie-back to an onshore production platform. This means the produced hydrocarbon and sand stream has to be transported from the wellhead through a long-distance multiphase export line, tie-back to floating or onshore production platforms. However, it is generally recognized that one of the major issues to be addressed before more widespread use of sand management technology in the petroleum industry is the effective transport of particles from sand face to surface processing facilities by oil-gas multiphase flow systems. Sand particle transport is one of the major flow assurance concerns during gas-oil-sand multiphase flows through wellbore, flowline and subsea tieback systems which if not addressed may erode the merit of the sand management technology. Figures 1.1 to 1.2 show sand flow patterns as a result of inefficient sand transport by the oil-gas multiphase flows lead to numerous problems such as sand deposition and bed development, increased pressure loss, enhanced pipeline erosion and corrosion, frequent and expensive cleaning operations and increased down time (Oudeman, 1993; Appah and Ichara, 1994; Appah, Ichara and Bouhroum, 1997). Because the cost of getting sand transport wrong in gas-oil production and transfer systems is so high,

adequate knowledge of the basic design parameters such as how much oil rate is required for optimal transport of produced sand; how to quantify pressure drop as a function of sand influx; how to determine local and axial distributions of slip (minimum or deposit) velocity, what is the particle velocity, particle holdup, particle flux and particle mass rate for sand erosion prediction and oil-gas-sand multiphase separator sizing; which system, operating and geometric variables affect the basic design parameters. Production and facility engineers often experience frustration due to lack of models to help them answer all these basic questions. Fundamental technical methodologies for good design and efficient estimation of sand deposition risk, system performance and optimization, effects of wellbore hydraulics and sand production induced stress on the productivity of the sand management wells are still very scare, even though sand management technology is widely used in the North Sea and Canada. This lack of adequate understanding of the physics and proper formulation of this problem has largely responsible for the rather slow pace of sand management technology acceptance in the petroleum industry.

The gas, liquid and solid phases may distribute in a number of geometrical configurations depending on flow rates, pipe size and geometry, fluid and solid properties in horizontal multiphase pipe and wellbore systems. The main parameters determining the distribution of solids in the in the liquid are gas-liquid flow patterns, gas and liquid velocities, solids loading, solids properties (particle diameter, particle diameter distribution, particle density, particle shape), physical properties of gas and liquid (viscosity and density). Solid flow patterns such as fully suspended symmetric, fully suspended asymmetric, moving bed, moving bed with stationary bed have been extensively reported in the open literatures. It should be stressed that the sand particle input volumetric fraction during sand management production operations may be up to 5 % by volume of crude oil (Gillies, et. al., 1997; Almedeija and Algharaib, 2005). However, the sand particle input volumetric fraction for most conventional (non-sand management production) wellbores and flowlines may be significantly as low as 5 – 40 Ib. per 1,000 barrel of produced crude oil, which is equivalent to 0.014 – 0.11kg sand per cubic meter of produced crude oil (Stevenson, et. al., 2001).

Three-phase gas-liquid-solid flow transport and management issues in subsea production and well systems continue to challenge petroleum industry. The design and cost-effective operation of the three-phase gas-liquid-solid transport systems has been hampered by poor knowledge of hydrodynamic processes associated with gas-liquid-solid multiphase flows. Previous studies have focussed on the prediction of minimum or critical transport velocity for a given multiphase production and transfer operations. For transport velocity above the critical value, sand particle will be delivered to the surface while for transport velocity below the critical value, the oil-gas multiphase flow systems is insufficient to lift the sand particles to the surface. More so, modelling of oil-sand and gas-oil-sand multiphase flow frictional pressure in horizontal wells remains a challenge to the petroleum industry. One effect of the increased friction pressure loss on horizontal wells is on the reservoir performance. The effect of increase pressure loss in horizontal wellbore translates to an increase in reservoir pressure drawdown. Recent results research efforts that incorporate the effects of frictional pressure drop in the horizontal wellbore stopped at the single-phase flow regime. Most of the existing models to evaluate the performance of oil-gas multiphase pipe flow systems subject to sand loading have made several simplifying

assumptions to reduce the complexity of their solutions. Phenomena such as medium to high sand loading, local and axial distribution of slip and sand particle velocities, relevant hydrodynamic processes controlling particle transport (for example, non-uniform three-phase hydrodynamic parameters, particle-gas, particle-pipe wall and particle-particle interactive forces) have been ignored in these models.

The key to achieving maximum production rate and realizing a significant workover and maintenance cost reduction is to determine the optimal transport velocity. This optimal transport velocity is dictated by system, operating and geometric parameters. Unfortunately, no method exists for predicting the optimal transport velocity, local and axial distributions of slip velocity and sand particle behaviour in gas-liquid-solid multiphase pipe and annular flow systems. Most of the three-phase gas-liquid-solid flows in pipes with considerable commercial interest are conducted under high pressure and low temperature. Fundamental study of the optimal transport velocity and flow behaviour of solid particles (local and axial distributions of slip velocity, solid phase velocity, solid phase volumetric fraction, solid phase flux, solid phase mass rates) and pressure drop distributions in the gas-liquid-solid multiphase pipe flow systems, particularly under high pressure and low temperature conditions, is thus very crucial. The identification of these solid transport parameters of interest in addition to liquid and bubble flow behaviour in gas-liquid-solid multiphase transport devices will enable more control and optimization possibilities of the hydrodynamic characteristics. Optimization of the gas-liquid-solid multiphase flow hydrodynamics in relation to system, design and operating conditions will result in a maximal performance of these flow facilities.

Theoretical studies have been reported for gas-liquid-solid multiphase flows in pipes by many investigators. These studies are based on multi-fluid models and empirical correlations. The multi-fluid model is not satisfactorily applicable yet because several constitutive equations for gas-liquid-solid multiphase pipe flows are insufficient as reported in many publications. Design and performance analysis of gas-liquid-solid multiphase pipe flows are mainly based on empirical and semi-empirical correlations gained from experimental data so far. Extrapolating use of these empirical correlations beyond the original operating conditions is highly risky. The strategy of stage-wise scale-up is costly and time-consuming and the satisfactory scale-up to large-scale gas-liquid-solid multiphase pipe flows cannot be guaranteed. Moreover, inaccurate prediction of solid transport in gas-oil multiphase pipe flows can result in severe problems such as productivity impairment, reduced flow capacity, sand deposition and accumulation, sand erosion and corrosion, and equipment failures.

1.2 Research Method and Approach

The fundamental objective of this thesis is to investigate experimentally and theoretically the particle transport behaviour in various three-phase gas-liquid-solid pipe flows. The scope of the experimental study has been limited to a handful of gas-liquid-solid three phase flow conditions. Certainly, the ranges of possible sand sizes and types and the number of possible gas-liquid two phase flows is far greater than could be experimentally investigated in any individual project. Based on this, an experimental multiphase flow loop was built that could be used to investigate flow behaviour of suspended solid particles in liquid-solid and gas-liquid-solid multiphase pipe flows under a variety of flow, operating and geometric conditions. A charged

couple device (CCD) measuring technique was used to measure local solid particle velocity, holdup, flux and mass rate.

The theoretical method used to deal with the solid transport behaviour issue was formulated based on the physics of the problem, accounting for the relevant transport mechanisms controlling particle motion in gas-liquid-solids multiphase flow systems. The model involves balance equations deduced from macroscopic mass and momentum conservation laws, constitutive equations and forces due to gravity, particle-multiphase, particle-turbulence, particle-particle and particle-wall interactions. Governing equations were solved by numerical method. The performance of the proposed model was evaluated with its comparison to prediction of the existing models using published and new experimental data. The proposed model predicts the solid transport behaviour in three-phase gas-oil-sand pipe flows with a better accuracy than the available methods. The fundamental feature of the developed physical model is the total absence of adjustable constants. Previous studies on sand transport in gas-oil multiphase pipe flows have been based on empirical and semi-empirical correlations. Improvement of gas-oil-sand multiphase production and transport system design and performance analysis may promote their reliability and efficiency.

As gas-oil-sand multiphase production and pipeline transport system design and performance guidelines become more reliable, their practical use would increase, allowing the sand management technology (SMT) to be a common production scheme. SMT offers the petroleum industry the potential for major reduction in capital cost and significant improvement in well productivity and reserve recovery from convention and non-conventional oil and gas fields with low formation pressure. The improvement in gas-oil-sand multiphase production and pipeline transport system design and performance guidelines will ultimately lead to better prediction, assessment and mitigation of sand deposition and erosion risks in gas-oil-sand multiphase wellbores, flowlines and pipelines. It will also lead to optimal sizing of gas-oil-sand multiphase separators and contribute appreciably to hydraulic optimization, increased sand management well productivity, elimination of costs of sand erosion, sand unloading, downtime, workover and equipment requirements. Sand volume fraction and mass rate monitoring for the control of smart sand management wells and reservoir management using downhole sensors and continuously updated three-phase flow models will also significantly enhance well performance and circumvent the need for over design provision.

The proposed physical model is suitable to design and assess the performance of gas-oil-sand multiphase wellbores and pipelines for any given system, operating geometric conditions. It may also help production engineers accelerate the full benefits of sand management production scheme by identifying an optimum safe operation (condition where pressure loss, sand deposition and erosion risk is minimized) for gas-oil-sand multiphase production and pipeline transport systems from comparison of the performance profiles for various alternatives. For the first time, the algorithm developed in this study is capable of answering a number of three-phase gas-liquid-solid pipe flow system design questions, which production engineers will want answers to:

- First, what is the energy consumption (pressure loss) per unit mass of sand particles transported at flow conditions?

- Second, what is the critical velocity for the incipient sand particle deposition in a three-phase gas-oil-sand pipe flows?

- Third, what is the optimal transport velocity at which the total pressure drop per unit length along a pipe becomes a minimum?

- Fourth, what is the methodology for predicting local sand particle flow rates and volumetric fractions, which is related to the local sand erosion risk, volume of produced sand to be disposed, size of possible dedicated sand management equipment, such as, desanders, filters, accumulator vessels, washing system and storage bins?

- Five, what are the guidelines for predicting safe operation and optimizing the performance of gas-oil-sand multiphase wellbores, flowlines, trunklines, production risers and pipelines?

- Six, how can we make a fast assessment of performance profiles of various gas-oil-sand multiphase flow wellbore, flowline, trunkline, production riser and pipeline system design options?

- Seven, what are the available quantitative experimental data on in-situ sand transport characteristics that can be used to calibrate or validate the predictive accuracies of widely used models for design and performance analysis of gas-oil-sand multiphase flow wellbores, flowlines, trunklines, production risers and pipelines?

In general, the following parameters are to be modeled in the gas-oil-sand multiphase production and transfer systems: local and axial distribution of sand phase velocity and volumetric fraction, local and axial distribution of particle slip (critical) velocity, local and axial distribution of pressure drop characteristics, optimal transport velocity for preventing sand deposition and bed development, impact of pressure effects on sand particle transport characteristics, impact of gas-oil (gas-liquid) multiphase flows on sand entrainment characteristics during production and sand unloading operations.

1.3 Structure of the Dissertation

Following this introduction is a critical review of previous experimental and theoretical studies on solid transport in gas-liquid multiphase pipe flow in Chapter 2. Also, presented in this chapter is the statement of research problem, significance and contribution of the present study; and research objectives. Chapter 3 is devoted to the development of the governing equations, formulation of the numerical solution and development of computer package for both solid transport and the hydraulic characteristic prediction in gas-oil-sand multiphase pipe flows. Chapter 4 introduces the details on the charged-couple device (CCD) measuring system, analytical measurement, experimental set-up and procedure. Chapter 5 presents experimental finding obtained in the laboratory-scale gas-water-sand multiphase flow loop along

side with the evaluation of the proposed model and existing model predictions against experimental data from the present and published studies is reported. Chapter 6 presents the field application studies of the proposed model to two case studies. Chapter 7 ends the thesis with a conclusion and a discussion of areas that should be explored for future work. And finally, five appendices give methods used for error analysis for model comparison, additional information on the computational flow diagrams, optimization and flow pattern flow charts.

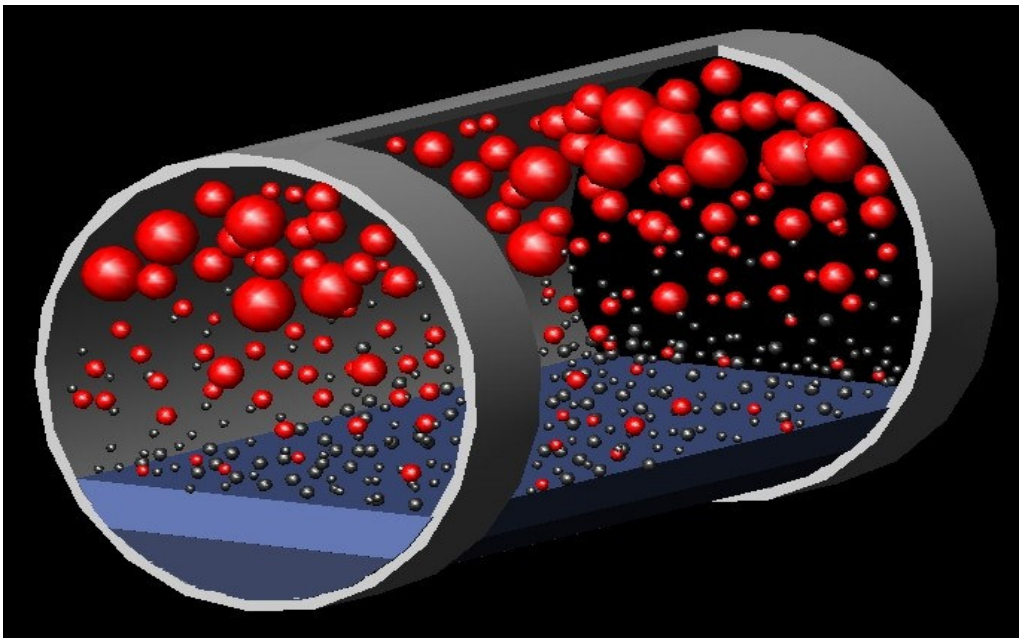

Figure 1-1: 3-D view of sand flow patterns in gas-oil two-phase flows through a pipeline

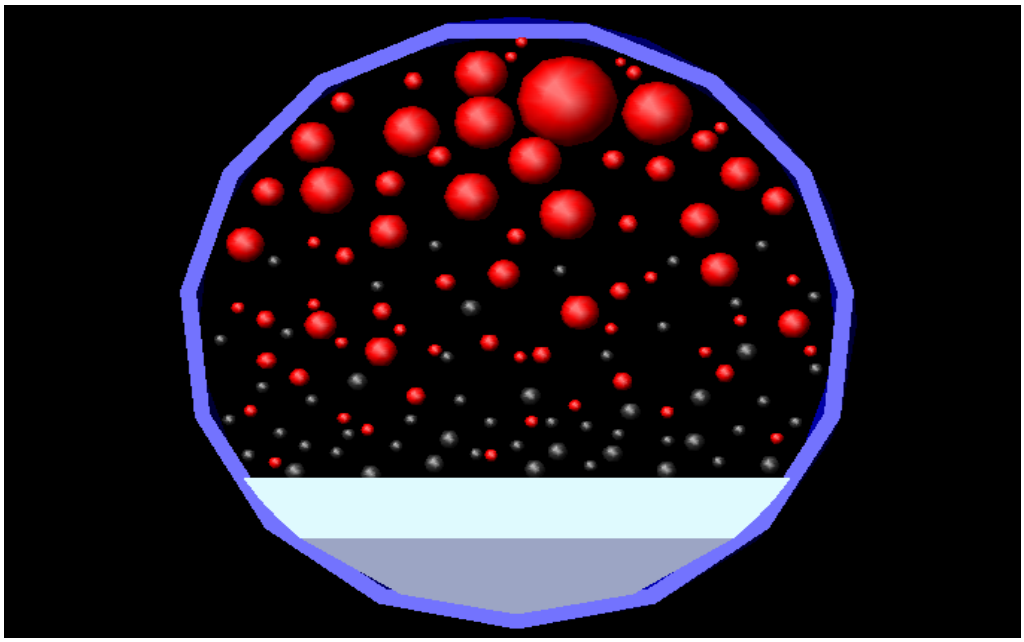

Figure 1-2: Cross-sectional view of sand flow patterns in 3-D gas-oil two-phase flows through a pipeline

2 STATE OF THE ART AND RESEARCH OBJECTIVES

2.1 Introduction

The transport of suspended and entrained sand particles in gas-liquid-solid multiphase flows through wellbore, flowline, risers, pipeline and annular systems is dependent upon several important sub-components, such as, characteristics of the gas-liquid two-phase pipe flow and interaction between the multiphase flow and the sand particles being transported. This chapter attempt to critically review past works documenting modeling and experimental studies on particles transport in gas-liquid multiphase flow through pipes. The current state of knowledge regarding this field and important unsolved problems from previous investigation are highlighted while new research challenges and technological needs undertaken in this study to bridge the knowledge gaps are also presented.

2.2 Solids Particle Transport in Two-Phase Gas-Liquid Flows through Pipes

2.2.1 Scott and Rao (1971)

Scott and Rao (1971) studied transport of solids by gas-liquid mixtures in horizontal pipes. In their experiments, two sizes of spherical particles (0.0001m and 0.0005m) with concentration range from 3.2% up to 14.0% by volume with or without air were pumped through 0.025m and 0.049m transparent glass pipes. The principal flow pattern studied were in the liquid-solid, bubble, plug and slug flow regimes. Liquid density, liquid viscosity, surface tension and particle density values were 1000kg/m^3, 0.001Pa.s, 0.101N/m and 2250kg/m^3, respectively.

The saltation velocities required to keep the solid particles barely skimming along the bottom of a horizontal pipe were determined by slowly decreasing the slurry velocities (at a fast gas rate) until a few particles were seen to remain stationary for a short time. The pressure drop was measured as a function of a range of gas/liquid ratios and concentrations of up to 14% solid particles by volume. The measured saltation velocities and pressure drop were compared with various correlations which have been suggested by previous investigators.

Durand correlation prediction gave the most fairly satisfactory agreement with the measured average saltation velocities. The experimental results also showed less dependence of the measured average saltation velocities on the bubble, plug and slug flow regimes. Although a slight increase in the saltation velocity was recorded at high concentration of particles, no reason was given for this phenomenon.

In another part of the study, the actual pressure drop was shown to be accurately predicted by Durand modified concentrated slurry used (14.1% by volume).

2.2.2 Sato et. al. (1991)

Sato et. al. (1991) studied transport of solids in a vertical three-phase air-water-solid slug flow through pipes. In their experiments, the velocity of a solitary particle lifted by an air-water two-phase flow and particles in crowds as the component of a three-phase air-water-solid flow through pipe was determined from the measured time taken for one particle to travel over 1.6m between two metal sensors. Experiments were carried out in a vertical acrylic resin pipe of 0.026m internal diameter and 6m long pipe at volumetric flow rates of 0.4m/s and 0.15 to 1.2m/s for air and water, respectively. The principal flow pattern studied were bubble, churn, plug and slug flow regimes. Two series of experiments were performed by the authors. In the first, a spherical-shaped aluminum particle with a 2690 kg/m^3 density and 0.006m particle diameter was used as the solid phase in the single (solitary) particle transport experiment. For the second three-phase air-water-solid flow experiment, two types of ceramic sphere with different densities (2540kg/m^3 and 3630 kg/m^3) were used. The range of the velocities of each flow was 0.5-0.8m/s, 0.5-1.3m/s and 0.0075-0.120m/s for air, water and solid phases, respectively. Ceramic tracer particles of the same density and size were introduced into the three-phase pipe flow systems (15-150 tracers) in order to determine the mean particle velocity. The mean velocity for the solitary particle in air-water two phase pipe flow and that of solid particles in the three-phase flows were found to have non-linear relationships with the air-water and air-water-particle mixture velocities.

Based on apparent mixture density and the authors' experimental data, an empirical model was developed to predict average velocity of solitary solid particle and particles in air-water and three-phase air-water-solid flows through vertical pipes. Sato et. al. (1991) correlation developed to predict the mean velocity of solid particles in three-phase pipe flow systems is given as:

$$V_S = C\left(\frac{G}{\rho_A}\right) + V_{PLS} \qquad [2.1]$$

Where
V_S = mean velocity of particles in a three-phase gas-liquid-solid pipe flow
C = distribution coefficient
ρ_A = apparent mixture viscosity
V_{PLS} = wall-affected settling velocity of the particles in three-phase flow

The apparent mixture density, ρ_A, is given by:

$$\rho_A = \left(\frac{\rho_S}{\rho_{LS,3}}\right)^n \rho_{LS,3} \qquad [2.2a]$$

Where
$\rho_{LS,3}$ = density of a three-phase mixture given as: $\rho_s = \rho_a H_G + \rho_L H_L + \rho_s H_s$

$\rho_{LS2,3}$ = density of slurry (water-solid particle mixture) in the three-phase flow

expressed by: $\rho_{LS2,3} = \rho_L \frac{H_L}{1-H_L} + \rho_S \frac{H_S}{1-H_G}$ [2.2b]

H_G, H_L and H_S the in-situ volumetric fractions of each of the phases.

n=1.5

The distribution coefficient and the total mass flux are given by:

$$C = 1 + C_1 \exp(-5H_S) \quad [2.2c]$$

$C_1 = 0.2$

$$G = \rho_G V_G + \rho_L V_L + \rho_S V_S \quad [2.2d]$$

The wall-affected settling velocity of the particles is given by:

$$V_{PSL} = \left[1 - \left(\frac{d_P}{D}\right)^2\right] V_{PL,3} \quad [2.3]$$

Where

$V_{PL,3}$ is the free-settling velocity of the particles in an imaginary three-phase mixture given as.

$$V_{PL,3} = \left[1 - \frac{H_S}{1-H_S}\right]^{2.4} \sqrt{\frac{\frac{\rho_L}{\rho_A}(S-1)}{S-1}} V_t \quad [2.4]$$

Where

S= specific gravity of particles in clear water (ρ_S / ρ_L)

V_t = free settling velocity of the particle in clear water

The model prediction was in good agreement with the experimental data within a mean error of $\pm 10\%$.

2.2.3 Angelson et. al. (1989)

Angelson et al. (1989) studied critical deposit velocities of sand particles in single and two-phase flow systems with internal pipe diameters of 0.025 to 0.1m and pipe length of 10 to 12m. Different sand particles in the size range of 30 to 150 μm were investigated in a pipeline system that could be tilted to an angle of inclination up to 15^0 and sand loadings of up to 1000ppm. Various sand particles flow and deposition mechanisms were deduced from visual, photo and video observations. Some of the major results were:

- The stratified flow in slightly inclined pipe was the most critical operating condition with respect to sand deposition
- Chemical additives and sand loadings of up to 1,000ppm had negligible effects on sand particle deposit characteristics

- The minimum liquid velocities calculated from the extended Wick's model for the particle transport in the stratified flow agreed relatively well with the measured values and bed development

2.2.4 Oudeman (1993)

Oudeman (1993) applied the general relation between sediment transport and fluid mechanical parameters in open channel flow to analyze the gas-liquid-solid multiphase flow in pipes under suspended, moving and stationary bed load conditions. Two dimensionless quantities were defined in terms of sand transport and fluid flow rates. A power law was used to correlate the dimensionless transport rate and flow rate, respectively. An expression for drag velocity was developed based on the conventional wall turbulence flow logarithmic approach. The values of m and n which depend on input gas fraction were obtained from experimental measurements. Details of the Oudeman's equation are given as follows:

$$\phi_S = \frac{F}{\sqrt{d_P^3 g(S-1)}} \qquad [2.5]$$

$$\phi_S = m\Psi^n \qquad [2.6]$$

$$\Psi = \frac{V_b^2}{g\, d_P\, (S-1)} \qquad [2.7]$$

Where

F = transport rate in grain volume per second per meter of sand bed width
ϕ_S = dimensionless sand transport rate
Ψ = dimensionless fluid flow rate
d_P = solid particle diameter
g = gravitational acceleration
V_b = drag velocity in sand bed
S = solid-liquid density ratio

Oudeman (1993) also experimentally studied gas-liquid-solid multiphase flow through pipe under varied operating conditions. Experimental data were based obtained in 0.07m internal diameter pipe using sand particle size range of 150 to 300 μm; input gas volume fractions of 0% to 20%; liquid velocity between 0.1 to 1.2m/s; pressure slightly over atmospheric condition and room temperature of about 20^0C. Ordinary water was used as liquid phase with carboxyl methyl cellulose (CMC) added to increase the liquid effective viscosity to 7mPa.s (0.007Pa.s). The effect of surface tension was also investigated by adding surfactant that reduced the surface tension value from 0.064 to 0.028N/m. Stratified wavy and slug flow patterns were deduced from visual observations. The total sand carry capacity (concentration and mass rate) in the system was invasively determined in samples taken from the riser section of the test loop. However, no information on the input solid particle loading, particle density and bed thickness for specific measurement was given by the author.

The entrainment rate of the sand particles from stationary bed to moving bed and moving bed to suspension mode was found to depend on the superficial liquid velocity and a weak function of the superficial gas velocity. However, sand transport rate increased strongly with increasing gas fraction than increasing the superficial liquid velocity. The author postulated that this trend was caused by increased turbulence effects and momentum transfer from the gas phase to the liquid phase in the multiphase flow system.

The author also proposed a methodology of using the developed model to establish the risk of sand deposition in horizontal multiphase trunklines connecting a subsea development to a nearby shallow water production platform.

2.2.5 Sakaguchi et. al. (1993a, 1993a, 1995)

Sakaguchi et. al. (1993a, 1993a, 1995) published extensive studies on pressure drop in gas-liquid-solid multiphase flow in vertical pipes for production of manganese nodules from ocean bed. Sakaguchi et. al. (1993a, 1993a, 1995) measured phase volumetric fractions, pressure drops in gas-liquid-solid multiphase slug and bubbly flows through vertical pipes. The effects of design and operating parameters on phase volumetric fractions and pressure drops were reported. The authors also presented semi-empirical models for pressure drop calculations using the experimental data as adjustable parameters. The proposed hydraulic models give good agreement with the measured data.

2.2.6 Gillies et. al. (1997)

Gillies et. al. (1997) developed an experimental flow loop to simulate and investigate the ability of gas-liquid mixtures to transport sand particles in a horizontal well at low velocities. The sand particles used had a density of 2650Kg/m^3 and median diameter of 10, 100 and 200 μm. The liquids employed in the experiments were water with density of 998Kg/m^3, viscosity of 1.0mPa.s and oil with density and viscosity of 872kg/m^3 and 78mPa.s, respectively. Time-averaged in-situ densities of the flowing mixtures were determined as a function of vertical position of the pipe using a traversing gamma ray gauge (gamma densitometers). Delivered sand concentrations were determined from samples collected at the pipe outlet. The results showed that the gas-liquid flow experiments conducted without sand were entirely in the slug regime for all the conditions studied. The Lockhart-Martinelli correlation predictions were in qualitative agreement with the holdup and pressure drop for air-water and air-oil flow without sand.

Results for sand transport characteristics by the gas-oil mixtures differed significantly from those for oil alone. Results were explained in terms of the effects of slippage and gas buoyancy on the multiphase flow. Gas and sand phases were observed to travel in separate parts of the pipe thereby making the bubble effects on sand transport and pressure drop to be insignificant. Gillies et. al. (1997) also extended and utilized the Meyer-Peter correlation for hydraulic conveying of high solids loading to estimate the delivered concentrations when the sand particle diameter is greater than 0.1mm and a

turbulent liquid flow. The extended Meyer-Peter proposed by Gillies et. al. (1997) is as follows:

$$\phi_d = \frac{q_{SM}}{\rho_S \left[g d_P^3 (s-1) \right]^{0.5}} \qquad [2.8]$$

Where

q_{SM} = volumetric flow rate of the mixture per unit bed width multiplied by the delivered volume fraction of solids

s = solid and liquid density ratio

d_P = particle diameter

g = gravitational acceleration

ϕ_d = dimensionless particle flux

$$\tau_d = \frac{\rho_L g\, d_P (s-1)}{\tau_0} \qquad [2.9a]$$

Where

τ_d = dimensionless shear stress

τ_0 = shear stress in the transporting medium

ρ_L = liquid density

$$\tau_0 = \frac{f V^2 \rho_{md}}{2} \qquad [2.9b]$$

Where

f = friction factor for flow over a bed with a relative roughness (d/D_{eq})

V = mean velocity of the flow above the sand bed ($V = Q/A_o$)

D_{eq} = hydraulic equivalent diameter

A_0 = contact flow area

ρ_{md} = mean density of the delivered mixture

The Meyer-Peter empirical equation that links ϕ_d and τ_d

$$\phi_d = \left[\frac{4}{\tau_d} - 0.188 \right]^{1.5} \qquad [2.9c]$$

The relationship between the interfacial stress in the Meyer-Peter equation and pressure gradient for the flow regime was given by Gillies et. al. (1997) as:

$$-\frac{dp}{dz} = \frac{\tau_o w + \tau_i s_i}{A} \qquad [2.9d]$$

Where

w = width of the sand bed

s_i = pipe perimeter

τ_i = interfacial stress

A = total cross-sectional area of an empty pipe

Gillies et. al. (1997) recommended the use of equation [2.6] if the transporting medium is liquid whereas the Lockhart-Martinelli should be used if the transporting medium is gas-liquid mixture. The authors also presented a correction for calculating the viscosity of the mixture as:

$$\frac{\mu_m}{\mu_L} = 1 + 2.5C + 10.0C^2 + 0.00273\exp(16.6C) \qquad [2.9e]$$

Where

C = mean in-situ solids volume fraction $= \dfrac{(A - A_o)C^*}{A}$ [2.9f]

C^* = concentration of the bed
A = total cross-sectional area of empty pipe
A_0 = contact flow area
μ_L = viscosity of carrier fluid
μ_m = viscosity of flow mixture

2.2.7 Salama (2000)

Salama (2000) developed a model based on the modified Wicks (1971) and Oroskar and Turian (1980) models for estimating minimum mixture velocity to avoid sand deposition in multiphase pipelines. The proposed model is given as:

$$V_{MTV} = \left(\frac{V_{SL}}{V_M}\right)^{0.53} d_P^{0.17} \left(\frac{\mu_L}{\rho_L}\right) \left(\frac{\mu_L}{\rho_L}\right)^{0.09} \left(\frac{\rho_S - \rho_L}{\rho_L}\right)^{0.55} D^{0.47} \qquad [2.10]$$

Where

V_{MTV} = minimum transport velocity to avoid sand settling in multiphase flowlines

$\frac{V_{SL}}{V_M}$ = ratio between liquid superficial velocity and mixture velocity at sand settling condition (for single phase, ratio=1)

d = particle diameter
D = pipe diameter

The model was validated using experimental data generated from a multiphase flow loop that is 12-m long with internal pipe diameter of 0.108m. The proposed model produced the measured settling (mixture) velocity fairly well in horizontal and near horizontal multiphase flowlines.

2.2.8 King et. al. (2001)

King et. al. (2001) presented experiments and modeling results regarding solids transport in multiphase flows under low and high viscosity fluid systems. The

experiments were conducted in a 120m long and 0.152m internal diameter acrylic pipe with a return bend after 60m and a dip of ± 1 deg downward and upward of the return bend. The process fluids generally were air and water, although various Carboxymethylcellulose (CMC) solutions were used to bring the viscosity of the water up to the values observed under field conditions. The different series of experiments were conducted corresponding to the fluid viscosity of 150mPa.s and 300 mPa.s Newtonian condition. Oil with viscosity of 3mPa.s was also used for some experiments. The particles used were reasonably typical of the produced sand from the south east forties field with a mean size of 255 μm and density of 2500Kg/m^3. The experimental flow loop was operated at atmospheric conditions. Particles were fed externally in the gas-liquid multiphase flow at the dip itself or 5-m downstream of the dip. The flowing water and air were in the range of 0.1- 0.57m/s and 0.85-4.66m/s, respectively for static and dynamic flowing water-sand multiphase tests. Tests showing the effect of liquid viscosity confirmed that the threshold velocity (minimum transport velocity) for the onset of sand particles suspension for the viscous crude oil was significantly higher than for the light crude. The observed behaviors of the entrained sand particles in the three-phase gas-liquid-solid pipe flow system were analyzed by formulating a mechanistic (empirical) model. The model developed by King et. al. (2001) was based on the traditional minimum transport velocity and pressure gradient accounting for both boundary layer and viscous drag effects. The King et. al. (2001) put forward an equation for pressure gradient required to transport solid in multiphase flow lines based on whether the particle diameter is larger or smaller than the thickness of the viscous sublayer.

For the case where the particle diameter is less than the laminar sublayer thickness, the friction shear velocity, V_o^*, at deposition for infinite dilution was given as:

$$V_o^* = \left[100 V_{PL} \left(\frac{\mu_L}{\rho_L dp} \right)^{2.71} \right]^{0.269} \qquad [2.11]$$

Where

V_{PL}= particle settling velocity (ft/s) under quiescent conditions
d_P = particle diameter (ft)

When the particle diameter is greater than viscous sublayer thickness the V_o^* was given instead as:

$$V_o^* = \left[0.204 V_{PL} \left(\frac{\mu_L}{\rho_L d_P} \right) \left(\frac{\mu_L}{\rho_L D} \right)^{-0.6} \left(\frac{\rho_S - \rho_L}{\rho_L} \right)^{-0.23} \right]^{0.714} \qquad [2.12]$$

Where
D = pipe diameter (ft)
ρ_s = solids density (lb/ft^3)
ρ_L = liquid density (lb/ft^3)

For moderately dense concentration, the assumption of the infinite dilution was corrected for the particle diameter greater than the viscous sublayer thickness as follows:

$$V_c^* = V_0^* \left[1 + 2.8 \left(\frac{V_{PL}}{V_0^*} \right)^{0.33} \sqrt{\lambda_S} \right] \qquad [2.13]$$

Where

V_c^* = corrected friction velocity (ft/s)

λ_S = input volumetric fraction (Holdup) of solids in the slurry = $\frac{q_S}{q_L + q_S}$

The thickness of the viscous sublayer δ, for a smooth pipe for Reynolds number below 10^7 was given by:

$$\delta = 62D \left[\frac{DV_{SL}\rho_L}{\mu_L} \right]^{-7/8} \qquad [2.14]$$

Where

V_{SL}= superficial liquid velocity (ft/s)

The expressions for particle settling velocities of different flow regions were given by King et. al. (2001) as follows:

$$V_{PL} = \frac{1488 g d_P^2 (\rho_s - \rho_L)}{18\mu_L} \qquad if\ \mathrm{Re}_P \langle 2\ [Stoke's\ law\ region] \qquad [2.15]$$

$$V_{PL} = \frac{3.54 g^{0.71} d_P^{1.14} (\rho_S - \rho_L)^{0.71}}{\rho_L^{0.29}\ \mu_L^{0.43}} \qquad if\ 2 \langle \mathrm{Re}_P \langle 500\ [Intermediate\ region] \qquad [2.16]$$

$$V_{PL} = 1.74 \sqrt{\frac{g d_P (\rho_S - \rho_L)}{\rho_L}} \qquad if\ \mathrm{Re}_P \rangle\ 500 [Newton's\ law\ region] \qquad [2.17]$$

$$\mathrm{Re}_P = \frac{1488 d V_p \rho_L}{\mu_L} \qquad [2.18]$$

Where g = gravitational acceleration (ft/s^2)

Based on the aforementioned analysis, King et. al. (2001) gave a correlation for calculating the pressure gradient corresponding to the minimum transport (frictional) velocity as:

$$\left[\frac{dP}{dX} \right]_{MTV} = \frac{4\rho_L (V_C^*)^2}{D} \qquad [2.19]$$

Where

$\frac{dP}{dX}$ = pressure gradient (Psi/ft)

The pressure gradient predicted by the above equation must be less than the oil-gas multiphase flow pressure gradient predicted by PROSPER for sand particles to be transported through the multiphase flowlines.

2.2.9 Stevenson et. al. (2002a, 2002b, 2003)

Stevenson et. al. (2001a, 2001b, 2002a, 2002b, 2002c, 2003) presented the results of a series of experiment sand modeling work aimed at better understanding of sand particle entrainment and transport characteristics in multiphase flowlines at low particle loading. Intermittent and stratified flow patterns in horizontal and near horizontal pipes were investigated in the presence of sand particles. High speed video system was used for flow visualization and analysis of sand particles entrainment and saltation in gas-liquid-solid three-phase intermittent and stratified pipe flows. Time-average sand particle velocities were estimated from the time needed for a given particle to pass a pre-set horizontal distance marked on the pipe wall. Stevenson et. al.(2002a, 2002b, 2003) also developed a mechanistic model for estimating average sand particle (V_p) and hold-up (H_p) in intermittent multiphase flowlines using long slug approximation and the critical flow velocity for sand particle motion in multiphase flowlines. Based upon the assumption of:

i. negligible gas drift through the slugs/plugs
ii. negligible effect of front of the slugs/plugs on pick-up and suspended sand particles transport enhancement
iii. forces on a hemispheric particle at rest in the viscous sublayer at a pipe wall
iv. approximation of intermittent flow with slug section as plug flow and the liquid film section as stratified flow

Critical velocity for incipient motion of small particle in viscous boundary layer at a pipe wall

Stevenson et. al. (2002c,) presented dimensionless correlation for calculating the values of V_C, the critical velocity for incipient particle motion as follows:

$$V_C = J - V_{PS} \qquad [2.20]$$

Where

J = average gas-liquid mixture superficial velocity ($V_{SG} + V_{SL}$)

V_{PS} = average particle velocity in the liquid slug zone

V_C, the critical velocity for incipient particle motion can be estimated depending on whether the particle diameter is smaller or greater than viscous sublayer thickness.

For particles diameter smaller than viscous sublayer thickness, the critical velocity is given by:

$$V_C = 2.19\left[f\, g\left(\frac{\rho_S}{\rho_L} - 1\right)\right]^{0.57} R_P^{0.57} D^{0.14} \left(\frac{\mu_L}{\rho_L}\right)^{-0.14} \qquad [2.21]$$

$$if\ \ \frac{R_P^2\, Q\, \rho_L}{\mu_L} \leq 0.5 \left(Stoke's\ law\ region\right)$$

$$V_C = 3.29\left[f\, g\left(\frac{\rho_S}{\rho_L} - 1\right)\right]^{0.41} R_P^{0.08} D^{0.14} \left(\frac{\mu_L}{\rho_L}\right)^{0.18} \qquad [2.22]$$

$$if\ \ \frac{R_P^2\, Q\, \rho_L}{\mu_L} \succ 0.5 \left(Intermediate\ region\right)$$

Where
R_p= radius of the hemisphere (which can be estimated as one-half (1/2) of the sand sieving diameter)
f = coefficient of static friction between the particle and pipe wall = 0.55 (a value of 0.55 was suggested for sand and Perspex)
D= internal diameter of pipe (m)
g = gravitational acceleration
Q = strain rate within the within the viscous sublayer

When the particle diameter is greater than the viscous sublayer thickness, the critical velocity (V_C) is calculated as follows:

$$V_C = 0.76\left[g\left(\frac{\rho_S}{\rho_L} - 1\right)\right]^{0.41} d_P^{-0.27} D^{0..5} \left(\frac{\mu_L}{\rho_L}\right)^{0.18} \qquad [2.23]$$

Particle transport in gas-liquid intermittent flow through pipeline system

Stevenson et. al. (2002a, 2002b, 2003) put forward the following equation for average particle holdup and velocity in gas-liquid intermittent pipe flow systems:

$$H_p = \frac{4q_S}{AD^2 V_P} = \frac{V_{SL} L_S}{V_P \rho_S} = \frac{V_{SS}}{V_P} \qquad [2.24]$$

$$V_P = \frac{V_{PS}\left(V_T - V_{PF}\right) + \frac{l_F}{l_S} V_{PF}\left(V_T - V_{PS}\right)}{\left(V_T - V_{PF}\right) + \frac{l_F}{l_S}\left(V_T - V_{PS}\right)} \qquad [2.25]$$

Where
H_P = average in-situ volumetric solid holdup
V_p = average sand particles velocities in gas-oil-sand multiphase flowlines

V_{ps} = average particle velocity in the liquid slug zone

V_{pf} = average particle velocity in the (gas slug) liquid film zone

V_T = translational velocity of slug nose

l_F = length of the film zone

l_S = length of the liquid slug zone

V_{SS} = solids superficial velocity

V_{SL} = liquid superficial velocity

Stevenson et. al. (2001a) used their acquired experimental data to develop a dimensionless correlation to predict the "saltation velocity" for an isolated grain in the liquid slug zone of horizontal intermittent flow:

$$V_{PS} = 0.95\left(V_{SL}\right)\left[\left(1+\frac{V_{SG}}{V_{SL}}\right)-\left(1.38\frac{V_{SG}}{V_{SL}}+0.88\sqrt{F_{rL}}\right)\left(\mathrm{Re}_L\, g\sqrt{F_{rL}}\left(\frac{d_P}{D}\right)^{1.5}\right)^{-0.180}\right] \quad [2.26]$$

$$F_{rL} = \frac{V_{SL}}{\sqrt{gD}} \quad [2.27]$$

$$R_{eL} = \frac{\rho_L V_{SL} D}{\mu_L} \quad [2.28a]$$

The V_{PS} can also be calculated from the critical velocity for incipient motion of small particle in viscous boundary layer at a pipe wall as follows:

$$V_{PS} = J - V_C \quad [2.29]$$

For the average particle velocity in the liquid film zone, V_{PF}, a dimensionless correlation developed by Stevenson and Thorpe (2002) for the velocity of isolated particles in stratified gas-liquid pipe flow is used:

$$V_{PF} = 1.03\, w_F\left[1-3.43\left(\frac{w_F\, d_P \rho_L}{\mu_L}\right)^{-0.34}\left(\frac{D_F\, g}{w_F{}^2}\left(\frac{\rho_S}{\rho_L}-1\right)\right)^{0.33}\right] \quad [2.30]$$

Where

D_F = Hydraulic diameter of the liquid film

w_L = average liquid stratum velocity

g = gravitational acceleration (m^2/s)

The liquid stratum (film) velocity, w_F, is calculated as follows:

$$w_F = V_T - \frac{A_P H_{LS}}{A_{Fi}} \left(V_T - \left(V_{SG} + V_{SL}\right)\right) \quad [2.31]$$

$$\frac{l_F}{l_S} = \frac{\left(V_{SL} + V_{SG}\right) H_{LS} - V_{SL}}{V_{SL} - w_F \left(\frac{A_{Fi}}{A_P}\right)} \quad [2.32]$$

The interfacial perimeter, S_i, was calculated from the following equation :

$$\tau_F S_F = \tau_G S_G + 2\tau_i S_i \quad [2.33]$$

$$\tau_F = 0.5 C_F^F \rho_F w_F^2 \quad [2.34]$$

$$\tau_G = 0.5 C_F^0 \rho_G V_T^2 \quad [2.35]$$

$$\tau_i = 0.5 C_F^F \rho_F (V_T - w_F)^2 \quad [2.36]$$

$$C_F^F = 0.048 \mathrm{Re}_F^{-0.2} \quad [2.37]$$

$$C_F^0 = 0.048 \mathrm{Re}_G^{-0.2} \quad [2.38]$$

$$\mathrm{Re}_F = \frac{w_F D_F \rho_F}{\mu_F} \quad [2.39a]$$

$$\mathrm{Re}_G = \frac{V_T D_G \rho_G}{\mu_G} \quad [2.39b]$$

$$D_F = \frac{4 A_F}{S_F} \quad [2.40a]$$

$$D_G = \frac{4 A_G}{\left(S_G\right)} \quad [2.40b]$$

$$S_F = \sqrt{H_{LS}} \quad [2.41a]$$

$$S_G = \sqrt{1 - H_{LS}} \quad [2.41b]$$

$$A_F = H_{LS} A \quad [2.42a]$$

$$A_G = A - A_F \quad [2.42b]$$

$$A_{Fi} = D_G \frac{(S_F + S_{iG})}{4} \quad [2.42c]$$

$$A_P = \frac{\pi D^2}{4} \quad [2.42d]$$

For the in-situ volumetric liquid holdup (H_{LS}) in liquid film zone, the semi-empirical correlation presented by Andreussi and Bendiksen (1989) was used by the authors:

$$H_{LS} = 1 - \frac{F_{rm} - F_o}{F_{rm} + F} \quad [2.43]$$

Where

$$F_{rm} = \frac{V_{SG} + V_{SL}}{\sqrt{gD}} = Mixture\ Froude\ Number \quad [2.44]$$

$$F_o = 2.6\left[1 - 2\left(\frac{D_o}{D}\right)^2\right] \quad [2.45]$$

$$D_o = 0.025m \quad [2.46]$$

$$F = 2400\left(1 - \frac{\sin\theta}{3}\right)B_o^{-0.75} \quad [2.47]$$

$$B_o = Bond\ Number = \frac{(\rho_L - \rho_G)gD^2}{\sigma_L} \quad [2.48]$$

$$\sigma_L = surface\ tension(N/m)$$

$$\theta = pipe\ inclination\ angle$$

For the slug nose translational velocity, V_T, the correlation of Manolis (1995) was used by the authors:

$$\begin{aligned} V_T &= 1.033(V_{SL} + V_{SG}) + 0.477(gD)^{0.5} \quad if\ F_{rm} < 2.86 \\ V_T &= 1.216(V_{SL} + V_{SG}) \quad if\ F_{rm} \geq 2.86 \end{aligned} \quad [2.49]$$

$$F_{rm} = \frac{V_{SG} + V_{SL}}{\sqrt{gD}} = Mixture\ Froude\ Number \quad [2.50]$$

The mechanistic model over-predicted the sand particle velocity when compared to the experimental sand particle velocity in slug flow by an average percentage relative error of 10 - 60% and a root mean square error (RMS) of about 40%. The difference between the predicted and measured particle velocity was explained based on the short slug/plug lengths in the laboratory measurement as compared to industrial multiphase flows with long slug/plug lengths.

2.2.10 Danielson (2007)

Danielson (2007) developed a theoretical model for predicting critical or minimum transport velocity that will result in sand bed formation in multiphase pipelines based on drift-shift model. By assumption of a linear function between the gas velocity and mixture velocity over a wide range of conditions, Danielson (2007) proposes a model for predicting sand particle holdup (H_S):

$$V_C H_S^2 + (V_{SL} + V_{SS} - V_C H_O) H_S - V_{SS} H_O = 0 \quad [2.51]$$

$$H_O = H_L + H_S \quad [2.52]$$

$$V_C = \frac{V_{SL}}{H_L} - \frac{V_{SS}}{H_S} \quad [2.53]$$

$$H_L = 1 - \frac{V_{SG}}{(CV_{SM} + V_O)} \quad [2.54]$$

Where C = 1.2 air/water mixture

The bubble rise velocity, V_O , was given by the author as follows:

$$V_O = 0.4\left(\frac{\rho_L - \rho_G}{\rho_L}\right)^{0.5} (gD)^{0.5} \quad [2.55]$$

$$V_{SM} = V_{SL} + V_{SG} \quad [2.56]$$

$$\left[\frac{V_{SL}}{H_L} - \frac{V_{SS}}{H_S}\right] H_S^2 + \left(V_{SL} + V_{SS} - \left[\frac{V_{SL}}{H_L} - \frac{V_{SS}}{H_S}\right][H_L + H_S]\right) H_S - V_{SS}[H_L + H_S] = 0 \quad [2.57]$$

$$V_S = \frac{V_{SS}}{H_S} \quad [2.58]$$

$$V_L = \frac{V_{SL}}{H_L} \quad [2.59]$$

$$V_G = C V_{MD} + V_O \quad [2.60]$$

$$V_C = (V_G + V_L) - V_S \quad [2.61]$$

$$V_{SG} = \frac{M_G}{\rho_G A} \quad [2.62a]$$

$$V_{SL} = \frac{M_L}{\rho_L A} \quad [2.62b]$$

$$V_{SS} = \frac{M_S}{\rho_S A} \quad [2.62c]$$

The model for the sand particle hold-up and critical solid-carrying velocity V_C gave a good fit to experimental data when compared.

2.2.11 Yang et. al. (2007)

Yang et al (2007) modeled and simulated sand transport in a stratified gas-liquid two-phase pipe flow system based on Ishii's one-dimensional multi-fluid model and mixture layer concept. The model consisted of one momentum for each mixture layer and four mass conservation equations for continuous liquid, continuous gas, droplets and sand particles. The proposed model predicted the pressure gradient and mean velocity for threshold of particle entrainment into suspension with reasonable accuracy when compared with experimental data from SINTEF multiphase flow loop.

2.3 Summary of review studies on sand particle transport in gas-oil two-phase pipe flow systems

It is a well known fact that there is a vast amount of petroleum resources in the offshore deep water and ultra deep water going by the petroleum industry discovery of more and more massive oil and gas fields in these highly challenging environments. The use of sand management and multiphase production technology has become conventional for the exploitation of these valuable resources. Increased water depths create a requirement for reliable subsea wells, flow lines, riser and pipelines to economically recover there deepwater fields and also minimize flow assurance problems. Sand particle transport is one of the major flow assurance concerns during deepwater production operations using sand management and multiphase technology. Ineffective sand transport in production and transfer systems can result in severe problems such as productivity impairments, sand deposition and bed formation, sand erosion, corrosion and equipment failure. Because the cost of getting sand transport wrong is so high, adequate knowledge of sand transport characteristics in oil-gas multiphase pipe flows is highly required. This justifies the vast number of theoretical and experimental studies on design and performance analysis of oil-gas-sand multiphase flows in subsea wells, flowlines, riser and pipelines systems.

Existing design practice for the three-phase gas-oil-sand flowlines is normally based on the use of minimum flow velocity that need to be achieved in the pipeline to prevent sand particle deposition and bed formation. Codes and guidance documents for the design of multiphase flowlines, such as the American Petroleum Institute Recommended Practice 14E (API RP 14E), suggest the sizing of three-phase gas-liquid-solid flowlines on the basis of empirical flow equation. However, this empirical flow velocity equation does not refer to any specific studies supporting these recommendations. Moreover, the empirical flow velocity equation does not take account of multitude of factors, such as pipe size; pipe geometry; gas-liquid flow patterns; sand loading; sand properties; particle-particle, wall-particle, aerated fluid-particle interactions (momentum transfer effect); pressure, temperature, oil and gas composition (pressure-volume-temperature effect).

Significant progress has also been made in understanding gas-liquid-solid multiphase flows phenomena in pipes and the ability to make quantitative prediction of sand particle flow behaviour. Particle transport parameters are important parameters in the calculation of gas-oil-sand mixture density, pipe erosion and sizing of sand management topside facilities. The critical and optimal velocities are also important to prevent sand deposition and bed development in horizontal three-phase gas-oil-sand multiphase wells and flowlines. Despite the fact that most industrial three-phase gas-oil-sand pipe flow systems operate at high pressures, almost all the existing models have been developed based on low pressures.

Although several attempts to develop minimum or critical transport velocity for sand particles in gas-oil multiphase pipe flows have been reported, their common setbacks is that they attempt to predict minimum instead of optimal transport velocity requirement. The optimal transport velocity exists that would yield the maximum sand carrying capacity and minimum total pressure loss in the multiphase flowline for a given mass flow rate of sand particles. Therefore existing methods only evaluate the lower limit of transport rate for a given gas-oil-sand multiphase production and transfer systems instead of generating optimal design parameters. Another setback of the previous attempt is that more of them use empirical or semi-theoretical approach lack generality since they are not physics based and beset with a number of problems (low, medium and high sand loading restrictions).

Historically, empirical and semi-empirical correlation is a very useful engineering approach and a large number of correlations appear in the literature. Although some of them are very widely used in the petroleum industry, empirical correlations are generally valid only for the parameter ranges for which they are generated. The Stevenson et. al. model which was an extensive study did not cover all flow configurations. They focused only on the average or overall critical (slip) velocity, solid particle velocity and holdup, but they did not treat both pressure gradient and sand particle transport characteristics in the entrance, middle and exit regions of gas-oil-sand multiphase pipe flow systems, which is very valuable for obtaining fundamentals understanding of the transport behaviour of solids in these long distance transport systems. With respect to the particle deposition, particle erosion and pressure drop in the gas-oil-sand multiphase wellbore, flowlines, risers, and pipelines, the entrance, middle and exit regions is of particular importance. The reasons are the

relatively high input sand fraction and its strong variation along these regions as compared with low sand loading. Therefore, understanding the effects of the multiphase flow phenomena in the entrance, middle and exit regions on the sand particle and hydraulic behaviour of the entrance region becomes very important for design, control and optimization of these systems. Previous literatures also offer no knowledge of the local and axial distribution of the sand particle behaviour in the gas-oil multiphase pipe flow systems. The local gas-oil two-phase pipe flow structure governs the local and axial distribution characteristics of sand particles and is interrelated in a complex way with system, operating and geometric parameters. It is therefore important and desirable to evolve adequate methodology to predict the local behaviour of the suspended and entrained sand particles. To the best of the author's knowledge, there is currently no published model and experimental data available on the local and axial distribution characteristic of particle slip velocity and solid particle parameters in gas-oil-sand multiphase flows through wellbores, flowlines, risers and pipelines. Local and axial distribution characteristics of particle behaviour in three-phase gas-oil-sand pipe flow are strongly linked with the internal flow structure and motion has not yet been well understood.

The Angelson et. al. (1989) study was limited to particle settling velocity while Salama (2000) investigated slip velocity in three-phase oil-gas-sand multiphase pipe flows using empirical modeling based on the extension of Wick (1971) equation. However, their models did not incorporate relevant oil-gas multiphase hydrodynamic parameters.

Gillies et. al. (1997) and King et. al.(2001) models reported on the prediction of pressure gradient, but they did not treat both, sand transport characteristics and optimal transport velocity.

Oudeman (1993) model reported on the entrainment rate prediction of sand particles from stationary bed to moving bed and moving bed to suspension mode. However, no information on the input solid particle loading, particle density, bed thickness and relevant oil-gas multiphase hydrodynamic parameters were given in the author's proposed model.

Danielson (2007) presented some improvement on overall (global) sand holdup and particle slip velocity mechanistic modeling. However, he did not incorporate the effects of sand particle properties such as, sand particle size, sand particle size distribution, sand particle density, sand particle shape factor or sphericity.

The multi-fluid model developed by Yang et. al. (2007) gives a sound approaches to the analysis of oil-gas-sand multiphase flows in pipes. However, the inherent complexity of three-phase oil-gas-sand multiphase pipe flows as well as the numerical methods for solving the governing and several constitutive equations are still largely under-developed and have not yet reached the sufficient successful stage where they can be used with confidence for design and operation of the wide-ranging gas-oil-sand multiphase pipe flow systems found in field practice. As a result, the multi-fluid model together with its relating constitutive equations, have only been marginally applied to horizontal three-phase gas-oil-sand stratified pipe flow systems. The major issues still unresolved for multi-fluid modeling approach are: (i) closure problems (ii) proper description of interface momentum transfer phase interaction (iii) identification of coherent turbulent structures and the quantification of their

contributions to the multiphase transport phenomena (iv) description of transient and three-dimensional flow patterns (v) near wall effects have not been analyzed and wall function have been used as boundary conditions (vi) results depend upon grid size and the discretization schemes used (vii) pressure effects; bubble-bubble coalescence and break-up and particle-particle collisions which have been reported to be hydrodynamic processes controlling solid particle and bubble behaviour in three-phase gas-liquid-solid flows through fluidized beds and bubble columns (Fan et. al. 2002, 2003, 2004, 2005). All these problems are under investigation throughout the world and satisfactory answers are awaited.

Sato et. al. (1991) and Sakaguchi et. al. (1993, 1995) studied three-phase gas-liquid-solid flows in vertical pipes. In other words, the research is applicable to manganese nodule production from ocean bed where the solid particle size is greater than 4mm. However, commonly produced reservoir sand particle size in the petroleum industry is much less than 1mm. More over, the parameters that govern flow behaviour of solid particles during production and transportation of petroleum fluids is high pressure and low temperature. Pressure affects the physiochemical properties of petroleum fluids (oil and gas) through these influences the fluid dynamics and transport phenomena. Density, viscosity, surface tension and gas solubility are the most sensitive to pressure. It is consequently evident therefore that empirical and semi-empirical models developed based on atmospheric experimental data cannot be extrapolated to operation at elevated pressure conditions.

The aforementioned predicaments and the need to address requirement for the development of gas-oil-sand multiple production and transfer systems in offshore deepwater environments using a physic-based predictive model and design tools becomes very crucial. A phenomenological modeling method has promising potential and has been developed in this study to predict particle transport parameters in high pressure three-phase gas-oil-sand multiphase flows through well and pipeline systems. Even if multi-fluid modeling and simulation methods prove to be successful, the simple phenomenological model is still expected to be useful to engineers practicing design as well as operations of three-phase gas-oil-sand wells and pipelines.

The lack of fundamental understanding and analysis of the sand particle behaviour in these systems has resulted in inhibition of sand management technology development and application. To stimulate greater use of this viable and cost-effective alternative to sand control technique, sound technical basis must be established for the adequate understanding of the hydrodynamics of the sand transport in gas-oil multiphase flows through subsea wells, flowlines, risers and pipelines. Such an approach must integrate the three-phase flow physics and various systems, operating and geometric parameters to result in an overall prediction and design tool. To the best of the author's knowledge, no investigation has been reported in the open literature regarding the nature and incorporation of pressure effects on sand particle transport behaviour on gas-oil multiphase pipe flows. Of fundamental importance is the extent to which the pressure effects occur and its implication on sand transport behavior in the three-phase gas-oil-sand pipe flow systems.

2.4 Statement of Research Problem

Sand particle transport in gas-oil multiphase production and well systems poses special flow assurance challenges and requires accurate multiphase flow prediction tools for efficient estimation of critical velocity for incipient sand particle deposition; gas-oil-sand multiphase flow system performance and optimization; system, operating and geometric effects on wellbore hydraulics; local and global flow rate and volume fraction of produced sand particles to be disposed, local erosion risk and sizing of possible dedicated sand management equipment, such as desanders, filters, accumulator vessels, washing systems and storage bins. Production and facility engineers often experience frustration due to lack of accurate models to help them answers basic design questions pertaining to gas-oil-sand multiphase wellbores, flowlines, trunklines, production risers and pipelines.

.

Conventional models for particle transport in gas-oil-sand multiphase production and well systems are generally based on hydraulic approximation and empiricism. These models have three major limitations: (i) the previous models lead to corrective measures rather than preventive ones, for example, critical velocity for incipient sand particle (bed) erosion instead of incipient sand particle deposition, which prevents sand deposition and bed development, production loss and downtime (ii) it does not incorporate the most important hydrodynamic processes governing the gas-oil-sand multiphase transport phenomena and the effects of system, operating and geometric parameters on local and global hydraulic and sand particle transport characteristics (iii) it is difficult to conduct off-line and on-line optimization and risk-based performance assessment and comparisons of gas-oil-sand multiphase wellbore, flowline, trunkline, production riser and pipeline system design options (minimizing sand deposition and erosion risks for long-term efficiency, reliability and integrity of assets).

Scientific and reliable design of gas-liquid-solid multiphase pipe flows requires accounting for hydrodynamic characteristics under different system, design and operating conditions. This demands sufficient experimental and theoretical investigations. Few studies on the macroscopic characteristics of solid phase in gas-liquid multiphase pipe flows have been reported. Since the macroscopic characteristics are governed by microscopic ones, much attention has been focused on the local and global solid phase hydrodynamic characteristics in this study. To the best of the author's knowledge, no mechanistic model has been reported to date in the petroleum industry to predict local and axial distributions of critical transport velocity; solid particle velocity, holdup, flux and mass rate; pressure drop characteristics and optimal transport velocity (rate) in gas-oil-sand multiphase pipe and annular flow systems. Moreover, experimental data on local and axial distributions of solid transport parameters in oil-sand and gas-oil-sand multiphase pipe flows is also scarce for the purpose of validation of hydrodynamic-based model. It is important but challenging task to obtain experimental data on local sand transport parameters for low to high sand concentration (loading) in oil-sand and gas-oil-sand multiphase pipe flow systems which will result in a better understanding of particle flow behaviour, system performance (pressure drop), wear and erosion characteristics.

The motivation for experimental and theoretical studies of three-phase gas-oil-sand pipe flows comes from the paramount need for a fundamental research, which provides practical solution that allows operators to produce oil at optimal economic

rate and still live pleasantly with sand production and transport issues. This need requires advancement of petroleum engineering practice from sheer prediction of minimum transport velocity and average particle velocity in gas-liquid-solid multiphase pipe flow systems to solving the problem of cash flow, which is traditionally tied to optimal oil rate, sand deposition and erosion risk assessment and management, minimum pressure drop (production optimization) and high ultimate recovery. This dissertation fills these gap-in-knowledge and technological needs for the first time by addressing solid transport behaviour issues in gas-oil-sand multiphase wellbores and pipelines based on fundamental and advanced experimental analysis.

2.5 Significance and Contribution of the Research Study

The most important contribution of this dissertation is six folds:

- First, the research presents an advancement of the analysis of particle transport in gas-liquid-sand multiphase pipe and annular flow systems using phenomenological modelling concept. This new model incorporates all relevant hydrodynamic processes controlling particle transport in liquid-solid and gas-liquid-sand multiphase pipe and annular flow systems
- Second, the research presents a novel method for predicting local and axial distributions of critical transport velocities, particle transport behaviour and pressure drop characteristics in liquid-solid and gas-liquid-sand multiphase pipe and annular flow systems
- Third, this research presents a design and optimization criteria for sand deposition prevention and hydraulic optimization of liquid-solid and gas-liquid-sand multiphase pipe and annular flow systems. Our investigation also elucidated several important trends and parameters dependencies that are far from obvious and not applied to problems of this type in the past.
- Fourth, the research presents an implementation of the hydrodynamic-based physical model in visual basic computer code for engineering applications. Computer package (software tool) enables the simulation of particle transport behaviour, determination of sand deposition risk and faster performance assessment of various design alternatives of the liquid-solid and gas-liquid-sand multiphase pipe and annular flow systems. The visual basic code can be run on any operating systems and capable of handling any pipe configuration, including vertical, inclined and horizontal pipes.
- Fifth, the field application of the new phenomenological modelling method for calculating particle velocity, particle holdup, critical velocity and pressure drop performance in optimal three-phase gas-oil-sand well and pipeline systems. The optimal transport velocity prediction and the significant impact of solid particle size distribution, solid article shape, operating pressure, particle-particle particle-multiphase flow, particle-wall interactions on solid transport parameters and pressure drop characteristics in gas-oil multiphase pipe flows is in particular novel. Prediction of sand management well performance is vitally important for enhancing sand management production scheme.
- Finally, the research presents new experimental data on local particle transport behaviour in liquid-solid and gas-liquid-solid multiphase pipe flow systems and the associated effects of system, operating and geometric parameters. To the best of the author's knowledge, although much research has been reported for solids transport in gas-liquid-solid multiphase pipe flows, virtually no

investigation has been reported on local solid phase velocity, phase holdup, phase flux and mass rate distributions in these flow systems using a non-invasive charged couple device measuring technique. Thus, this information about the effects of system, design and operating conditions on solids transport characteristics is valuable and useful.

2.6 Research Objectives

The purpose of this dissertation is to:

- experimentally investigate local and global particle transport behaviour in three-phase gas-liquid-solid pipe flow systems for a variety of flow patterns and conditions using light sheet charged couple device (particle image and particle tracking velocimetry) measuring technique
- use the acquired experimental data to better understand particle transport characteristics in three-phase gas-liquid-solid pipe flows with respect to its dependency on system, operating and geometric properties
- develop a realistic phenomenological model for predicting particle transport parameters, critical (deposition) velocity and optimal transport velocity in three-phase gas-liquid-solid wellbore, flowline, production riser and pipeline systems under wide ranging conditions found in practice. The predictive model has the capability of properly accounting for the relevant mechanisms controlling particle transport in gas-oil-sand multiphase pipe and annular flows
- formulate a numerical model to solve the phenomenological model and implement the solution in a visual basic computer code (package) for engineering applications
- validate and compare the proposed model and existing methods using experimental data obtained from present study and open literature
- demonstrate the field applications of the new methodology with several case studies

2.7 Conclusions

The research reviewed in this chapter details the research work that has been previously investigated in the field of sand transport in multiphase pipe flow systems, which provides a foundation for the observation made in the present work. Sand transport in three phase gas-liquid-solid pipe flow system has been developed for average or global slip velocity, particle velocity and holdup. There is still limited knowledge of local and axial distribution characteristics of particle slip velocity, particle velocity, holdup, flux, mass rate and the impact of system, operating and geometric parameters. Furthermore, there exist no methodology (criterion) of determining the optimal oil rate for minimizing pressure drop and preventing sand deposition in gas-oil-sand multiphase production and transfer systems. Settling flow (sand deposition) is usually avoided in any good design. In addition, no dedicated computer package currently exists for the evaluation and optimization of particle and hydraulic behaviour of a wide range gas-oil-sand multiphase wellbores, flowlines, rises and pipeline system design for complete lifecycle conditions. The research presented herein fills this knowledge gap and technological needs.

In addition, there has been relatively little use of advanced experimental flow measurement techniques application to study particle transport in gas-oil multiphase flow conditions. These techniques such as electrical capacitance tomography (ECT), nuclear magnetic resonance imaging (MRI) pulsed ultrasonic Doppler velocimetry (PDA), particle image velocimetry (PIV), particle tracking velocimetry (PTV), Laser Doppler velocimetry (LDA) flows in fluidized beds and high speed charged couple device (CCD) tracking techniques are established methods which have been deployed to visualize, elucidate and analyze multiphase flows in fluidized beds and bubble columns (Fan et. al. 2002, 2003, 2004, 2005). They have numerous advantages over the existing methods (direct sampling probe, stop watch, quick-closing valves and particles collection) because of their non-invasive character. The fast response and valuable insight into the physical mechanisms controlling sand particle transport in gas-oil multiphase pipe flow justify the choice of CCD measuring technique for this study. The advantage of CCD imaging technique is its feasibility in practice that gives adequate results of both visualization and quantitative measurements can be obtained by a conventional high speed CCD camera coupled to a video system which is easily facilitated in laboratory and quite cheap. However, it needs a very good computer program algorithm for image processing and calculation of local solid particle velocity, holdup, flux and mass rate.

Past experimental and modeling research studies done on particle transport in gas-liquid multiphase pipe flow systems can be used to verify and validate the predictive accuracy and applicability of the newly developed model results. Current study will also utilize part research results to help collaborate and interpret the behaviour of sand particles in gas-liquid multiphase pipe flow in cases where direct observation cannot be made.

3 MATHEMATICAL MODEL DEVELOPMENT

3.1 Introduction

This chapter presents a theoretical analysis of particle transport and hydraulic characteristics in oil-sand and gas-oil-sand multiphase pipe flow systems. The system of governing equations developed to for local and axial distributions of particle velocity, hold-up, flux and mass rate; local and axial distributions of slip (critical) velocity; performance and optimal transport velocity is based upon a phenomenological description of oil-sand and gas-oil-sand multiphase flow behaviour in a pipe. The mathematical model involves balance equations deduced from macroscopic mass and momentum conservation laws, constitutive models and forces due to drag force, gravitation force, buoyancy force, particle-liquid turbulent interaction force, particle-particle interaction force and particle-pipe wall interaction force. The governing equations are solved by fourth order Runge-Kutta numerical method which computational algorithm is implemented in visual basic computer code. The proposed mathematical model provides guidelines in the decision making processes, because it uses optimization techniques to obtain optimal transport velocity that prevents sand deposition, minimizes pressure drop, minimizes sand erosion, reduces downtime and cost of maintenance over the life cycle of the production and transfer systems. The computational method is also capable of determining best among various design alternatives.

3.2 Particle Transport Model Development

The gas-liquid-solid multiphase production and pipeline transport system operating under high pressure is considered. A typical sketch of the gas-liquid-solid multiphase flow in a pipe and control volume systems is represented in Figures 3.1 and 3.2. The blue colour in figures 3.1 and 3.2 represents the liquid phase while the red and black colours connote gas and solid phases, respectively. The forces acting on a suspended single particle in a three-phase pipe flow systems are represented in Figures 3.3 and 3.4. P is the system pressure of the three-phase gas-liquid-solid pipe flow between points 1 and 2 of the control volume element. V denotes the phase velocity of each of the flowing three-phase between points 1 and 2 of the computational cell. The theoretical analysis and mathematical model for the oil-sand and gas-oil-sand multiphase pipe flow system is developed under the following assumptions:

a. The gas-liquid-solid multiphase flow is one-dimensional, fully developed, steady state and isothermal
b. The three-phase flowing mixtures are assumed to be Newtonian fluids. Both the liquid and solid phases are incompressible (constant density) and the gaseous phase is considered as real gas. The real behaviour of the gas phase remains a good approximation for operating conditions not too close to the critical point
c. The effects of the flow distribution and large scale fluctuations and non-uniformity induced by gas-phase (liquid phase) are neglected; the hydrodynamic variables for the gas and liquid phases are uniform over the cross-section and axial length of the pipe
d. The flow field is governed mainly by body and interaction forces between the three flowing phases

e. Acceleration effects are negligible in the absence of interfacial mass transfer between the phases
f. The radial and tangential components of the velocity vector are assumed to be negligible
g. No interaction between fine-fine and coarse-coarse particles is assumed but there is interaction between fine-coarse particles
h. Bubble-bubble interactions are considered to be negligible
i. Bubble coalescence and break up are negligible
j. The pressures in all phases are the same within a computational cell
k. The holdup is considered as average for particular gas and liquid flow rate within a computational cell
l. The influence of solid particle motion on the continuous phase (carrier fluid) is not accounted for in the developed model

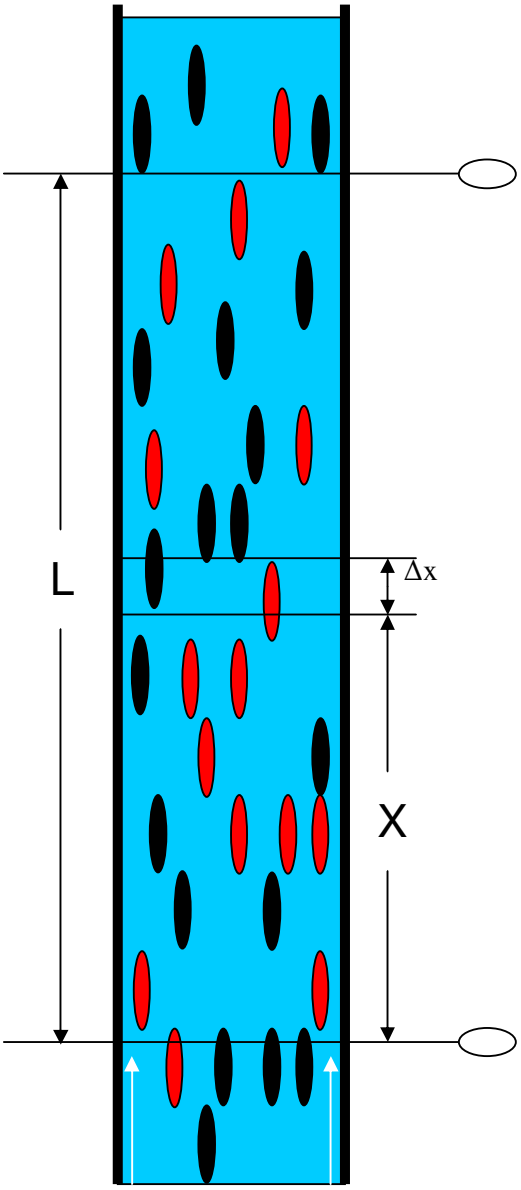

Figure 3-1: Schematic representation of a gas-liquid-solid multiphase flow through a vertical pipe

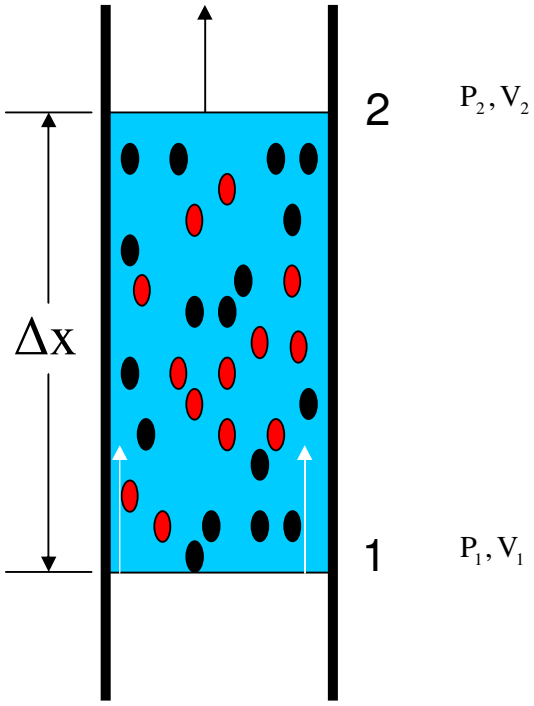

Figure 3-2: Schematic representation of the control volume in a gas-liquid-solid multiphase flow through a pipe

In Figures 3.3 and 3.4, F_{IS} is the interfacial drag force on particle exerted by the gas-liquid two-phase flow. It is the driving force that keeps the particle in motion. F_{BS} is buoyancy force acting on the solid phase. F_{GS} is gravity force acting on the solid phase. F_{PS} is the particle-particle collision force. F_{WS} is friction force transferred from the pipe wall to the solid phase. F_{TS} is the turbulent dispersive force. Virtual mass forces acting due to the acceleration of the multiphase flows and Saffman lift forces (F_{LS}) are considered negligible in the present analysis.

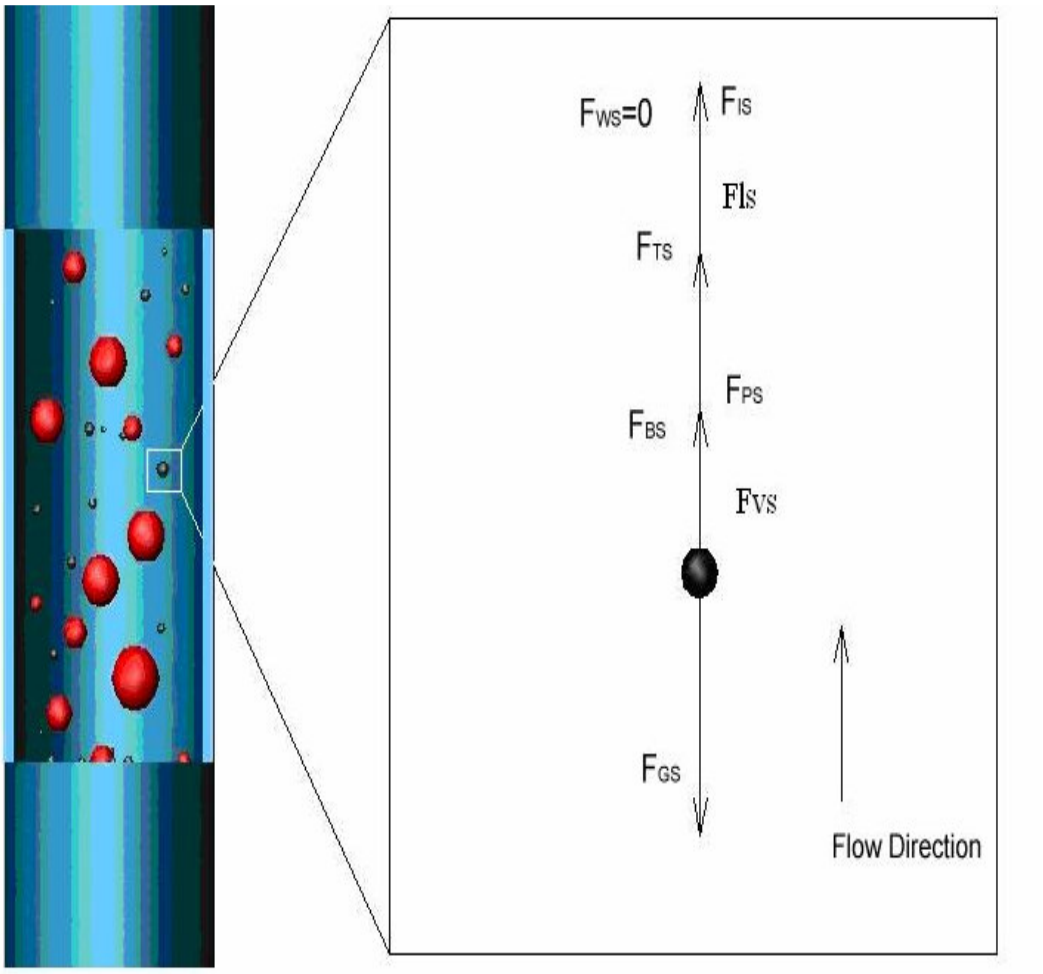

Figure 3-3: Force body diagram of a fully suspended particle in gas-oil- sand multiphase flow through a vertical pipe

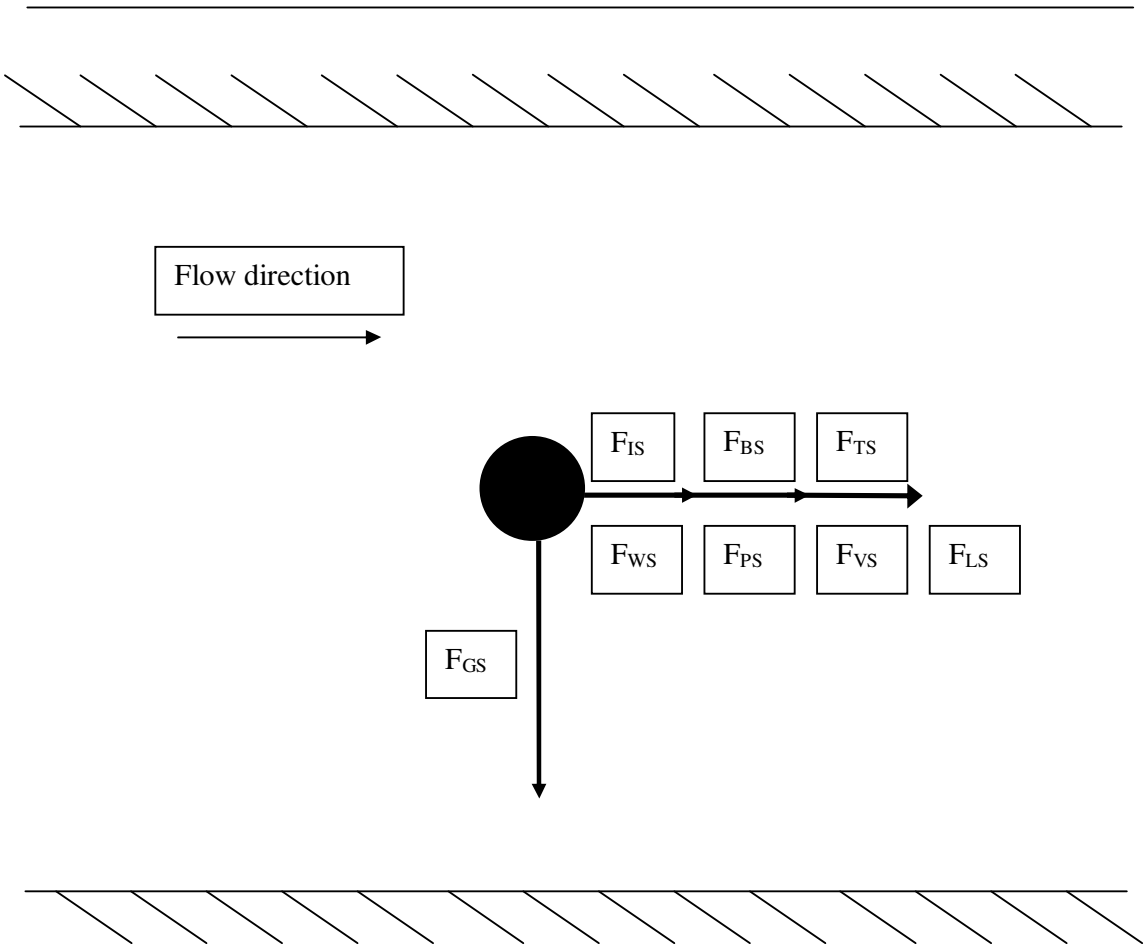

Figure 3-4: Force body diagram of a fully suspended particle in gas-oil-sand multiphase flow through a horizontal pipe

3.2.1 Conservation equations

The conservation equation of mass and momentum which governs the solid phase in the gas-liquid-solid three-phase flow in a pipe are given by:

Continuity equation for the solid phase

$$\frac{\partial(\rho_S)}{\partial t} + \frac{\partial(\rho_S V_S)}{\partial x} = 0 \qquad [3\text{-}1]$$

Solid phase momentum equation

$$\frac{\partial(\rho_S V_S)}{\partial t} + \frac{\partial(\rho_S V_S^2)}{\partial x} = \sum_{i=1}^{8} F_{vi} \qquad [3\text{-}2]$$

The F_V is force per volume with several components (interfacial drag, buoyancy, gravity, particle-particle, particle-wall, turbulent dispersive, virtual mass and Saffman lift forces per volume). Dividing equation [3-2] by particle volume ($\frac{\pi}{6} d_p^3$) with negligible effect of the momentum flux term and macroscopic analytical treatment of it gives a one-dimensional equation of motion of a single particle suspended in a liquid flow, isolated from other particles may be expressed as:

$$M_P \frac{dV_S}{dt} = F_{IS} + F_{PS} + F_{WS} + F_{TS} + F_{VS} + F_{LS} + F_{BS} + F_{GS} \qquad [3\text{-}3]$$

Where x and t represent the spatial (axial) and time coordinate respectively. The solid particle velocity is V_S. M_P is the solid particle mass which is a function of particle density and volume. In this investigation, only the interfacial drag, buoyancy, gravity, wall friction, turbulent dispersive and particle-particle collision forces are considered. Due to the small solid particle size, the virtual mass and Saffman lift forces are ignored due to their negligible influences.

Equation [3-3] therefore reduces to:

$$M_P \frac{dV_S}{dt} = F_{IS} + F_{PS} + F_{WS} + F_{TS} + F_{BS} + F_{GS} \qquad [3\text{-}4]$$

where
M_P, represents the solid particle mass and its given as follows:

$$M_P = \frac{\pi}{6} d_p^3 \rho_S \qquad [3\text{-}5]$$

where ρ_S the solid density is. d_P is solid particle diameter

Considering the equality for a fully developed flow:

$$\frac{dV_S}{dt} = V_S \frac{dV_S}{dx} \qquad [3\text{-}6]$$

Substituting equations [3-5] and [3-6] into equation [3-4] to give:

$$V_S \frac{\pi}{6} d_p^3 \rho_S \frac{dV_S}{dx} = F_{IS} + F_{PS} + F_{WS} + F_{TS} + F_{BS} + F_{GS} \qquad [3\text{-}7]$$

Equations [3-1 to 3-7] represent the equations governing the solid phase transport in gas-liquid multiphase flow through a pipe. Equation [3-7] is used to estimate the local and axial distributions of solid phase velocity, holdup and flow rate in three-phase gas-liquid-solid pipe flow for dispersed bubble, bubbly and annular flow patterns. This requires the closure models for all the acting hydrodynamic forces in the three-phase gas-liquid-solid pipe flow systems. The solid phase velocity distributions in three-phase gas-liquid-solid slug flow in a pipe are calculated using a similar method developed by Wang et. al. (2002) for predicting corrosion rate in oil-water-gas multiphase pipe flow:

$$V_S = V_{S1}\left(\frac{t_{sf}}{t_{avg}}\right) + V_{S2}\left(\frac{t_{sm}}{t_{avg}}\right) \qquad [3\text{-}8]$$

where

t_{avg} = average time for one slug unit

t_{sf} = time for one slug film

t_{sm} = time for one slug mixing zone

V_{S1} = sand particle velocity in liquid film zone

V_{S2} = sand particle velocity in liquid slug mixing zone

V_S = sand particle velocity in gas-liquid-solid multiphase slug flow

$$t = t_{sf} + t_{sm} \qquad [3\text{-}9]$$

$$t = \frac{1}{f_{slug}} \qquad [3\text{-}10]$$

The slug frequency, f_{slug}, is calculated as follows:

$$Log\left(f_{slug}\frac{D}{V_{sl}}\right) = m\left(v_m^1 + b\right)$$

$$m = 4x10^{-5}\theta^3 + 5x10^{-4}\theta^2 - 2.5x10^{-2}\theta + 0.7 \qquad [3\text{-}11]$$

$$b = -4x10^{-4}\theta^3 - 4.1x10^{-3}\theta^2 + 2\theta - 1.7$$

where

f_{slug} = slug frequency

D = pipeline diameter

V_{sl} = superficial liquid velocity

θ = pipeline inclination angle from horizontal

$$v_m^1 = v_{3m}^1 = \frac{w}{\rho_{3m}^1 A} = \text{total gas-oil-sand velocity} \qquad [3\text{-}12]$$

The average mixing zone time, t_{sm}, is estimated as follows:

$$t_{sm} = \frac{LMZ}{V_t} \qquad [3\text{-}13]$$

Where the average length of mixing zone, LMZ, is calculated using the correlation given Maley and Jepson (1997)

$$LMZ = 0.051F_r + 0.18 \qquad [3\text{-}14]$$

Where

V_t = transitional mixing zone velocity = 1.25 (V_{SL} + V_{SG})

$$Fr = \ film\ Froude\, number = \frac{V_t - V_{LF}}{(gh_{EF})^{0.5}} \qquad [3\text{-}15]$$

V_{LF} = slug film velocity = V_{SL}

The effective slug film height, h_{EF}, is calculated from published correlations (Wang et. al., 2002)

$$\frac{h_{EF}}{D} = 0.059\exp\left(-0.34 Fr_{GO}^{0.25}\ \mathrm{Re}_{LO}^{0.19}\ X^{0.6}\right) \qquad [3\text{-}16]$$

Where

h_{EF} = effective slug film height

$$Fr_{GO} = \frac{V_{SG}^2}{g\,D} \qquad [3\text{-}17]$$

$$\mathrm{Re}_{LO} = \frac{\rho_L V_{SL}\, D}{\mu_L} \qquad [3\text{-}18]$$

$$X = \frac{V_{SG}\,\rho_G}{V_{SG}\,\rho_G + V_{SL}\,\rho_L} \qquad [3\text{-}19]$$

Both V_{S1} and V_{S2} is determined by equation [3-7] depending on whether the particle is in the liquid slug zone or in the liquid film zone. However, the average particle velocity in a slug unit which comprises the liquid slug zone and the liquid film zone is estimated using equation [3-8] and its relating equations [3-9 to 3-19].

The solid particle hold-up in each of the gas-liquid-solid multiphase flow through a pipe system is calculated as follows:

$$H_S = \frac{V_{SS}}{V_{S_i}} \qquad [3\text{-}20]$$

V_{SS} is given by equation [3.52].

The in-situ solid particle mass rate in each of the gas-liquid-solid multiphase flow through a pipe system is calculated as follows:

$$\int_0^{Q_{S2}} dQ_S = \int_0^A V_S \, \rho_S \, dA \qquad [3\text{-}21]$$

$$Q_S = V_S \, \rho_S \, A \qquad [3\text{-}22]$$

The critical velocity is the velocity at which sand particle bed start to form and develop. A bed of sand particles represents an inefficient operation and should be avoided in a good design. The design velocity in a gas-oil-sand multiphase pipe flow should therefore be the critical velocity plus some margin of 10% or so for the effects of input sand loading fluctuations. A higher than necessary design velocity is energy inefficient and results in excessive wear of the flow conduit. A design velocity that is too low, however, can result in sand particle bed deposition and bed development. The critical or slip velocity in a gas-liquid-solid multiphase flow through a pipe system is calculated in relation to the in-situ gas and liquid mixture velocity and the in-situ particle velocity as follows:

$$V_C = V_M - V_S \qquad [3\text{-}23]$$

where V_C is the critical or slip velocity. V_M is the actual or in-situ gas-liquid mixture velocity while V_S is the actual or in-situ sand particle velocity.

3.2.2 Flow regime prediction

The Beggs and Brill (1973) expression is utilized for the gas-liquid flow regime prediction. The expressions are given as follows:

- $N_{Fr} = \dfrac{v_{2m}^2}{gD}$ [3-24]

- $\lambda_L = \dfrac{q_L}{q_L + q_g}$ [3-25]

- $L_1 = 316\lambda_L^{0.302}$ [3-26]

- $L_2 = 0.0009252\lambda_L^{-2.4684}$ [3-27]

- $L_3 = 0.10\lambda_L^{-1.4516}$ [3-28]

- $L_4 = 0.50\lambda_L^{-6.738}$ [3-29]

The segregated (annular or stratified) flow regime exists if:

$\lambda_L \angle 0.01$ and $N_{Fr} \angle L_1$ or $\lambda_L \geq 0.01$ and $N_{Fr} \angle L_2$ [3-30]

The intermittent (slug) flow regime occurs if:

$0.01 \leq \lambda_L \angle 0.4$ and $L_3 \angle N_{Fr} \leq L_1$ or $\lambda_L \geq 0.4$ and $L_3 \angle N_{Fr} \leq L_4$ [3-31]

The distributed (bubble or dispersed) flow regime occurs when:

$\lambda_L \angle 0.4$ and $N_{Fr} \geq L_1$ or $\lambda_L \geq 0.4$ and $N_{Fr} \succ L_4$ [3-32]

The transition flow regime occurs when:

$\lambda_L \geq 0.01$ and $L_2 \angle N_{Fr} \leq L_3$ [3-33]

3.2.3 Formulation of forces acting on a particle in gas-liquid-solid multiphase pipe flow system

The governing equations [3-1 to 3-7] do not form a closed system. The constitutive equations or expressions are required in order to close the governing equations. The quantities that are needed include F_{IS}, F_{PS}, F_{WS}, F_{TS}, F_{BS}, F_{GS} and the respective multiphase flow parameters.

The frictional interaction force between the sand particle and the flow conduit in the vertical flow is assumed negligible because the particle flow has been reported not to exist in the boundary layer region of an upward vertical pipe flow (Xia, et. al., 2004).

A. <u>Frictional drag force</u>

The drag force (F_{IS}) transferred from liquid-phase to a single suspended solid particle is calculated by:

$$F_{IS} = \beta(V_M - V_S) \quad [3\text{-}34]$$

where β is the momentum transfer coefficient and the $V_M - V_S$ is the particle slip velocity between solid and liquid-gas mixture considering the presence of the gas phase.

$$\beta = C_{DS} \frac{\rho_M (V_M - V_S)}{2} \frac{d_p^2 \pi}{4} \quad [3\text{-}35]$$

The d_P is the equivalent particle diameter used for multi-sized mixtures (n is the number of class intervals in the particle size distribution). The d_P can be represented as:

$$d_P = \frac{\sum_{i=1}^{n} f_i \, d_i}{\sum_{i=1}^{n} f_i} \qquad [3\text{-}36]$$

The C_{DS}, is estimated using the drag coefficient correlation developed by Swamee and Ojha (1991) for spherical and non-spherical particles in incompressible fluids based on the Corey shape factor (Ψ). The Swamee and Ojha (1991) correlation is given as follows:

$$C_{DS} = \frac{48.5}{\left(1 + 4.5\Psi^{0.35}\right)^{0.8} \mathrm{Re}_P^{0.64}} + \left(\frac{\mathrm{Re}_p}{\mathrm{Re}_p + 100 + 100\Psi}\right)^{0.32} \left(\frac{1}{\Psi^{18} + 1.05\Psi^{0.8}}\right) \qquad [3\text{-}37]$$

The equation was stated to be applicable in the range:

$0.3 \prec \Psi \prec 1$ and $1 \prec \mathrm{Re}_P \prec 10{,}000$

The particle Reynolds number, Re_P, is defined as follows:

$$\mathrm{Re}_P = \frac{d_P V_{PL} \rho_S}{\mu_L} \qquad [3\text{-}38]$$

Where Ψ is the solid particle shape factor. The Ψ and d_i in this study are estimated from over 100 different sand particles (ρ_S = 2,600 kg/m^3) via scanned electron microscope and using the following equation:

$$\Psi = \frac{c}{\sqrt{a\,b}} \qquad [3\text{-}39]$$

$$d_i = \sqrt[3]{a\,b\,c} \qquad [3\text{-}40]$$

For a geometrically irregular solid particle a, b and c are the length of the three main axes being a and c the longest and shortest respectively.

Several correlations are available to predict particle terminal velocity, V_{PL}, in a liquid-solid medium with liquid as the continuous phase and its given as:

$$V_{PL} = \left[\frac{4(\rho_S / \rho_L - 1)\, g\, d_p}{3 C_{DS}} \right]^{0.5} \quad [3\text{-}41]$$

The g denotes the acceleration due to gravity (9.8m/s^2).

The actual gas and liquid velocities at the inlet and outlet of each computational cell during gas-liquid-solid three phase flow is estimated as follows:

$$V_G = = \frac{V_{SG}}{H_G} \quad [3\text{-}42]$$

$$V_L = = \frac{V_{SL}}{1 - H_G} \quad [3\text{-}43]$$

The value of the actual liquid velocity in liquid-solid two phase pipe flow system is calculated from an iterative procedure:

$$V_L = = \frac{V_{SL}}{H_L} \quad [3\text{-}44]$$

V_L is guessed at the beginning of iteration as a product of

$$H_L = = \frac{V_{SL}}{V_{MIX}} \quad [3\text{-}45]$$

Where

$$V_{MIX} = \frac{1}{\rho_{SS}} \left[\lambda_L V_{SL} \rho_L + \lambda_S V_{SS} \rho_S \right] \quad [3\text{-}46]$$

$$\lambda_G = \frac{q_G}{q_G + q_L + q_S} \quad [3\text{-}47]$$

$$\lambda_L = \frac{q_L}{q_G + q_L + q_S} \quad [3\text{-}48]$$

$$\lambda_S = \frac{q_S}{q_G + q_L + q_S} \quad [3\text{-}49]$$

$$V_{SL} = \frac{\dot{m}_L}{\rho_L A} \quad [3\text{-}50]$$

$$V_{SG} = \frac{\dot{m}_G}{\rho_G \, A} \qquad [3\text{-}51]$$

$$V_{SS} = \frac{\dot{m}_S}{\rho_S \, A} \qquad [3\text{-}52]$$

where $\dot{m}_G$, $\dot{m}_L$ and $\dot{m}_S$ are mass rates of gas, liquid and solid phases, respectively. V_M and ρ_M are the gas-liquid mixture velocity and gas-liquid mixture density which are expressed as follows:

$$V_M = V_G + V_L \qquad [3\text{-}53]$$

$$\rho_M = \rho_G H_G + \rho_L (1 - H_G) \qquad [3\text{-}54]$$

For the gas-liquid mixture case, the sum of volumetric fractions for gas and liquid phase is regarded as:

$$H_G + H_L \approx 1 \qquad [3\text{-}55]$$

Where H_G and H_L are the volumetric fractions for gas and liquid phase respectively.

In horizontal and upward inclined pipes, the volumetric fraction for the gas-phase, H_G, used in this study is calculated based on the correlation proposed by Woldermayat and Ghajar (2007) for different flow patterns. This expression is given as follows:

$$H_G = \frac{V_{SG}}{V_{SG}\left[1+\left(\frac{V_{SL}}{V_{SG}}\right)\left(\frac{\rho_G}{\rho_L}\right)^{0.1}\right] + 2.9\left[\frac{g\,D\sigma(1+\cos\theta)(\rho_L-\rho_G)}{(\rho_L)^2}\right]^{0.25} + [1.22+1.22\sin\theta]\,\frac{P_{atm}}{P_{system}}} \qquad [3\text{-}56]$$

where P_{atm} and P_{system} are the atmospheric and system pressures respectively.

The volumetric fraction, H_G, for gas-liquid two phase flows through vertical pipes are estimated using the correlation given by Kabir and Hassan (1998):

Dispersed bubble flow parameters

Gas holdup fraction

$$H_{GD} = \frac{V_{SG}}{V_{SG} + V_{SL}} \qquad [3\text{-}57]$$

Bubble flow parameters

Gas holdup fraction

$$H_{GB} = \frac{V_{SG}}{1.2V_M + V_{BR}} \qquad [3\text{-}58]$$

where

$$V_{BR} = 1.40\left[1 - \frac{D_B}{D}\right]\left[\frac{g\sigma\Delta\rho}{\rho_L^2}\right]^{0.25} \qquad [3\text{-}59]$$

$$d_B = \left[\frac{3\,\sigma}{g\,\Delta\rho}\right]^{0.5} \qquad [3\text{-}60]$$

where d_B is bubble size diameter, D is the pipe diameter and d_B is the hydraulic diameter defined by equation [3.91].

Slug flow parameters

$$H_G = \frac{V_{SG}}{V_{TY}} \qquad [3\text{-}61]$$

$$V_{TY} = 1.2\left(V_{SL} + V_{SG}\right) + 0.35\left(g\,D_H\right) \qquad [3\text{-}62]$$

Where V_{TY} is the Taylor bubble velocity

Annular Flow

Holdup Fraction

$$H_{GA} = \frac{V_{SG}}{V_{SG} + E\,(V_{SL})} \qquad [3\text{-}63]$$

where the vapour entrainment, E, is estimated from the following conditions:

If $V_{SGC}\,(10^4) \le 4$ then $E = 0.0055[V_{SGC}\,(10^4)]^{2.86}$

If $V_{SGC}\,(10^4) \ge 4$ then $E = 0.857\log\,[V_{SGC}\,(10^4)] - 0.20$

The critical vapor velocity, V_{SGC} , is calculated as from:

$$V_{SGC} = \frac{V_{SG}\,\mu_G\,(\rho_G / \rho_L)}{\sigma_L} \qquad [3\text{-}64]$$

Z-factor is computed using the Brill and Beggs (1974) method. This method is expressed as follows:

$$A = 1.39\,(T_{\mathrm{Pr}} - 0.92)^{0.5} - 0.36 T_{\mathrm{Pr}} - 0.10 \qquad [3\text{-}65]$$

$$B = (0.62 - 0.23 T_{\mathrm{Pr}}) P_{\mathrm{Pr}} + \left[\frac{0.066}{T_{\mathrm{Pr}} - 0.86} - 0.037\right] P_{\mathrm{Pr}}^2 + \frac{0.32 P_{\mathrm{Pr}}^6}{10^E} \qquad [3\text{-}66]$$

$$C = 0.132 - 0.32 \log\,(T_{\mathrm{Pr}}) \qquad [3\text{-}67]$$

$$D = 10^F \qquad [3\text{-}68]$$

$$E = 9\,(T_{\mathrm{Pr}} - 1) \qquad [3\text{-}69]$$

$$F = 0.3106 - 0.49 T_{\mathrm{Pr}} + 0.1824 T_{\mathrm{Pr}}^2 \qquad [3\text{-}70]$$

$$Z = A + \frac{1 - A}{\exp^B} + C P_{\mathrm{Pr}}^D \qquad [3\text{-}71]$$

Where

$P_{\mathrm{Pr}} = \dfrac{p}{P_C}$ = Pseudo-reduced pressure

$T_{\mathrm{Pr}} = \dfrac{T}{T_C}$ = Pseudo-reduced temperature

$P_C = \sum_{i=1}^{n} p_{ci}\, y_i$ = Pseudo-critical pressure

$T_C = \sum_{i=1}^{n} T_{ci}\, y_i$ = Pseudo-critical temperature

$$\rho_G = \frac{p M_g}{zRT} \qquad [3\text{-}73]$$

The gas viscosity (μ_G) computed using the Lee-Gonzalez-Eakin Method (1966). This method is expressed as follows:

$$\mu_G = 10^{-4}\, K \exp\left[X\, \rho_G{}^{Y}\right] \qquad [3\text{-}74]$$

Where

$$K = \frac{(9.4 + 0.02 M_G) T^{1..5}}{209 + 19 M_G + T} \qquad [3\text{-}75]$$

$$X = 3.5 + \frac{986}{T} + 0.01 M_G \qquad [3\text{-}76a]$$

$$Y = 2.4 - 0.2\, X \qquad [3\text{-}76b]$$

Where

M_G = y_i MW_i = Molecular weight of the gas mixture

The gas gravity (γ_G) and gas mixture density (ρ_G) are calculated as follows:

$$\gamma_G = \frac{\sum_{i=1}^{n} MW_i\, y_i}{\gamma_{AIR}\, 28.97} \qquad [3\text{-}77]$$

T = Absolute temperature

ρ_g = *gas mixture density*

μ = *gas mixture viscosity*

n = number of components

MW_i = molecular weight of component i
y_i = molecular fraction of component i
M_G = molecular weight of gas mixture
p = operating pressure
T = operating temperature
z = gas compressibility factor

B. Particle-Particle interaction force

The particle-particle interaction force (F_{PS}) in gas-liquid-solid three-phase pipe flow can be written using the mixture model as follows:

$$F_{PS} = \frac{\pi}{4}(d_P)^2 \frac{\dot{m}_S}{A}(V_M - V_S) \quad [3\text{-}78]$$

Where $\dot{m}_S$ is the input solid-phase mass flow rate or sand mass production rate into the wellbore or pipeline. A is the pipe cross-sectional area. d_P is the solid particle equivalent diameter.

C. Particle-Liquid (turbulent) interaction force

The particle-liquid (turbulent) interaction force (F_{TS}) in gas-liquid-solid three-phase pipe flow can be written using the mixture model as follows:

$$F_{TS} = \rho_L \frac{\pi}{4}(d_P)^2 \quad (v^1)^2 \quad [3\text{-}79]$$

Where v^1 is the turbulent fluctuation velocity. The η_L and ρ_L are the liquid dynamic viscosity and density, respectively. d_P and D are the solid particle equivalents and pipe diameters, respectively. Davies (1987) proposed a model for estimating the eddy fluctuation force (or the force of the turbulent eddies) acting on asymmetric fully suspended solid particle in liquid-solid two-phase pipe flow with the turbulent fluctuation velocity defined by:

$$v^1 = (0.16)^{1/3}\left(\frac{\eta_L}{\rho_L}\right)^{1/12} v_m^{0.92} d_P^{1/3} D^{-0.42} \quad [3\text{-}80]$$

The v_m is the minimum mean flow velocity required to suspend solid particles in a pipe flow and can be calculated as follows:

$$v_m = 1.08(1+\alpha\lambda_S)^{1.09}(1-\lambda_S)^{0.55n}\left(\frac{\eta_L}{\rho_L}\right)^{-0.09} d_P^{0.18}\left[2g\frac{\rho_S - \rho_L}{\rho_L}\right]^{0.54} D^{0.46} \quad [3\text{-}81]$$

Where α is a constant given by Davies (1987) to be 3.64. n is a constant which accounts for hindered settling. n is about 4 when $1 \prec \mathrm{Re}_P \prec 10$ and decreasing to 3 when $\mathrm{Re}_P \approx 100$. λ_S is the local input volume fraction of solid particles which is given as:

$$\lambda_S = \frac{q_S}{q_L + q_S} \quad [3\text{-}82]$$

D. Gravity force

The gravity force (F_{GS}) in liquid-solid two-phase and gas-liquid-solid three-phase pipe flow is calculated by:

$$F_{GS} = \frac{1}{6}\pi d_p^3 \rho_S \, g \qquad [3\text{-}83]$$

Where ρ_S is the particle density

E. Buoyancy force

The buoyancy force (F_{BS}) in gas-liquid-solid three-phase pipe flow can be written using the mixture model as follows:

$$F_{BS} = \frac{1}{6}\pi d_p^3 \rho_M \, g \qquad [3\text{-}84]$$

Where ρ_M is the mixture density defined by equation [3-54]

F. Frictional normal contact force

For the general case of a pipe sloping upward at an angle of θ to the horizontal, the time-averaged gravitational force acting down the slope due to the weight of the solid particle and the frictional resistance (particle-wall sliding friction) provided by the pipe invert is:

$$F_{WS} = \frac{1}{6}\pi d_p^3 \, g \, (\rho_M - \rho_S) \, \delta \qquad [3\text{-}85]$$

Both equations [3.83] and [3.84] have been lumped into equation [3.85]. The factor δ allows for the effect of the solid frictional resistance and normal contact force provided by the pipe inclination from horizontal to vertical section and it is given by:

$$\delta = \sin \theta + f_{SS} \cos \theta \qquad [3\text{-}86]$$

The solid particle suspension friction factor, f_{SS}, is an empirical quantity. A number of empirical correlations are available to determine the solid particle suspension friction factor, f_{SS}. However, there are far fewer correlations for solid particle suspension friction factor, f_{SS}, than there are for f_G and f_L. For this study, f_{SS}, is calculated using the empirical correlations proposed by Doron et. al. (1987) and Davies (1987) for Newtonian fluids:

Doron et. al. (1987)	**Davies (1987)**	
$f_{SS} = \dfrac{0.046}{\mathrm{Re}_{PS}^{0.2}}$	$f_{SS} = \dfrac{0.079}{\mathrm{Re}_{PS}^{0.25}}$	[3-87]

Where

$$\mathrm{Re}_{PS} = \frac{\rho_{SS}\, v_{Mix}\, D_H}{\mu_L} \qquad [3\text{-}88]$$

$$\rho_{SS} = \frac{\rho_G\, q_G + \rho_L\, q_L + \rho_S\, q_S}{q_G + q_L + q_S} \qquad [3\text{-}89]$$

$$v_{Mix} = \frac{1}{\rho_{SS}}\left(\lambda_G V_{SG}\rho_G + \lambda_L V_{SL}\rho_L + \lambda_S V_{SS}\rho_S\right) \qquad [3\text{-}90]$$

The hydraulic diameter occupied by the liquid (D_H) can be evaluated by:

$$D_H = \frac{4\,A_L}{S_L} \qquad [3\text{-}91]$$

Where

$$(S_L)^2 = (1 - H_G) \qquad [3\text{-}92a]$$

$$A_L = (1 - H_G)\,A \qquad [3\text{-}92b]$$

Kim and Ghajar (2006) related the effective wetted-perimeter to flow pattern factor by the expression given as:

$$(S_L)^2 = (1 - H_G) + H_G F_S^2 \qquad [3\text{-}93a]$$

$$F_S = \frac{2}{\pi}\tan^{-1}\left(\sqrt{\frac{\rho_G (V_G - V_L)^2}{g\,D(\rho_G - \rho_L)}}\right) \qquad [3\text{-}93b]$$

The F_S is only applicable for slip ratios ($k = \dfrac{V_G}{V_L}$), which is common in gas-liquid slug flow and represents the shape changes of the gas-liquid interface.

3. 2.4 Formulation of the Governing Equation

If we add the expressions for the hydrodynamic forces, Equation Equations [3-7] becomes:

$$\frac{(\pi d_p^3 \rho_S)}{6} V_S \frac{dV_S}{dx} = C_{DS} \rho_M \frac{d_p^2 \pi}{4} \frac{(V_M - V_S)^2}{2} + \frac{\pi}{4}(d_P)^2 \frac{\dot{m}_S}{A}(V_M - V_S) + \rho_L \frac{\pi}{4}(d_P)^2 (v^1)^2 \frac{1}{6}\pi d_p^3 g(\rho_M - \rho_S)\delta \quad [3\text{-}94]$$

Equation [3-94] could be re-arranged to:

$$\frac{dV_S}{dx} = \alpha V_S + \frac{1}{V_S}\left[\alpha V_M^2 + \beta V_M + J(v')^2 + \gamma\right] - 2\alpha V_M - \beta \quad [3\text{-}95]$$

Where

$$\alpha = \frac{3}{4}\frac{C_{DS}\rho_M}{d_P \rho_S} \quad [3\text{-}96]$$

$$\beta = \frac{3}{2}\frac{\dot{m}_S}{d_P \rho_S A} \quad [3\text{-}97]$$

$$\gamma = \frac{(\rho_M - \rho_S)}{\rho_S} g\,\delta \quad [3\text{-}98]$$

$$J = \frac{3}{2}\frac{\rho_L}{d_P \rho_S} \quad [3\text{-}99]$$

The ordinary differential equation [Equation 3-95] is initial value problem and must be solved for the dependent variable V_S (solid phase velocity distribution) subject to the following initial conditions:

$$V_S\big|_{X=0} = \frac{\dot{m}_S}{A\rho_S} \quad [3\text{-}100]$$

where $V_S\big|_{X=0}$ is the initial solid particle velocity. $\dot{m}_S$ is input solid-phase mass flow rate. A is the constant cross-sectional area of the wellbore or pipeline.

3.3 Hydraulic Model Development

The conservation equation of mass and momentum which govern each phase in gas-oil multiphase flow through vertical pipes are given by Azzopardi (2006):

Continuity Equation for the Gas phase

$$\frac{\partial}{\partial t}(\rho_G) + \frac{\partial}{\partial x}(\rho_G V_G) = 0 \qquad [3\text{-}101]$$

Continuity Equation for the Liquid phase

$$\frac{\partial}{\partial t}(\rho_L) + \frac{\partial}{\partial x}(\rho_L V_L) = 0 \qquad [3\text{-}102]$$

Momentum Equation for the Gas phase

$$\frac{\partial}{\partial t}(\rho_G V_G) + \frac{\partial}{\partial x}(\rho_G V_G^2) = -\frac{\partial P}{\partial x} - \frac{2 f_G \rho_G V_G^2}{D} - \rho_G g \sin\theta \qquad [3\text{-}103]$$

Momentum Equation for the Liquid phase

$$\frac{\partial}{\partial t}(\rho_L V_L) + \frac{\partial}{\partial x}(\rho_L V_L^2) = -\frac{\partial P}{\partial x} - \frac{2 f_L \rho_L V_L^2}{D} - \rho_L g \sin\theta \qquad [3\text{-}104]$$

Further macroscopic analytical treatment of equations [3-101 to 3-104] with steady state assumption gives:

$$\frac{d}{dx}(\rho_G V_G^2) = -\frac{dP}{dx} - \frac{2 f_G \rho_G V_G^2}{D} - \rho_G g \sin\theta \qquad [3\text{-}105]$$

$$\frac{d}{dx}(\rho_L V_L^2) = -\frac{dP}{dx} - \frac{2 f_L \rho_L V_L^2}{D} - \rho_L g \sin\theta \qquad [3\text{-}106]$$

Where x and t represent the spatial (axial) and time coordinate respectively. ρ_G and ρ_L represent the gas and liquid densities, respectively. The mean gas and liquid velocities are denoted by V_G and V_L.

The efflux terms in the momentum equations [3-105 and 3-106] can be expanded as follows:

$$\frac{d}{dx}(\rho_G V_G^2) = V_G \frac{d}{dx}(\rho_G V_G) + \rho_G V_G \frac{dV_G}{dx} \qquad [3\text{-}107]$$

$$\frac{d}{dx}\left(\rho_L V_L^2\right) = V_L \frac{d}{dx}\left(\rho_L V_L\right) + \rho_L V_L \frac{dV_L}{dx} \qquad [3\text{-}108]$$

At steady state condition, $\frac{d}{dx}\left(\rho_G V_G\right)$ and $\frac{d}{dx}\left(\rho_L V_L\right)$ become zero and hence equations [3-107 and 3-108] reduce to:

$$\frac{d}{dx}\left(\rho_G V_G^2\right) = \rho_G V_G \frac{dV_G}{dx} \qquad [3\text{-}109]$$

$$\frac{d}{dx}\left(\rho_L V_L^2\right) = \rho_L V_L \frac{dV_L}{dx} \qquad [3\text{-}110]$$

For a pipeline with constant cross-sectional area (A)

$$\left(\rho\, V\right)_{inlet} = \left(\rho\, V\right)_{outlet} = \frac{\dot{m}}{A} \qquad [3\text{-}111]$$

Then, equations [[3-108 and [3-106] become:

$$-\frac{dP}{dx} = \frac{\dot{m}_G}{A}\frac{dV_G}{dx} + \frac{2 f_G \rho_G V_G^2}{D} + \rho_G\, g \sin\theta \qquad [3\text{-}112a]$$

$$-\frac{dP}{dx} = \frac{\dot{m}_L}{A}\frac{dV_L}{dx} + \frac{2 f_L \rho_L V_L^2}{D} + \rho_L\, g \sin\theta \qquad [3\text{-}112b]$$

Due to large density difference between the disperse phase (gas) and the continuous phase (liquid), the mixture modelling concept is applicable. The mixture modelling approach is based on the principles of continuum mechanics for a single phase but generalized to the two gas and liquid inter-penetrable continua. This means the single density and velocity in the momentum equation is replaced by the gas-liquid mixture density and velocity. More so, additional term is introduced into the mixture momentum equation due to slip of the dispersed gas phase relative to the continuous liquid phase. The slip velocity is usually accounted for in form of an algebraic equation. The mixture model is derived in the literature applying various approaches (Ishii and Mishima, 1984)

Using the mixture model and assuming the pressure gradients due to $\frac{\dot{m}_G}{A}\frac{dV_G}{dx}$ and $\frac{\dot{m}_L}{A}\frac{dV_L}{dx}$ to be equal to the pressure gradients due to form drag (liquid-gas interaction) calculated by using the following expression (Azzopardi, 2006):

$$\frac{1}{8} C_{Db} [\rho_L (1-H_G) + \rho_G H_G] \frac{(V_G - V_L)^2}{L} \qquad [3\text{-}113]$$

Where C_{Db} is the bubble drag coefficient. Equations [3-112a and 3-112b] become:

$$-\frac{dP}{dx} = g [\rho_L (1-H_G) + \rho_G H_G] \sin\theta + \frac{2 f_T \rho_L (V_{SL} + V_{SG})^2}{D_H} +$$

$$\frac{1}{8} C_{Db} [\rho_L (1-H_G) + \rho_G H_G] \frac{(V_G - V_L)^2}{L} \qquad [3\text{-}114]$$

Where f_T is the mixture wall friction factor (see equations 3.122 to 3.125).

The pressure gradient due to interactions between the dispersed gas and solid phases, $\frac{M_S}{A}\frac{dV_S}{dx}$, is added to equation [3-114a] as follows:

$$-\frac{dP}{dx} = g [\rho_L (1-H_G) + \rho_G H_G] \sin\theta + \frac{2 f_T \rho_L (V_{SL} + V_{SG})^2}{D_H} +$$

$$\frac{1}{8} C_{Db} [\rho_L (1-H_G) + \rho_G H_G] \frac{(V_G - V_L)^2}{L} + \frac{\dot{m}_S}{A}\frac{dV_S}{dx} \qquad [3\text{-}115]$$

Where L is the length of the flow conduit.

The pressure drop in a computational cell is given as follows:

$$\Delta p_i = (\Delta p)_{el} + (\Delta p)_f + (\Delta p)_I \qquad [3\text{-}116]$$

According to Lain et. al. (1999), the bubble drag coefficient, C_{Db}, can be calculated as follows:

$$C_{Db} = \frac{16}{\mathrm{Re}_b} \qquad \text{If} \quad \mathrm{Re}_b \prec 1.5 \qquad [3\text{-}117]$$

$$C_{Db} = \frac{14.9}{\mathrm{Re}_b^{0.78}} \qquad \text{If} \quad 1.5 \prec \mathrm{Re}_b \prec 80 \qquad [3\text{-}118]$$

$$C_{Db} = \frac{48}{\mathrm{Re}_b}\ (1 - \frac{2.21}{\mathrm{Re}_b^{0.5}}) \qquad \text{If} \quad 80 \prec \mathrm{Re}_b \prec 700 \qquad [3\text{-}119]$$

Where

$$\mathrm{Re}_b = \frac{d_b (V_G - V_L)\rho_L}{\mu_L} \qquad [3\text{-}120]$$

d_b, the maximum bubble size in the flow region is given by Barnea et. al. (1982) as follows:

$$d_b = 0.725 + 4.1 H_G^{0.5} \left(\frac{\sigma}{\rho_L}\right)^{3/5} \left(\frac{2 f_T}{D}(V_{SL} + V_{SG})^2\right)^{-2/5} \qquad [3\text{-}121]$$

Equation [3-121] is only valid for a gas void fraction of less than 0.52

f_T is the mixture wall friction factor. For Newtonian laminar flow, the expression for the liquid-wall friction factor has been given by Hagen-Poisseulle:

$$f_T = \frac{16\mu}{\rho v D} = \frac{16}{N_{\mathrm{Re}t}} \qquad [3\text{-}122]$$

For laminar flows, that is,

$$N_{\mathrm{Re}t} = \frac{\rho_L (V_{SL} + V_{SG}) D_H}{\mu_L} \leq 2100 \qquad [3\text{-}123]$$

For turbulent flow, f_T can be obtained from the Moody diagram or calculated from one of the numerous empirical correlations that have been reported in the open literature.

For smooth pipe walls, f_T is determined from a Blasius-type equation (Wallis, 1969; Govier and Aziz, 1972) as follows:

$$f_T = \frac{0.046}{N_{\mathrm{Re}t}^{0.2}} \qquad [3\text{-}124a]$$

For the limitation given as follows:

$$300 \le N_{\mathrm{Re}t} \le 100{,}000 \qquad [3\text{-}124b]$$

For rough pipe walls, f_T is estimated using the Chen equation, which is an explicit approximation of the Colebrook equation (1939). The Chen equation for f_T calculation is given as follows:

$$\frac{1}{\sqrt{f_T}} = -4 \cdot \log_{10}\left(\frac{\varepsilon/D}{3.7065} - \frac{5.0452}{N_{\mathrm{Re}t}} \cdot \log_{10}\left(\frac{(\varepsilon/D)^{1.1098}}{2.8257} + \left(\frac{7.149}{N_{\mathrm{Re}t}}\right)^{0.8981}\right)\right) \qquad [3\text{-}125]$$

Where ε/D is the relative roughness ratio of the pipe

3.4 Numerical Solution of the Governing Equations

The fourth order Runge-Kutta explicit method was chosen to solve the basic governing equations [3-95 and 3-115] for the dependent variables, V_S and P. The Runge-Kutta explicit method is an ideal numerical scheme for solving ordinary differential equations because it is self-starting with good stability characteristic. The step-size can be changed as desired without any complications for higher-order schemes.

The fourth (4^{th}) order Runge-Kutta explicit method was applied to solve the governing equation and predicted local and axial distribution of the slip velocity, particle velocity, particle holdup, particle flux and mass rate.

The expression for the fourth order Runge-Kutta explicit method is given as follows:

$$\frac{dV_S}{dx} = \alpha V_S + \frac{1}{V_S}\left[\alpha V_M^2 + \beta V_M + J\left(v'\right)^2 + \gamma\right] - 2\,\alpha V_M - \beta \qquad [3\text{-}126]$$

$$f(x, V_S) = \alpha V_S + \frac{1}{V_S}\left[\alpha V_M^2 + \beta V_M + J\left(v'\right)^2 + \gamma\right] - 2\,\alpha V_M - \beta \qquad [3\text{-}127]$$

Where knowing the value of V_{Si}=$V_{S,0}$ at x_i, we can find the value of V_S=$V_{S\,i+1}$ at x_{i+1},

For the initial boundary conditions of:

i = 0, $x_0 = 0$ and $V_{S,0} = \frac{M_S}{A\rho_S}$

And given that $m = 20$ and $h = \frac{L}{20}$

$$k_1 = f(x_0, V_{S,0}) \quad [3\text{-}128a]$$

$$k_1 = \alpha V_S + \frac{1}{V_S}\left[\alpha V_M^2 + \beta V_M + J(v')^2 + \gamma\right] - 2\alpha V_M - \beta \quad [3\text{-}128b]$$

$$k_2 = f\left(x_0 + \frac{1}{2}h, V_{S,0} + \frac{1}{2}k_1 h\right) \quad [3\text{-}129a]$$

$$k_2 = \alpha V_S + \frac{1}{V_S}\left[\alpha V_M^2 + \beta V_M + J(v')^2 + \gamma\right] - 2\alpha V_M - \beta \quad [3\text{-}129b]$$

$$k_3 = f\left(x_0 + \frac{1}{2}h, V_{S,0} + \frac{1}{2}k_2 h\right) \quad [3\text{-}130a]$$

$$k_3 = \alpha V_S + \frac{1}{V_S}\left[\alpha V_M^2 + \beta V_M + J(v')^2 + \gamma\right] - 2\alpha V_M - \beta \quad [3\text{-}130b]$$

$$k_4 = f\left(x_0 + \frac{1}{2}h, V_{S,0} + \frac{1}{2}k_3 h\right) \quad [3\text{-}131a]$$

$$k_4 = \alpha V_S + \frac{1}{V_S}\left[\alpha V_M^2 + \beta V_M + J(v')^2 + \gamma\right] - 2\alpha V_M - \beta \quad [3\text{-}131b]$$

$$V_{S,1} = V_{S,0} + \frac{1}{6}(k_1 + 2k_2 + 2k_3 + k_4)h \quad [3\text{-}132]$$

Where, $V_{S,1} = V_S(x_0 + h)$ is the approximate sand particle velocity at $x_1 = x_0 + h$

For $i = 0$

$$x_1 = x_0 + h$$
$$V_{S,1} = V_S(x_0 + h) \quad [3\text{-}133]$$

$$k_1 = f(x_1, V_{S,1}) \quad [3\text{-}134a]$$

$$k_1 = \alpha V_S + \frac{1}{V_S}\left[\alpha V_M^2 + \beta V_M + J\left(v'\right)^2 + \gamma\right] - 2\,\alpha V_M - \beta \qquad [3\text{-}134b]$$

$$k_2 = f\left(x_1 + \frac{1}{2}h,\ V_{S,1} + \frac{1}{2}k_1 h\right) \qquad [3\text{-}135a]$$

$$k_2 = \alpha V_S + \frac{1}{V_S}\left[\alpha V_M^2 + \beta V_M + J\left(v'\right)^2 + \gamma\right] - 2\,\alpha V_M - \beta \qquad [3\text{-}135b]$$

$$k_3 = f\left(x_1 + \frac{1}{2}h,\ V_{S,1} + \frac{1}{2}k_2 h\right) \qquad [3\text{-}136a]$$

$$k_3 = \alpha V_S + \frac{1}{V_S}\left[\alpha V_M^2 + \beta V_M + J\left(v'\right)^2 + \gamma\right] - 2\,\alpha V_M - \beta \qquad [3\text{-}136b]$$

$$k_4 = f\left(x_1 + \frac{1}{2}h,\ V_{S,10} + \frac{1}{2}k_3 h\right) \qquad [3\text{-}137a]$$

$$k_4 = \alpha V_S + \frac{1}{V_S}\left[\alpha V_M^2 + \beta V_M + J\left(v'\right)^2 + \gamma\right] - 2\,\alpha V_M - \beta \qquad [3\text{-}137b]$$

$$V_{S,2} = V_{S,1} + \frac{1}{6}\left(k_1 + 2k_2 + 2k_3 + k_4\right)h \qquad [3\text{-}138]$$

Where, $V_{S,2}$ is the approximate sand particle velocity at $x_2 = x_1 + h$ and

$$V_{S,2} = V_S\left(x_1 + h\right) \qquad [3\text{-}139]$$

The model is also used to estimate solid phase holdup, mass rate and pressure drop distributions and optimal velocity to prevent sand bed development during gas-oil-sand multiphase production and transfer operations. The program assumes that friction factors, gas compressibility, gas and liquid density, gas and liquid viscosity is constant within the computational cell of the pipeline. With this the pressure, friction factors and gas compressibility, density and viscosity is updated after every convergence of solid phase settling velocity at specified (stepwise) computational cell of the pipeline.

3.5 Development of Particle Entrainment Model in Straight and Annuli Pipes

Sand particles can be transported along a gas-liquid multiphase pipe in the following ways: in suspension within the flow; as individual particles moving in continuous or intermittent contact with the pipe wall; as separated phase moving slowly in the viscous boundary layer at the pipe wall; as a surface layer of particle moving over a continuous deposit of stationary sand bed.

The entrainment mass rate of sand particles resting at the pipe wall or on continuous deposit of sand bed can be evaluated as follows:

$$\dot{M}_{SE} = E_F\,(1-\varphi_P)\,A_b \rho_P V_{DPL} \qquad [3\text{-}140]$$

Where

$\dot{M}_{SE}$ = entrainment mass rate (kg/s)
E_F = entrainment function (-)
φ_P = sand bed porosity (%)
ρ_P = entrained sand particle density (kg/m^3)
V_{DPL} = entrained sand particle settling velocity (m/s)
$A_b = \pi\left(r_e^2 - r_b^2\right)$ = cross-sectional area sand bed in contact with flow (m^2)
r_e = empty pipe radius (m)
r_b = sand bed height or thickness (m)

The expression for the entrainment function for bed sediment into suspension in open channel flow has been given by Garcia and Parker (1991) as follows:

$$E_F = \frac{A Z_U^5}{1 + \frac{A}{0.3} Z_U^5} \qquad [3\text{-}141]$$

$$A = 1.3\ x\ 10^{-7} \qquad [3\text{-}142]$$

$$Z_U = \frac{V_x^1}{V_{DPL}}\ \mathrm{Re}_{PD}^{0.6} \qquad [3\text{-}143]$$

$$V_x^1 = \frac{g^{0.5}}{C^1} V_{DMIX} \qquad [3\text{-}144]$$

$$V_{DMIX} = V_{SL} + V_{SG} \qquad [3\text{-}145]$$

$$C^1 = 18 \log\left(4\frac{r_b}{d_P}\right) \qquad [3\text{-}146]$$

$$\mathrm{Re}_{PD} = \frac{\left(g\,\rho_S\,d_P d_P\right)^{0.5}}{\mu_L} \qquad [3\text{-}147]$$

$$V_{DPL} = \frac{4\left(\rho_S / \rho_L - 1\right)\ g\ d_P}{3 C_{DS}} \qquad [3\text{-}148]$$

Where

d_P = entrained sand particle diameter (m)

μ_L = liquid viscosity (Pa.s)

g = acceleration due to gravity (m/s^2)

C_{DS} = drag coefficient (-)

The equivalent diameter, D_{Eq} and cross-sectional area, A_{Eq}, for annular pipe geometries are calculated as follows:

$$D_{Eq} = D_0 - D_i \qquad [3\text{-}149a]$$

$$A_{Eq} = \frac{\pi\left(D_0^2 - D_i^2\right)}{4} \qquad [3\text{-}149b]$$

Where

A_{Eq} = flow area (m^2)

D_{Eq} = equivalent diameter (m)

D_0 = internal diameter of production tubing or flowline (m)

D_0 = external diameter of wash pipe or coiled tubing (m)

3.6 Development of Optimization Model

The optimal design of oil-sand and gas-oil-sand multiphase production and transfer systems remains up to date a very challenging task due to poor knowledge of the hydraulic behaviour. A systematic study of these problems, especially utilizing fundamental approaches, is lacking.

The optimization model proposed in this study consists of an objective function described by minimizing the pressure drop and maximizing the monetary benefits of enhanced oil production rate, with the sand particle transport model acting as the constraints. Optimization problem is formulated by considering the minimum pressure drop as a decision (optimization) variable, while the system, operating and geometric variables may be considered as optimization parameters that should be evaluated using the sand transport simulation model. In addition to the simulation model, the objective function is subjected to a number of constraints, which are mainly imposed to narrow the search domain of the optimization. Such constraints help in reducing the processing time and avoid convergence to local minimums (Perry, Green and Maloney, 1998).

In this study, the flexibility of the visual basic programming environment has been effectively utilized to solve the proposed optimization problem. The approach followed is based on solving the mathematical model at every iteration of the optimization procedure. For each iteration, the parameters required by the objective function are obtained by solving the simulation model. The optimization model was solved using the Newton-Raphson search (optimization) algorithms.

The Newton-Raphson search (optimization) algorithms for optimal design and operation are formulated to predict the minimum total pressure drop per unit length along oil-sand and gas-oil-sand multiphase production wellbores and flowlines for a given system, operating and geometric parameters. The optimal design point is normally the one at which the total pressure drop per unit length becomes a minimum for a given mass flow rate of sand particles.

The objective function for the optimal design is described as follows:

$$\sum_{i=j}^{n} \Delta P_i = \min \qquad [3\text{-}150]$$

under restrictions:

$$\Delta P_i \geq \Delta P_{i,\min} \qquad [3\text{-}151a]$$

$$\Delta P_i \leq \Delta P_{i,\max} \qquad [3\text{-}150b]$$

The optimality is found between:

$$q_{i,\min} \langle q \langle q_{i,\max} \qquad [3\text{-}151]$$

Where

$q_{i,\min}$ = Minimal acceptable oil production rate

$q_{i,\max}$ = Maximum acceptable oil production rate

$q_{i,\max}$ / $q_{i,\min}$ = Upper and lower levels of search limits

3.7 Prediction Algorithm and Computer Package Development

3.7.1 Prediction algorithm development

The computational algorithms for the prediction of the local and axial distributions of particle velocity, holdup, flux and mass rate; local and axial distributions of slip (minimum/critical/depositional) velocity; local and axial distributions of pressure drop; optimal transport velocity are shown in Appendices B, C, D and E. The computational scheme solves the flow field in a stepwise fashion; namely knowing the upstream flow properties (inlet pressure, inlet temperature, superficial velocities, flow pattern, densities, viscosities, surface tensions, mass flow rates, input volumetric fractions, mean velocities) at point 1 of the computational cell and the downstream flow properties (inlet pressure, inlet temperature, superficial velocities, flow pattern, densities, viscosities, surface tensions, mass flow rates, input volumetric fractions, mean velocities) at point 2 of the computational cell are obtained using the gas-liquid-solid multiphase flow governing, closure and numerical equations.

I. Main algorithm for calculation of local and axial distributions of solid particle parameters (particle velocity, holdup, flux, mass rates) and slip velocity; pressure drop and optimal transport velocity.

The step-by-step computational procedure for the governing equations [3.95 and 3.115] is given as follows:

a. Select the flow geometry
b. Segment the flow conduit into different computational cells (length increments)
c. Assign entrance values (input initial system, operating and geometric parameters) to the first computational cell
d. If the inlet pressure value into the first computational cell is given then guess outlet pressure corresponding to the first computational cell
e. Calculate the average pressure in the first computational cell using the expression, $P_{ave} = P_1 + P_2 / 2$
f. Calculate the gas properties such as compressibility factor, density and viscosity based on the P_{ave} value
g. Determine flow pattern type and its specific multiphase flow parameters
h. Calculate the equivalent solid particle diameter
i. Estimate terminal velocity of the equivalent solid particle
j. Solve the governing equation using the Runge-Kutta fourth order algorithm described in detailed in Section 3.4 and calculate the solid particle velocity at the outlet of the computational cell [Equation 3.95]
k. Calculate the solid particle holdup at the outlet of the computational cell
l. Calculate the total pressure drop, Δp_i, in the first computational cell due to interactions between the dispersed phases (gas and solid) and the continuous phase for the computational cell using the governing equation [Equation 3.115]
m. Estimate the outlet pressure for the first computational cell using the calculated total pressure drop, Δp_i, in the first computational cell
n. Check for convergence between the calculated and guessed outlet pressure of the first computational cell) using the method described in Appendix A
o. Repeat the steps [d-n] until the calculated and guessed outlet pressure of the first computational converges within a reasonable error limit
p. Repeat steps [d-o] for the remaining fragments of pipe length until the end of the pipe length has arrived
q. If the end of the pipe length has arrived, calculate the total pressure drop and write output of the pressure drop , predicted solid particle velocity, solid particle holdup, solid particle flow rate and pressure distribution to excel and stop

II. Main algorithm for calculation of optimal flow rate at minimum pressure drop and/or prevent solid deposition in oil-gas-sand multiphase pipe flow systems

An iterative procedure is devised to calculate the optimal flow rate (optimal transport velocity) in vertical, inclined and horizontal pipes as follows:

a. Select the flow geometry
b. Guess the value of $V_{OPTIMAL}$
c. Segment the flow conduit into different computational cells (length increments)
d. Assign entrance values (input initial system, operating and geometric parameters) to the first computational cell
e. If the inlet pressure value into the first computational cell is given then guess outlet pressure corresponding to the first computational cell
f. Calculate the average pressure in the first computational cell using the expression, $P_{ave} = P_1 + P_2 / 2$
g. Calculate the gas properties such as compressibility factor, density and viscosity based on the P_{ave} value
h. Determine flow pattern type and its specific multiphase flow parameters
i. Calculate the equivalent solid particle diameter
j. Estimate terminal velocity of the equivalent solid particle
k. Solve the governing equation using the Runge-Kutta fourth order algorithm described in detailed in Section 3.4 and calculate the solid particle velocity at the outlet of the computational cell [Equation 3.95]
l. Calculate the solid particle holdup at the outlet of the computational cell
m. Calculate the total pressure drop, Δp_i, in the first computational cell due to interactions between the dispersed phases (gas and solid) and the continuous phase for the computational cell using the governing equation [Equation 3.115]
n. Estimate the outlet pressure for the first computational cell using the calculated total pressure drop, Δp_i, in the first computational cell
o. Check for convergence between the calculated and guessed outlet pressure of the first computational cell) using the method described in Appendix A
p. Repeat the steps [d-n] until the calculated and guessed outlet pressure of the first computational converges within a reasonable error limit
q. Repeat steps [d-o] for the remaining fragments of pipe length until the end of the pipe length has arrived
r. If the end of the pipe length has arrived, compare the previously calculated pressure drops to know if the minimum pressure drop has been reached within the preset minimum and maximum velocities preset using the Newton-Raphson iterative method
s. If the value calculated in step (r) is not a minimum pressure drop, then a new guess is made for $V_{OPTIMAL}$ and calculation goes back to step (b). This cycle of calculation is repeated until minimum pressure drop has been reached
t. If yes, write output the predicted optimal liquid velocity and the corresponding minimum solid velocity flow and pressure drop to excel and stop

3.7.2 Computer package development

Appendix B shows a conceptual formulation of the computer package while appendix C to E gives the details of the computational procedures developed using the version 7.0 of the Microsoft Visual Basic language. The whole program is made up of distinct but interrelated modules.

I. The input parameters module

This module is used to fill in all input parameters. These included three groups of parameters:

(a) fluid system parameters such as density, viscosity and surface tension; solid system parameters such as particle size, particle size distributions, particle density, particle shape

(b) operating parameters such as flowing bottomhole or wellhead pressure; flowing bottomhole or wellhead temperature; gas, liquid and mass rates; selection of the type of liquid-solid or gas-liquid-solid multiphase flow systems; selection of the type of operation systems (production without sand bed, production with sand bed, sand bed clean out)

(c) geometric parameters such as pipe diameter, pipe length, pipe roughness; selection of the type of flow geometry (vertical, inclined or horizontal); selection of the type of flow direction (bottomhole to wellhead, wellhead to separator, separator to wellhead, wellhead to bottomhole)

II. The flow characteristic and pattern module

This module is used to determine the following parameters:

(a) estimate pipe cross-sectional area
(b) estimate input rates and superficial velocities of the given phases
(c) estimate input volumetric fraction of each of the given phases
(d) calculate gas compressibility factor, gas density, gas viscosity
(e) predict the type of flow pattern
(f) calculate the in-situ gas phase holdup
(g) calculate the in-situ or actual velocities of the gas and liquid phases
(h) calculate the in-situ or actual gas-liquid mixture velocity
(i) calculate the superficial liquid-solid or gas-liquid-solid mixture velocity
(j) calculate the two-phase friction factor
(k) calculate the solid-phase friction factor

III. The sand transport module

This module is used to predict the following parameters:
(a) estimate the local and axial distributions of the sand particle velocity
(b) estimate the local and axial distributions of the sand particle holdup
(c) calculate the local and axial distributions of the sand particle flux
(d) calculate the local and axial distributions of the sand particle mass rate
(e) calculate the local and axial distributions of the slip velocity
(f) calculate the local and axial distributions of the pressure drop
(g) carry out sensitivity analysis of sand particle transport and hydraulic parameters with respect to system, operating and geometric variables

IV. The optimization module

This module is used to predict the following parameters:

(a) calculate the optimal transport velocity with respect to the given system, operating and geometric variables

V. Other modules

A number of subroutine modules were also built into the computer model. These modules include calculation of productivity index profile for horizontal wells with sand production effects and discharge pressure.

3.8 Conclusion

In this chapter, both the particle transport and hydraulic models were developed. A solution to the problem under investigation is obtained by a numerical integration of the set of ordinary differential equations using a fourth order Runge-Kutta method.

Newton-Raphson iteration method is used to determine the particle settling velocity and optimal transport velocity for both oil-sand and gas-oil-sand multiphase flows through production and transfer systems.

The implementation of the governing equation in a computer package is also carried out using Microsoft Visual Basic Language.

4 EXPERIMENTAL SET-UP AND PROCEDURES

4.1 Introduction

This chapter deals with the experimental investigation of hydrodynamic characteristics of solid particles in gas-liquid (air-water) two-phase pipe flow systems using high-speed charge coupled device (CCD) measuring systems. The CCD measuring technique offers a deep insight into the particle transport mechanisms which makes possible both qualitative observations and quantitative analysis of the hydrodynamic processes governing particle motion in three-phase pipe flow systems. The hydrodynamic parameters investigated include the sand particle velocity, hold-up and flux.

The experimental programme was mainly focussed on gas-liquid-solid three-phase pipe flow systems where particle solids deposition and bed development is prevented.

The measurements provided a dataset, which together with published experimental data was used to validate the particle transport model developed in Chapter Three.

4.2 Analytical Measurements

4.2.1 Sieving

A 300 gram sample of dry sand was sieved through a series of sieves with standard sieve meshes. The sample fraction remaining in each sieve is weighed on a mass balance. The fractions by mass are re-calculated to obtain a percentage of the mass of the entire sample.

4.2.2 Sedimentation tests

A 50 gram sample of sand particle was collected in a cup at the top of a sedimentation column filled with water. The cup was opened and the time which the sand particles need to reach the bottom of the sedimentation column was measured. The sedimentation column is of 0.05m internal diameter while the distance between the cup and sedimentation column bottom is 1.0m. The product of the distance between the cup and sedimentation column bottom over the travel time gives the particle settling velocity. The results of the settling velocities are given in Table 4.1. The main aim of this effort is to use the settling data to verify the accuracy of the particle settling velocity equation used in the proposed phenomenological model.

4.2.3

The gas pycnometer was switched on and allowed to attain the required temperature after ten to fifteen minutes. The helium gas bottle was opened and adjusted to 22.1psi. The empty sample chamber (cell) was weighed in an analytical mass balance having an accuracy of $\pm$ 0.0001g. The sand grains were charged into the sample chamber (cell) of known volume (7.52 cm^3). The sample chamber (cell) plus the sand grains were then weighed and the net weight of the grain obtained. The sand grains in the sample chamber (cell) were sealed by closing vent valve. The pressure in the chamber was built up (17psi) by allowing the helium gas to flow into the sample chamber (cell)

and later close the valve on the gas flowline. The stabilized pressure (P_2) within the sample chamber (cell) was measured during the sealing. An isolated reference sample chamber (cell) of known volume (5.22 cm^3) was pressurized and the stabilized pressure (P_1) read.

The volume of the particle grain in the sample chamber (V_P) is calculated as follows:

$$V_P = V_C - \left[V_R \left(\frac{P_1}{P_2} \right) - 1 \right] \qquad [4\text{-}1]$$

Where

V_P = volume of sand particle (cm^3)

V_C = volume of sample cell (cm^3)

V_R = reference volume (cm^3)

P_1 = pressure reading after pressurizing the reference volume (Psi)

P_2 = pressure reading after pressurizing the sample cell with the sand grain (Psi)

The particle density (ρ_S) is calculated as follows:

$$\rho_S = \frac{sand\ \ particle\, weight}{sand\ \ particle\, volume} = \frac{w_P}{V_P} \qquad [4\text{-}2]$$

4.2.4 Particle shape characterization

The equipment used for the particle shape characterization is the Autoscan U-1 scanning electron microscope (SEM). It consists of three main parts that are interconnected by several interfaces: a SEM, an energy-dispersive x-ray analyzer (EDX) and an image processing system (IPS). The IPS hosts the computer interface panel that controls all the pertinent functions of the SEM and EDX. The SEM system is capable of determining mineralogy, grain texture, pore structure and sphericity of the sand particle samples. Sand particle submitted for the SEM analysis is attached to a SEM specimen plug with epoxy and dried overnight in a low temperature drying oven. The sample is coated with gold, a conductive metal. The coating is required to obtain a clear image of the solid particle sample. The coated SEM sample is placed in the sample chamber in the electron optics column and evacuated to high vacuum. The SEM image is formed by an internally generated electron beam. The beam is created by heating a tungsten filament in the electrons gun until the filament emits electron. The electrons are accelerated through the electron optics column and focused through a series of electromagnetic lenses into a finely focused beam, which bombard the sample. The interaction between the primary electron beam and the sample produced various form of radiation, such as, secondary electron, backscatter electron, characteristics x-rays. The three-dimensional SEM image is formed from the collection of the secondary electron generated by the primary beam. The SEM image is then digitized and stored in the IPS memory. The SEM image gives polygonal contour information of the sand particle sample. The sand particle shape factor or sphericity and the particle size are estimated using the following equations:

$$\Psi = \frac{c}{\sqrt{ab}} \quad [4\text{-}3]$$

$$d_S = \sqrt[3]{abc} \quad [4\text{-}4]$$

Where Ψ is the solid particle shape factor which is between 0.3 and 0.95. The d_S is the sand particle diameter. For a geometrically irregular solid particle a, b and c are the length of the three main axes. The a and c the longest and shortest respectively. The results of some of the analytical measurements is given Table 4.1

Table 4-1: Physical properties of sand particles

S/N	Grain size range (µm)	Average particle size (µm)	Grain density (kg/m^3)	Grain Shape factor (-)	Settling velocity (m/s)	Particle Reynolds number (-)
1	300-425	320	2600	0.759	0.086	3.2
2	425-630	600	2600	0.712	0.118	33.6
3	630-800	750	2600	0.686	0.138	53.25
4	800-1,250	810	2600	0.647	0.169	62.37
5	1,250-1,600	1,300	2600	0.610	0.120	156

4.3 Flow Loop

A schematic diagram of the flow loop for flow visualization and particle transport in three-phase air-water-sand flow in a pipe is shown in Figure 4.1a. The test section is a transparent 0.04m internal diameter straight Plexiglas with a length to diameter ratio of 150. The pipe was made of carefully flanged, 2-m long, interchangeable section mounted on the bench by precision supports. The test section rests atop a carbon steel beam that is supported by a pivoting foot and a stationary foot that incorporates an hydraulic screw-jack. The beam is approximately 6.5m in length and can be inclined to an angle of approximately 90 degree from horizontal.

In order to develop various two-phase flow patterns (by controlling the flow rates of gas and liquid), a two-phase gas and liquid flow mixer was constructed (see Figure 4.1b). The mixer consisted of a perforated stainless steel tube (0.008 ID) inserted into the liquid stream by means of a tee and a compression fitting. A cylindrical sieving screen (2.0mm) was fitted to the end of the stainless steel tube. The two-phase flow leaving the mixer entered the calming section. The calming section served as a flow developing and turbulence reduction device. The flow pattern was observed in the test section at a length to diameter ratio of 100. Water, oil-free air and sand were used as liquid, gas and solid phases respectively. The water was supplied by a 6.0 KW stainless steel centrifugal slurry pump from a 0.4 m^3 stainless steel slurry tank into a 25 mm ID stainless steel pipe, where its flow rate was measured using an electromagnetic induction flow meter. The flow rate of the water was controlled by the rotational speed of the centrifugal pump.

Air was supplied via an industrial air compressor mounted inside the basement of the institute and isolated to reduce vibration unto the laboratory floor. The air passed through a coolant to adjust the temperature of the air to room temperature. The air was then filtered and condensate removed in a coalescing filter. The oil-free pressurized air was fed to the mixing chamber through the cylindrical sieving screen attached to the stainless steel pipe. The flow rate of the air was measured by an orifice meter and controlled by a needle valve. The solid phase used were black and white sand particles supplied by Erich Friedrich Handel GmbH, Germany with normal mean diameter of 0.6 mm and density of 2600 kg/m^3. The sand particles in the hopper were supplied to the water tank by an electric solid feeder and then fed with water into the test section by the centrifugal pump. The particle loading of the sand was controlled by the vibration frequency of the electromagnetic feeder.

The in-put sand loadings (concentrations) were estimated by sampling the loop several times during the water-sand and air-water-sand mixture flow experiments to determine the concentration of particle suspended in the water. Samples of transported sand particles were collected by discharging the air-water-sand mixture into a calibrated collecting cylindrical vessel through a three-way valve over a specific time period. When the three-way valve was opened air-water-sand mixture was discharged into collecting cylindrical vessel. Previous tests on dredging pipelines (Matousek, 1997) suggested that a sample collected this way would realistically represent all fractions in transported solids. The discharged solid particles collected were dried using hot-air dryer and weighed by an electronic mass balance. In addition, the discharged water was measured by a graduated cylinder and the input sand particle loading and mass rate determined. The uncertainty of sand particle loading measurement is within $\pm$ 0.002 kg/m^3. The sand particle input volumetric fraction (ϕ) is defined as a ratio of the input sand particle input volumetric flow rate and input water volumetric rate. The resulting fractional value is expressed in percentage. The mixture flows back into the slurry tank and the air vented to the atmosphere. The sand particle was separated from water by means of a sand screen filter and the water re-circulated into the system. Table 4.1 gives the physical properties of sand particles investigated in the study.

Three dimensional process flow diagrams of the experimental diagram are drawn using AutoCAD 2005 and presented in Figure 4.2 to 4.7 for vertical, inclined and horizontal viewing planes. Pipelines in the three dimensional process flow diagrams with red, yellow, green and light blue lines represent water-sand, compressed air, compressed air-water-sand and mixing chamber, respectively.

4.4 Digital high-speed charged coupled device (CCD) measuring system

The digital high-speed video system is based on the direct measurement of air-water-sand through a pipe by continuous imaging of the flow in the transparent Plexiglas pipe. The cylindrical pipe is enclosed in a rectangular shaped-box to improve the test section for better optical access and to avoid optical distortions The enclosed rectangular shaped box filled with water (the flowing liquid inside the pipe) in order to achieve index of refraction matching. Three dimensional schematics and digital pictures of some of the experimental set-up including the cylindrical pipe enclosed in the rectangular box are shown in Figures 4.8 to 4.13.

Films on the water-sand and air-water-sand multiphase flows were captured using a VDS Vosskühler high-speed HCC-1000 camera with mega-pixel resolutions and features for high-speed motion analysis. The VDS Vosskühler video system consists of a high-speed camera with in-built charge coupled device sensor, lens, AC supply, remote control panel, light source and transmission cable. The digital high-speed video system has a standard shooting speed of 1,000 frames per second with 1280 x 1024 pixels. The test pipe was illuminated by 1000 Watt halogen lamp. The high speed camera was mounted and fixed at right angle to the flow. The films were recorded in the grey format and the video signal from the high-speed camera was sent to a 17 inches high resolution computer monitor. Since the refractive indices of air, water and glass are 1.0, 1.33 and 1.52 at wavelength 589.3nm, respectively, the refraction and reflection of light occur at the interface. If the incident angle of light to an interface is smaller than the critical angle determined by Snell's law, the light is partly reflected at the interface and partly passes through it. However, when the incident angle of light is equal or larger than the critical angle, total reflection occurs. Such complicated light path results in distortion of images. To minimize the effect of light refraction and/or reflection, the high speed camera was calibrated (camera mis-alignment and lens) and the positions of light source were carefully chosen by trial and error method. In processing the images, a scale or magnification factor is determined according to the outside diameter (D = 0.045m) of the test pipe.

The scale or magnification factor is defined as:

$$F_{scale} = \frac{pipe\ outside\ diameter\ in\ the\ image}{real\ pipe\ outside\ diameter} \qquad [4\text{-}5]$$

F_{scale} is a very important parameter in order to obtain the real information from the image processing. The features of the high speed video recording camera system used are given in Table 4.2.

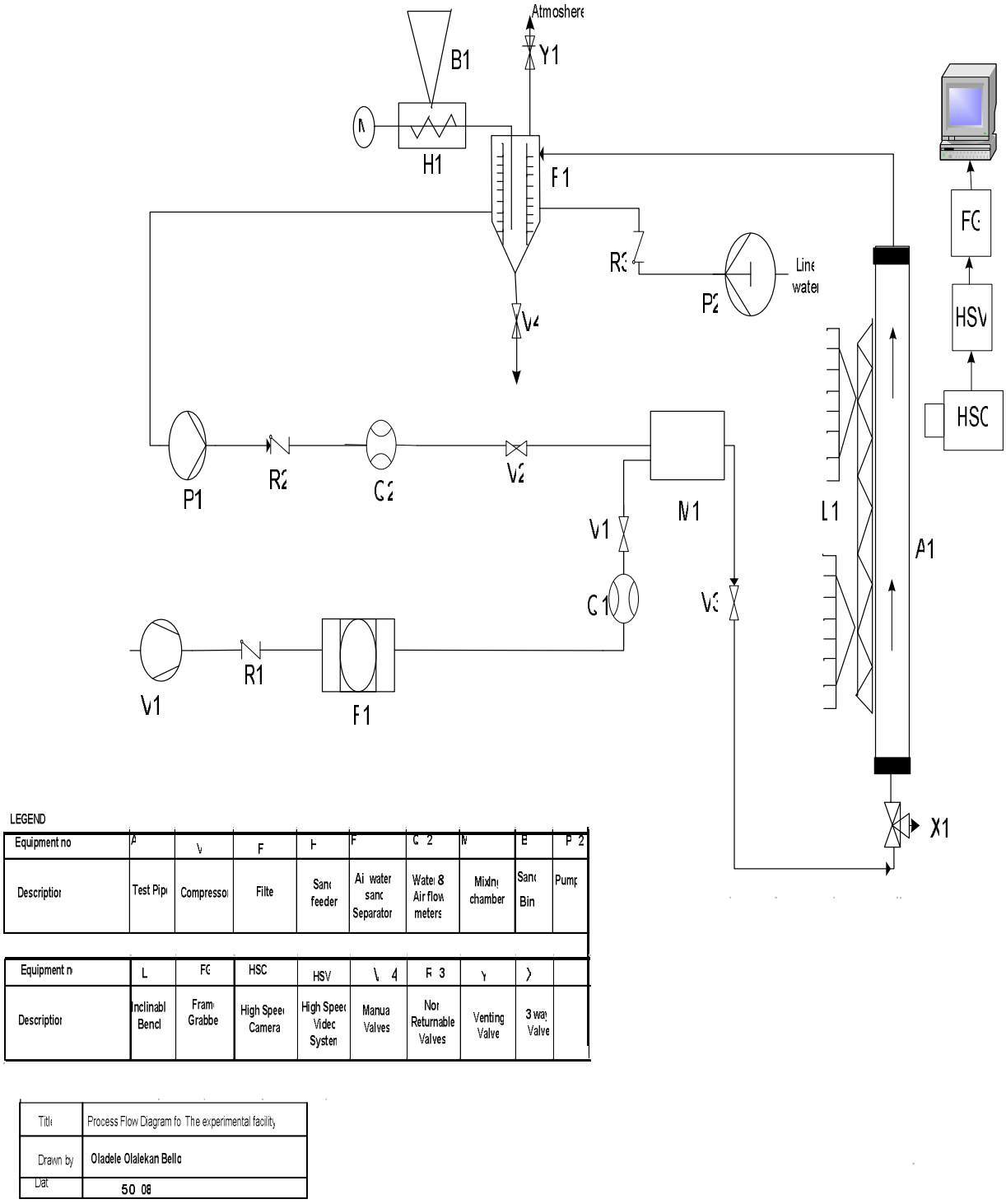

Figure 4-1a: Schematic diagram of the experimental set-up

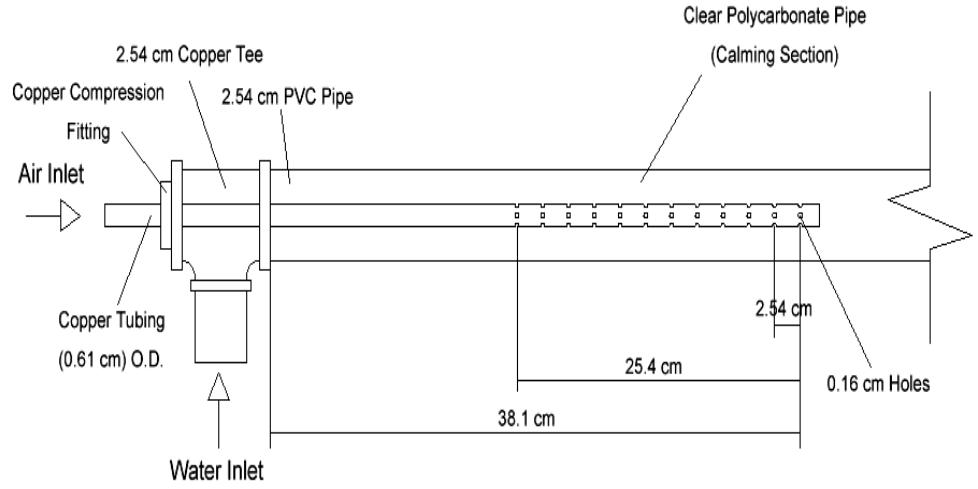

Figure 4-1b: Schematic diagram of the mixing chamber

LEGEND

A1	=	Test pipe	V1	=	Compressor
F1	=	Filter	H1	=	Sand Feeder
Q1-2	=	Water and Air Flow Meter (Liquid)	LI	=	Inclinable Bench
V1-4	=	Manual valve	Y1	=	Venting valve
X1	=	Three-way valve	V4	=	Non-returnable valve
B1	=	Sand bin	M1	=	Mixing chamber
PI-2	=	Pumps	PT	=	Pressure Taps
DP	=	Differential Pressure Transducer	AD	=	AD Converter
DB	=	Data Acquisition System	HSC	=	High Speed Camera
HSV	=	High Speed Video System	FG	=	Frame Grabber
PC1	=	Personal Computer for Imaging Acquisition			
PC2	=	Personal Computer for Differential Pressure Fluctuation Acquisition			

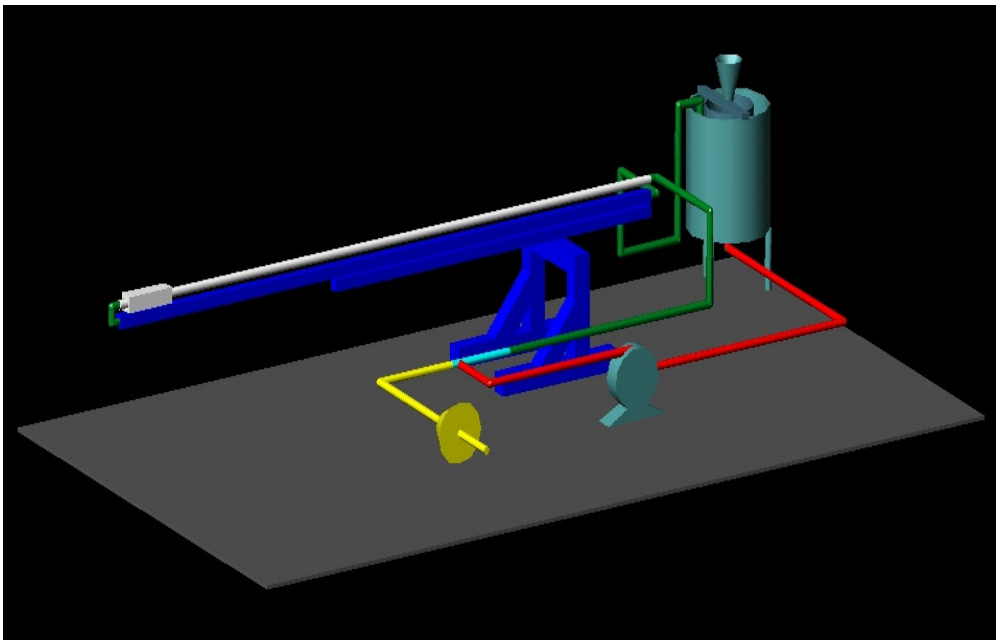

Figure 4-2: Left view of the 3-D experimental set-up (horizontal plane)

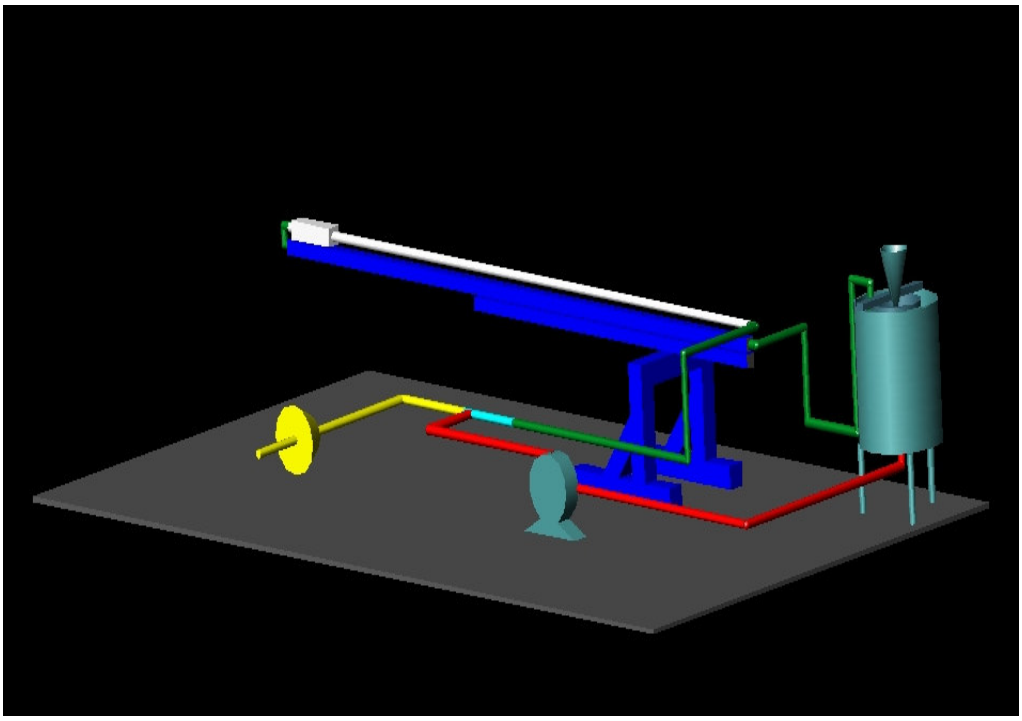

Figure 4-3: Right view of the 3-D experimental set-up (horizontal plane)

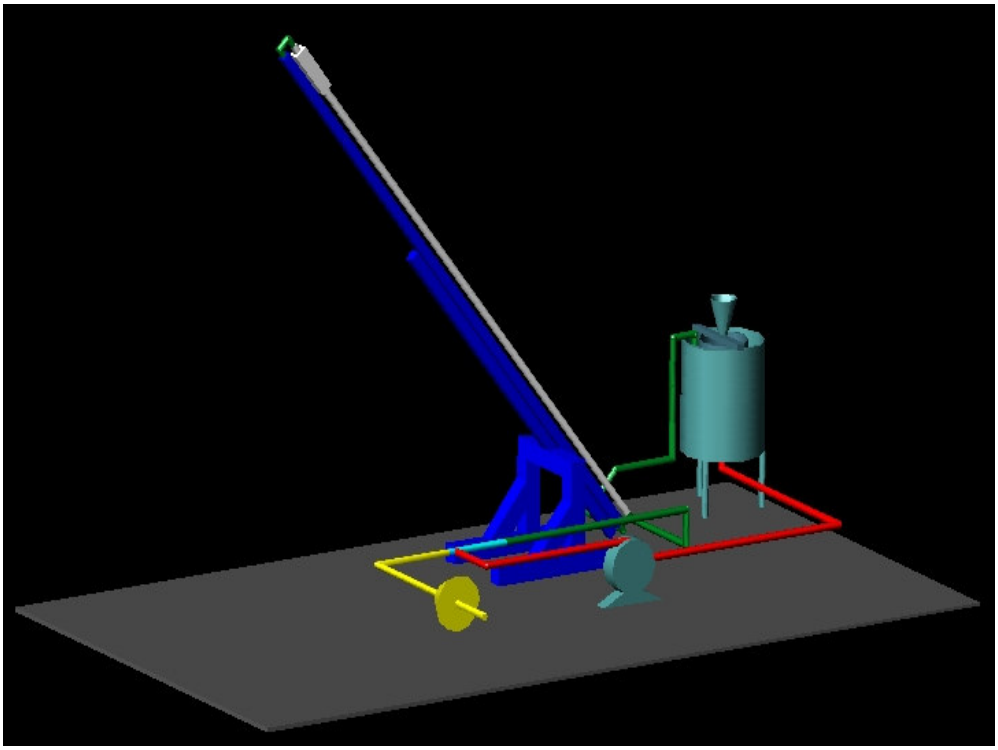

Figure 4-4: Right view of the 3-D experimental set-up (inclined plane)

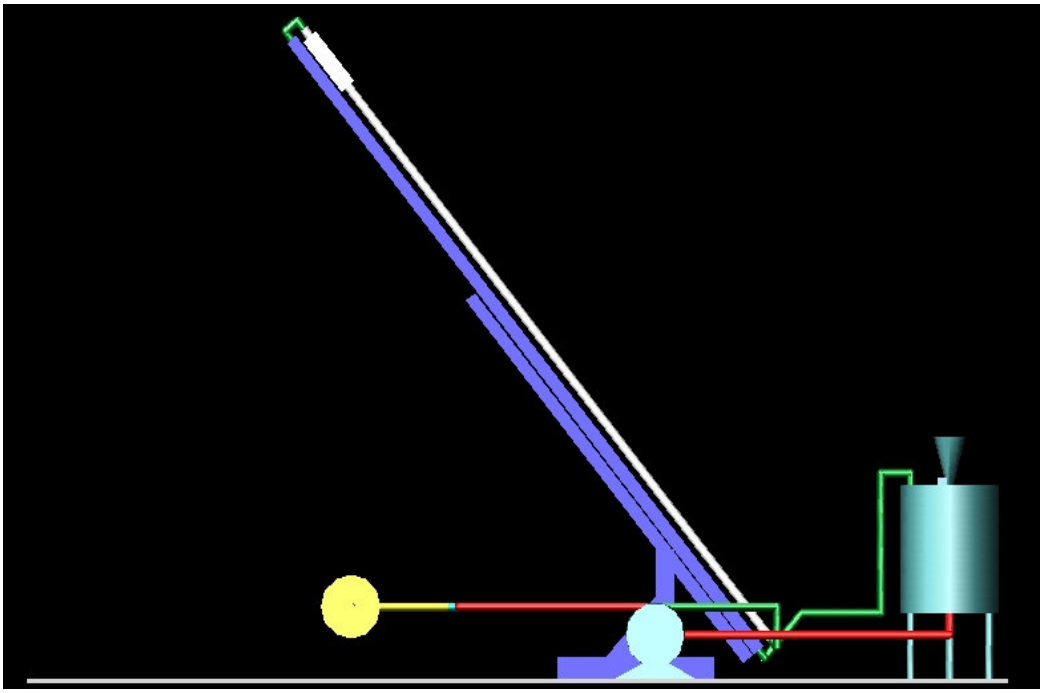

Figure 4-5: Principal view of the 3-D experimental set-up (inclined plane)

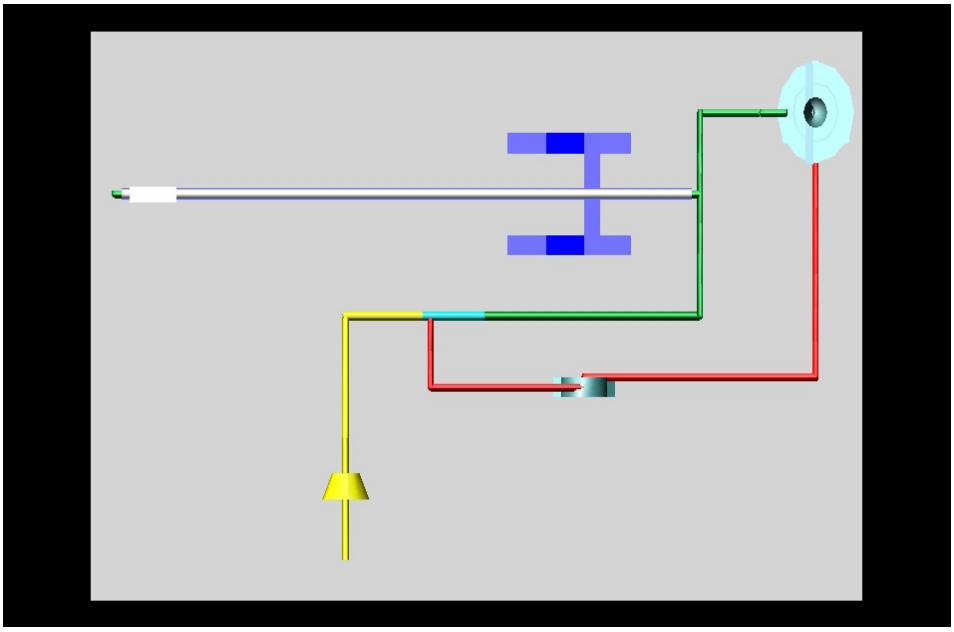

Figure 4-6: Top view of the 3-D experimental set-up (inclined plane)

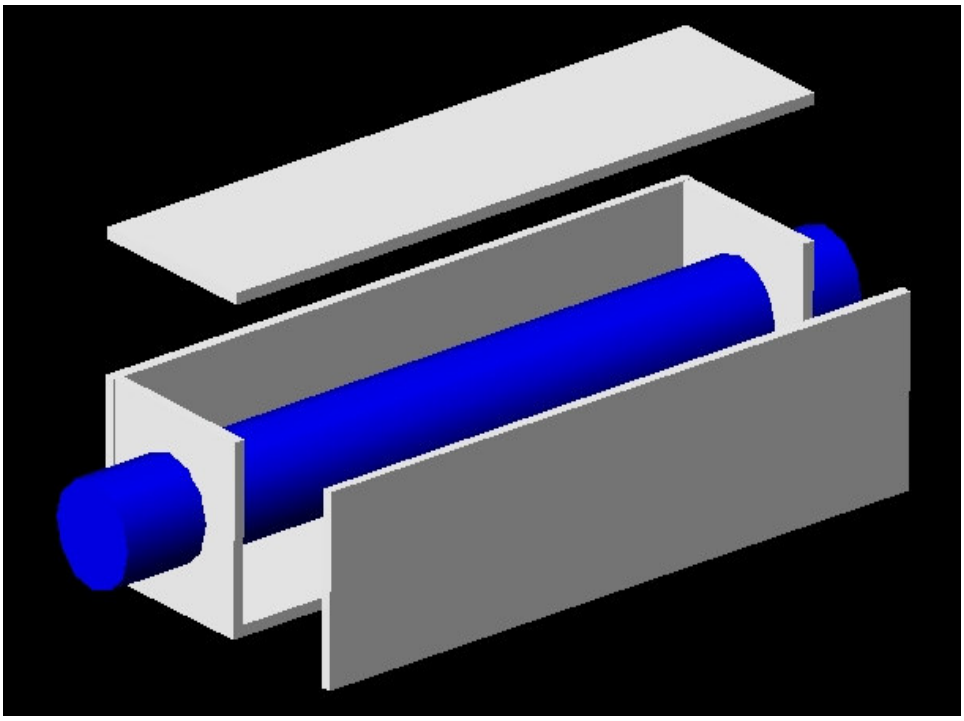

Figure 4-7: 3-D schematic diagram of the measurement zone in the test section

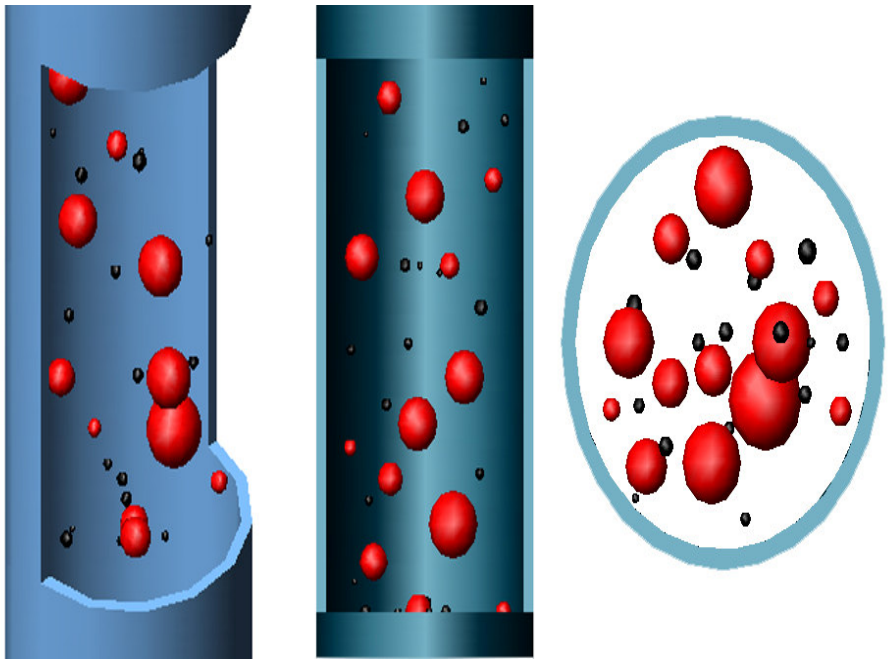

Figure 4-8: 3-D schematic visualization of the air-water-sand flow through the measurement zone

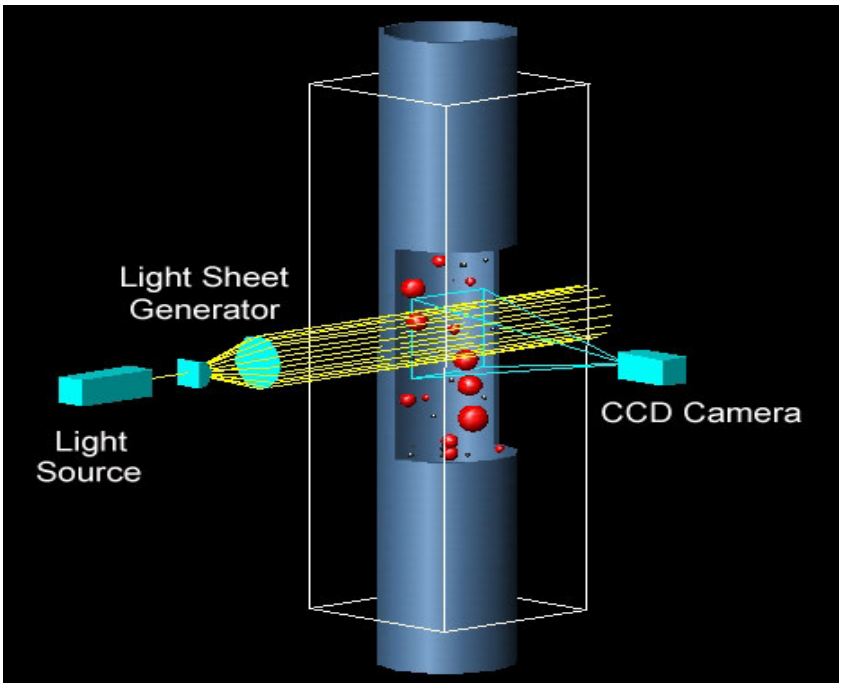

Figure 4-9: 3-D schematic diagram of the CCD measuring system (right view)

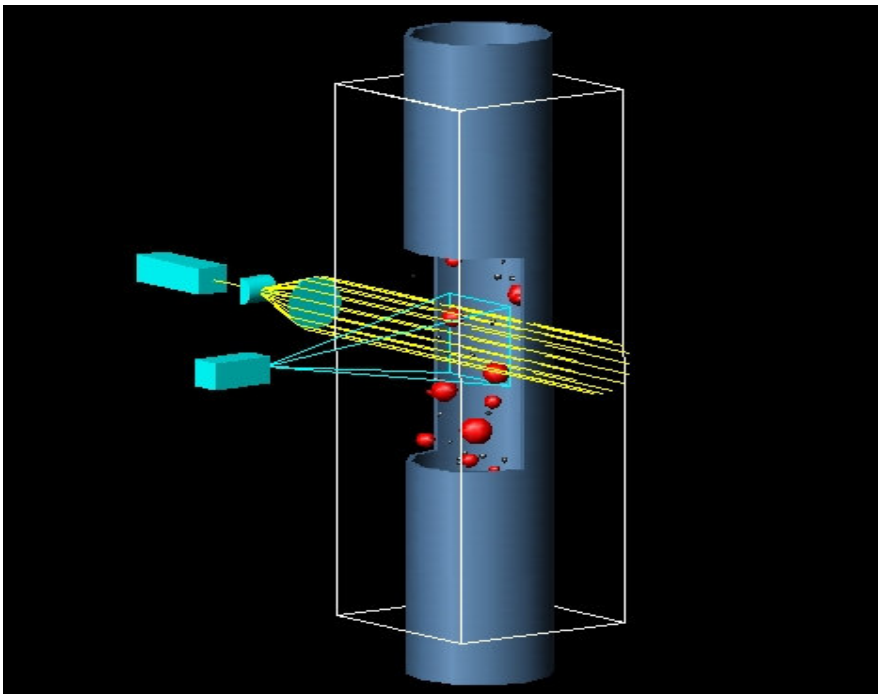

Figure 4-10: 3-D schematic diagram of the CCD measuring system (left view)

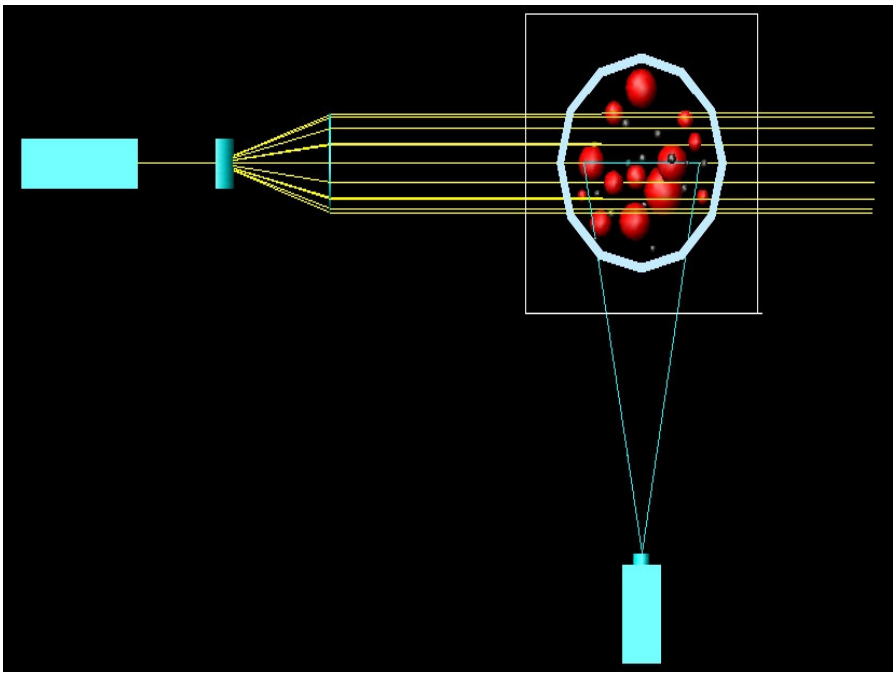

Figure 4-11: 3-D schematic diagram of the CCD measuring system (top view)

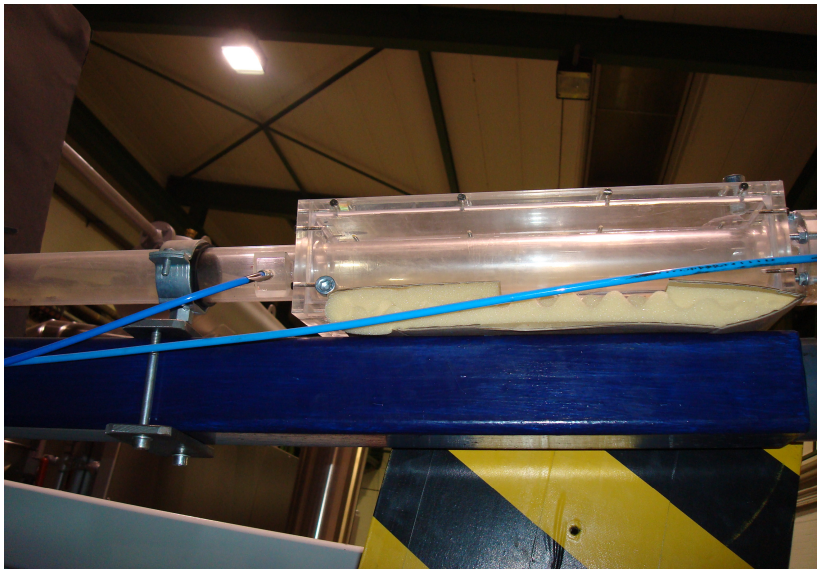

Figure 4-12: Digital picture of the test pipe enclosed in a rectangular box

Figure 4-13: Digital picture of the ITE multiphase flow loop

Table 4-2: Features of the VDS Vosskühler high-speed CMOS HCC-1000 system used

Image Resolution	Up to 1024 x 1024
Frame Rate	923 fps
Number of Images	128 images
Pixel size	10 x 10-6m x 10 x 10-6m
Active sensor size	2.56 (H) mm x 2.56 (V) mm
Sensor array	Linear CMOS-Sensor
Memory	512 Mbytes
Shutter	Global electronic shutter with exposure time from 2ms
Particle	Pixel coordinates of the particle position are always displayed on the screen
Digital Output	8-bit (mono)
Computer control	RS-232 interface
Output frame rate	Up to 4000 frames per second
Output Pixel Clock	33 MHz
Power Supply	12 V DC, 500 mA
Playback rates	User selectable variable play-back
Lens Mount	Standard C - mount
Camera Control Software	Matrix Vision Frame grabber
Images recording file format	Bmp, Jpeg, Tiff and Avi
Analysis features	Microsoft excel compatible features includes linear and angular velocity measurement. Track multiple points over multiple frames.

4.5 Estimation of Local and Global Sand Particle Velocity

In recording the velocity of the sand particles in a water-sand and air-water-sand multiphase pipe flow systems, some of the particles were painted red using a commercial dye for cloth. In the video image processing, such coloured particles were picked up and tracked. No appreciable difference between the motion of the coloured

and the normal particles was seen. The displacement of the sand particles and the time evolution of particle position in the air-water-sand multiphase pipe flow system were measured in a series of successive video images and the instantaneous velocity and the total average velocity of the particle was estimated. As shown in Figure 4.10, one tracing particle moves from point A to point B, the displacement of this particle in x-axis and y-axis is Δx and Δy, respectively. The velocities of the particle can be determined from:

$$V_{SX} = \frac{1}{F_{Scale}} \frac{\Delta x}{\Delta Frames\, \tau} \qquad [4\text{-}6]$$

Where τ is the exposure time or the time interval between two continuous frames which is derived from the shutter speed. $\Delta Frame$ is the total number of frames. Δx_i is the displacements measured in terms of the images. This study only investigated the local sand particle velocity in the axial direction. The global sand particle velocity is estimated as the ensemble cross-sectionally averaged value of the local sand particle velocity distribution over the entire measured points along the pipe. Local sand particle velocities were also estimated using the Chemical 2.0 image analysis software developed by Liu, et. al. (2006). The CCD measuring technique utilizes particle tracking algorithm to determine the velocity fields. This mode of operation is commonly referred to as particle tracking velocimetry (PTV).

4.6 Estimation of Local and Global Sand Particle Holdup

The local sand particle holdup is defined as the ratio of the solid flow cross-sectional area to the imaged flow viewing area. To calculate the local sand particle holdup in the air-water-sand three-phase pipe flow system, the particle cross-sectional area was calculated assuming the particles to be approximately spherical in shape and multiplied with the counted numbers of solid particles in the particular flow image. Next, the area of the 2-dimensional rectangular flow image was calculated. The local sand particle holdup of any acquired 2-dimensional flow image can be calculated as follows:

$$A_S = \frac{\pi d_P^2}{4} N \qquad [4\text{-}7]$$

$$A_I = \frac{[Width][Height]}{F_{Scale}} \qquad [4\text{-}8]$$

$$H_S = \frac{A_S}{A_I} \qquad [4\text{-}9]$$

Local sand particle holdups were also estimated using the Chemical 2.0 image analysis software developed by Liu, et. al. (2006). The Chemical 2.0 image analysis software discriminates between sand particles and gas bubbles based on the size of the recorded image of the objects. A full description of the Chemical 2.0 image analysis software can be found in Liu et. al. (2006). The global sand particle holdup is

estimated as the ensemble cross-sectionally-averaged value of the local sand particle holdup distribution over the entire measured points along the pipe.

4.7 Particle image velocimetry (PIV) set-up and measurement

4.7.1 PIV system set-up and description

A commercially available PIV from LaVision GmbH was used to measure the flow field at several cross-sectional stations along the length of the pipe. It consisted of a dual-cavity 50 mJ Nd:Yag, dual-frame charged couple device (CCD) camera, a three-dimensional traverse system and a commercial image software (DaVis) running on a personal computer for system control, data management and data pre- and post-analysis. The CCD camera is mounted on a 3-D traverse and has its focal axis perpendicular to the plane of the laser sheet. The exposure time of the CCD camera was controlled by an electronic shutter installed in the CCD camera. A photograph of the PIV system set-up is shown in Figure 4.4. The light source is a frequency double pulse Nd:Yag laser giving pulse of green (532 nm wavelength) coloured beams, pulsed at a frequency of 15Hz and with a pulse duration of 6ns. Light sheet forming optics mounted at the exit portal of the laser system generated a thin, focusable light sheet by means of a series of lenses. The laser light went through a prism, a cylindrical lens, a spherical lens and another cylindrical lens before forming a light sheet focused along the center-plane of the pipe. The spatial location of the illumination system was fixed during all the tests. Visualization tests and measurements were performed under varied steady state water, water + air and air + water + sand particle flow conditions. The test section was enclosed in a rectangular box filled with water to obtain images without any optical distortion. Testing under single-phase water flow conditions involved using glass hollow spheres as tracer particles. The average diameter of the sphere was 2.0×10^{-6}m with a density of 1120 kg/m3. This test was used to provide a baseline flow field characteristics within the pipe flow system. The recorded images were analyzed using the commercial image software DaVis provided by LaVision. Velocity profiles were formed from a number of multi-point wise measurements of local velocities in the horizontal and vertical directions. From the instantaneous velocities, both averaged (mean) and root mean squared velocities (RMS) were calculated. Significant physical phenomena regarding the water-air-sand flow structure was explored.

4.7.2 PIV image measurement and analysis

The basis relation of displacement divided by time to yield velocity is the fundamental principle of the PIV technique. The displacement information is provided by seeding of tracer or sand particles, which were suspended in the water or water-air pipe flow system. Tracer or sand particle suspended in the water or water-air pipe flow system were illuminated using the thin laser sheet, which was pulsed to freeze the particle motion. The light scattered from the particles was recorded by from a direction normal to the light sheet, at two instances in time using a high speed CCD camera. The two sequential digital images were then sub-sampled at particular areas via a prescribed interrogation window, and a spatial cross-correlation was performed using a fast fourier transfer (FFT) analysis. The separation time between the light pulses was selected so as to have particles displace several pixels within the interrogation area, at most common remain common to both images. A high cross-correlation value was observed where many particle images match up with their

corresponding spatial partners and this is considered to represent best match of particle images between the sequential recordings. The displacement vector of cross-correlation peak from the center (origin) of the two-dimensional interrogative window denotes the average distance traveled by the particles within the interrogative area. Accurate estimation of the displacement vector to sub-pixel resolution was performed by locally fitting the two-dimensional array of correlation values in the vicinity of the peak. The absolute displacement vector was then calculated from a calibration of the magnification factor between the pixel domain of the digital recording device and the physical field of view. Finally, division of the displacement vector, determined for each interrogation area along the entire pixel domain by the time separation between the two sequential laser pulses yields the velocity vector field in the physical area under investigation.

Data records of 200 pair images were collected under varied three-phase water-air-sand flow conditions. An interrogation area of 32 x 32 pixels was chosen for processing each pair of images, which yielded a spatial resolution of 0.65 mm^2. It was found that this interrogation area size gave the best performance in terms of signal-to-noise without significant compromise in spatial resolution and correlation performance due to particle drop-out as a result of out of plane motion. Calibration of the field of view was performed by using the diameter of the test section pipe cross-section, imaged at focus of the camera, to determine the magnification factor. Digital pictures of the PIV measuring system together with other accessories is shown in Figure 4.14.

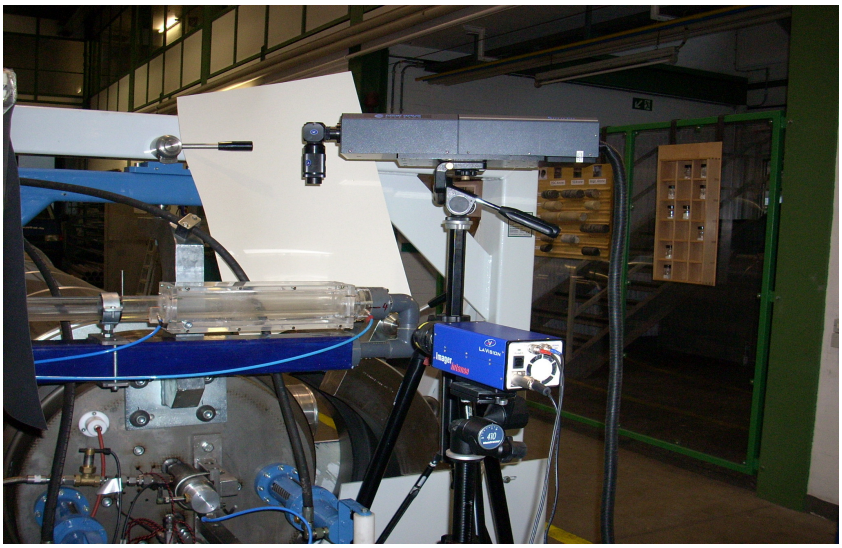

Figure 4-14: Photograph of the PIV visualization and measurement system

4.8 Measurement error

The measurement error is reduced by averaging six times measurement of local particle velocity and holdup for the given operating and system parameters.

4.9 Conclusion

The experimental facility mimics the gas-oil-sand multiphase flows in production and transfer systems under different system, operating and geometric conditions. The CCD measuring techniques were successfully utilized to investigate varied the flow structures and solid particle transport characteristics in the three-phase pipe flow systems which result in a better understanding of the effects of gas-liquid multiphase flow phenomena on the local and global solid particle transport characteristics. The series of experiments also provide a useful well-defined data set against which the present and existing models for predicting sand particle transport in gas-oil multiphase wellbore, flowline, riser and pipeline systems can be validated.

The two CCD measuring techniques, particle image velocimtery (PIV) and particle tracking velocimetry (PTV) are analyzing methods for image pairs in a seeded flow field with known temporal separation. The distance between the particle positions in the two images divided by the time separation yields the local velocity information. While the PTV method directly track single particle, the PIV method uses the cross-correlation function to estimate the displacement of a particle ensemble on two separate frames. The PTV method operates at low seeding densities (typically a few particles per mm^2 viewed) while the PIV functions using a moderately to high seeding densities. The possible accuracy of the PTV algorithm is given by the accuracy of the detection of particle position whereas the PIV method is limited to by the accuracy of locating the correlation peak.

The results are shown as a function of axial length for various system, operating and geometric conditions.

5 EXPERIMENTAL RESULTS AND MODEL VALIDATION

5.1 Introduction

In this chapter the results of the experimental investigation are presented. Special attention is paid to the theoretical analysis of the observed phenomenon. Moreover, the validity of the proposed model together with the other existing sand transport predictive methods for three-phase production and well systems is examined by comparing the predicted with the measured sand transport data. Data sets obtained from three independent sources (open literature) and present study were used for the model validation and comparative study. Statistical analysis of the measured and predicted values is also evaluated and reported.

In this study, the flow pattern identification for the different system, operating and geometric experimental conditions used was based on visual observation and video analysis of flow images. Although there are other various flow pattern interpretation (traditional and modern) methods but no generalized procedure exists at present. It is also fair to say that the gas injection methods have formidable effects on flow pattern formation and evolution. The porous pipe method was used in this study even though perforation pitch and nozzle techniques also exist.

5.2 Sand particle velocity

5.2.1 Axial distribution of solid phase velocity

Figure 5.1 shows experimental results for the axial velocity for the solid phase in horizontal three-phase air-water-sand pipe flow system determined according to section 4.5. Intermittent flows (includes elongated bubble and slug flows) were observed under this operating conditions. As can be seen, the local solid phase velocity increases as the superficial liquid velocity increases. The increment can be explained based on the flow visualization where the increase of in-situ liquid velocity enhances the turbulence of the flow and the energy exchange between liquid micro-liquid units. Part of the gas bubble kinetic energy absorbed in the liquid phase is transferred to the suspended sand particle resulting in non-uniform velocity distribution. However, the significance of the effect becomes less as the superficial liquid velocity increases and a degree of permanent flow equilibrium was attained.

The strong slug turbulence is favorable to for the fragmentation of gas bubbles and decrease of the bubble size. Due to high buoyancy, these small gas bubbles gather near the central axis of the pipe, which results in the fluctuation of the liquid velocity gradient and increase in non-uniformity of the axial sand particle distribution.

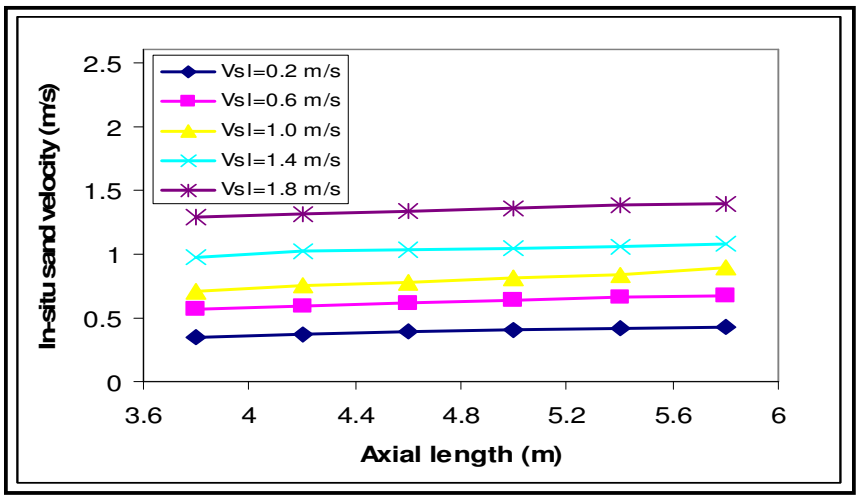

Figure 5-1: In-situ velocity profiles of sand particle as a function of pipe length and different superficial liquid velocities (d_P = 0.0003m, V_{SG} = 0.4m/s and ¢ = 0.4%)

The effect of superficial gas velocity, V_{SG} on the axial distribution of local sand particle velocity has also been studied experimentally, as shown in Figure 5.2, illustrating the remarkable influence of superficial gas velocity on sand particle velocity and motion. The uniformity of the sand particle velocity distribution in the axial direction of the pipe flow is decreased. This fluctuation may be associated with the characteristics of the observed intermittent flow patterns. The increase of gas velocity leads to more bubbles, which initiate stronger turbulence and vortex formation in the pipe flow. With a further increase in the gas velocity, the lateral migration distance of the gas bubble to the central axis of the pipe and the size of vortex increases. These vortices would create a mixing effect which produces high flow instability. This is well recognized phenomenon observed among previous investigators such as Gopal and Jepson (1997) and Sakaguchi et. al. (1997).

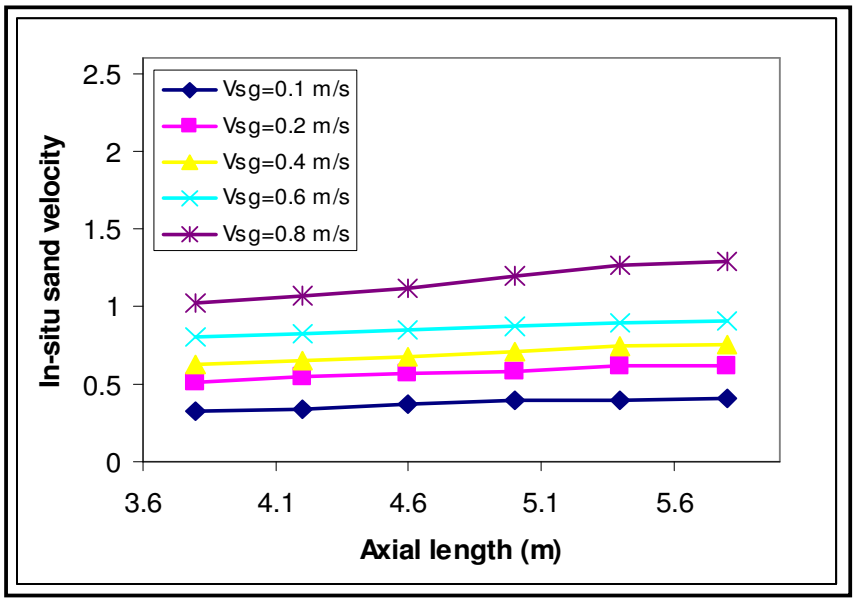

Figure 5-2: In-situ velocity profiles of sand particle as a function of pipe length and different superficial gas velocities (d_P = 0.0003m, V_{SL} =1.2m/s and ¢ = 0.6%)

The sand loading is one of the most important features of a three-phase gas-liquid-solid pipe flow systems. The existence of sand particles can enhance the disintegration of gas bubbles and the turbulence of the liquid phase both unfavourable to uniform sand velocity distribution (Sakaguchi et. al., 1992; Kundakovic and Vunjak-Novaakovie, 1995). The variation of sand loading has an apparent effect on the axial distribution of the local sand velocity.

Figure 5.3 shows the effect of sand loading in the horizontal three-phase air-water-sand slug pipe flow on the axial distribution of the local sand velocity. The notable feature of the plot is the slight decrease in the particle velocity with increased in sand loading rates. Apparently, particle-particle interactions increases at higher loading rates lead to increased momentum transfer to the wall and lower local average particle velocities. Moreover, the decrease can also be explained based on the turbulence dampening effect and the subsequent decrease in liquid velocity. This obviously makes the local sand velocity distribution in the axial direction to be less uniform.

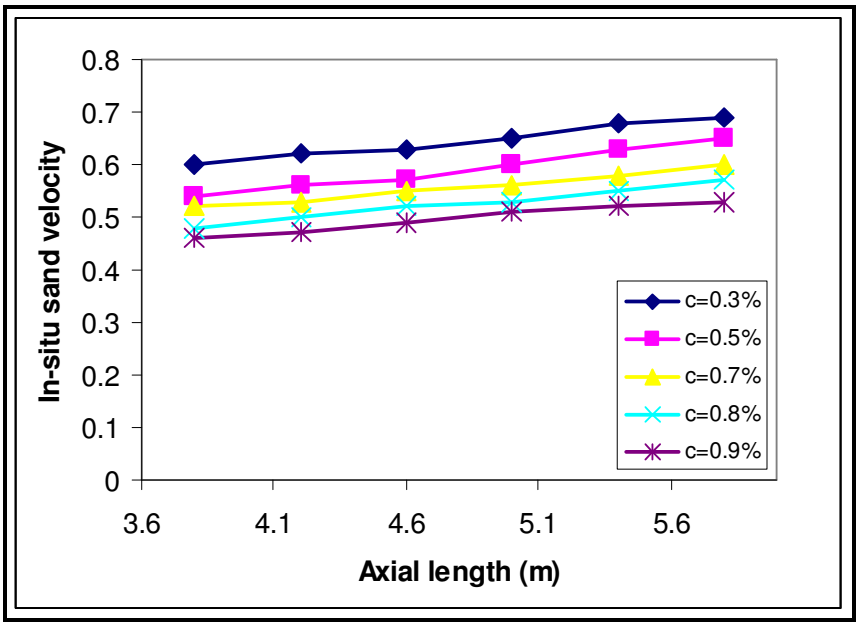

Figure 5-3: In-situ velocity profiles of sand particle as a function of pipe length and different sand particle volumes (d_P = 0.0003m, V_{SL} = 0.6m/s and V_{SG} = 0.5m/s)

5.2.2 Axial distribution of solid velocity in different flow regimes

Figure 5.4 shows the results of the experiments on the effects of flow patterns on in-situ sand particle velocity profiles in horizontal three-phase air-water-sand pipe flow systems. The high enhancing effects of the slug flow operating conditions could be observed as compared to the elongated bubble and stratified flow regimes. Obviously, the high mixing characteristics seems to be responsible for the in-situ sand particle velocity enhancement in the three-phase pipe flow systems.

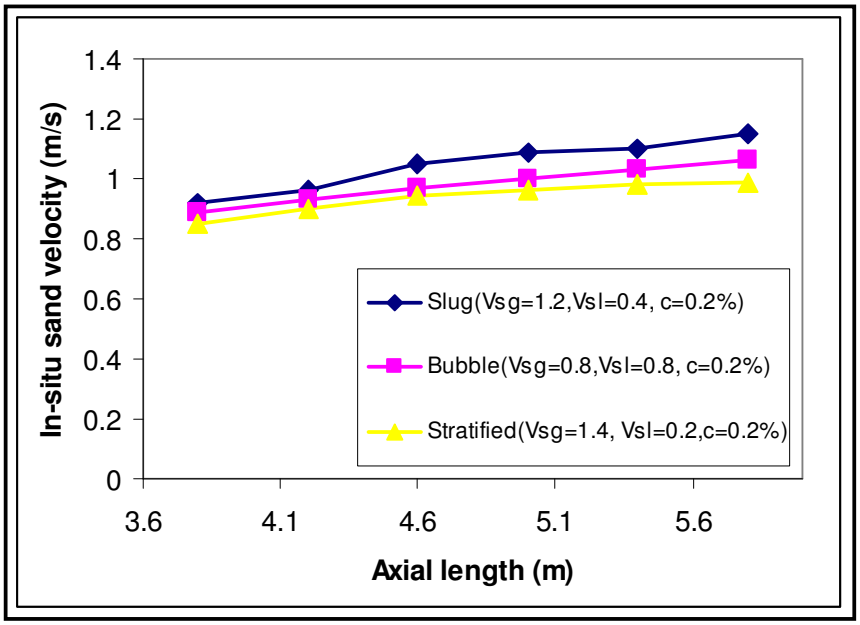

Figure 5-4: In-situ velocity profiles of sand particle as a function of pipe length and different flow regimes (d_P= 0.0003m)

5.2.3 Axial distribution of solid velocity for in different direction of flow

Figure 5.5 shows the effect of three-phase air-water-sand pipe flow direction on the local average in-situ particle velocity. It can be seen that the local average in-situ particle velocity is larger in vertical pipes than those in inclined and horizontal pipes.

This trend can be explained in terms of pipe effects on the morphology of the gas-liquid two-phase flow. The bubbles rise faster in a vertical pipe as compared to a horizontal pipe, which significantly affect the transfer of momentum to the in-situ liquid phase and the sand particle motions. In the horizontal pipe, the bubble rise to the top of the pipe wall as a result of buoyancy force reducing its impact on the liquid and solid phase velocities.

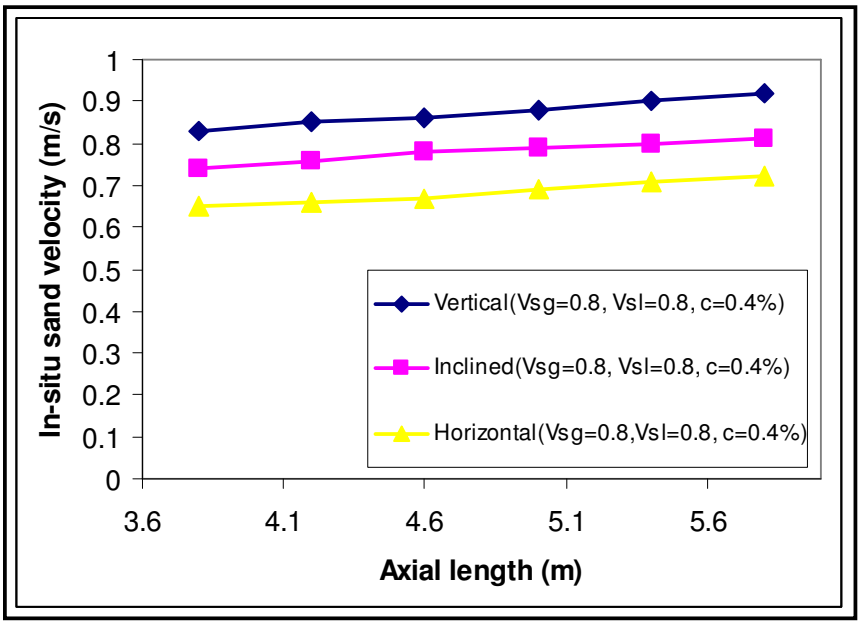

Figure 5-5: In-situ velocity profiles of sand particle as a function of pipe length and different flow geometries (d_P = 0.0007m, V_{SL} = 0.8m/s and V_{SG} = 0.8m/s)

5.2.4 Effect of liquid velocity on measured global solid velocity

Figure 5.6 presents the influence of superficial liquid velocity on the global average sand particle velocity at different superficial gas velocities and fixed particle loading. Four superficial gas velocities were considered. As expected, the higher superficial gas velocity gives rise to higher mean sand velocity. The figure shows a rapid acceleration of the mean sand particle, which quickly approach their equilibrium value of velocity and thereafter, remain almost constant.

This trend can be attributable to the particle shape factor (sphericity) and surface-to-volume ratio. Small particle size with a high surface-to-volume ratio and specific surface area tends to encounter a relatively high drag force (lifting effect), which results in increase velocity.

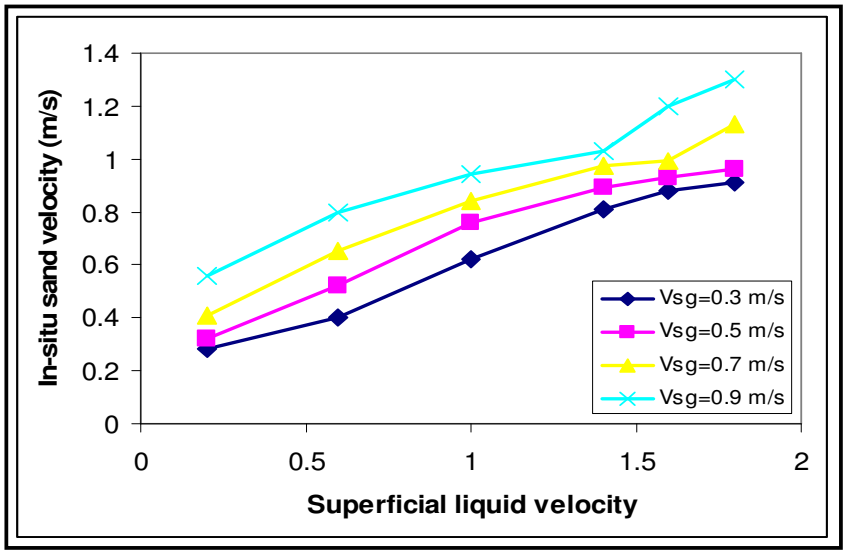

Figure 5-6: In-situ velocity of sand particle as a function of superficial liquid velocities and different gas velocities (d_P = 0.0006m, ¢ = 0.4% and L= 5.3m)

5.2.5 Effect of gas velocity on measured global solid velocity

Figure 5.7 shows the mean sand velocity with the superficial gas velocity at different superficial liquid velocities and fixed particle concentration. As the superficial gas velocity increases, the sand velocity increases. Because of the increase of the superficial gas velocity, more turbulence is produced, resulting in a better momentum from the liquid phase to the suspended sand particles. Hence, the liquid phase velocity of the multiphase flow system increases. This leads to the increase of the mean sand velocity.

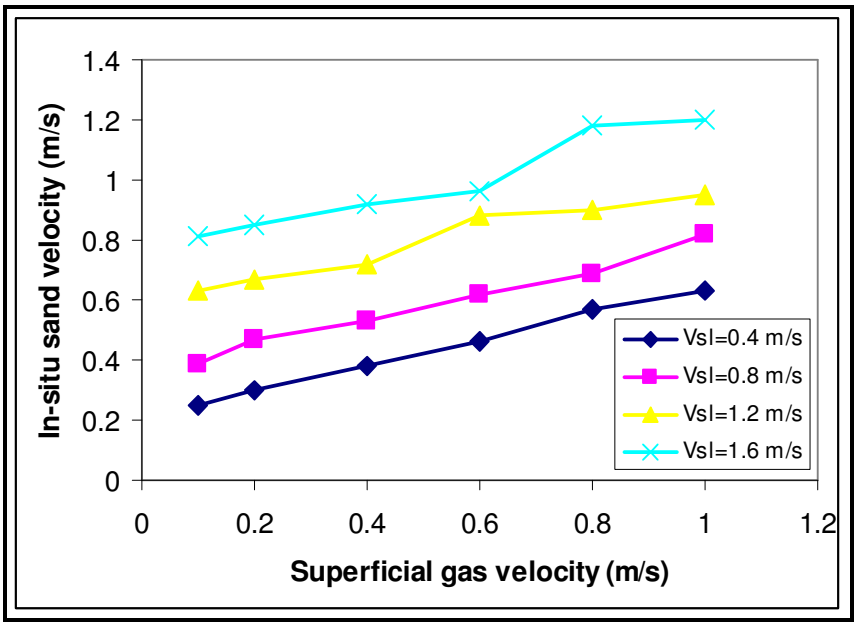

Figure 5-7: In-situ velocity of sand particle as a function of superficial gas velocities and different liquid velocities (d_P = 0.0006m, ¢ = 0.6% and L= 5.3m)

Figure 5.8 shows the measured mean sand velocity as a function of particle loading at different superficial gas and liquid velocities. The result shows that the mean sand particle velocity decreases with increasing particle loading. The effect of the particle loading on the mean sand particle velocity can be interpreted from the following aspects: (i) the increase of particle loading causes the decrease of liquid velocity which invariably decreases the mean sand velocity. The superficial liquid velocity was quite constant for a changing input sand particle volumetric fraction. The effect decreases with increases of the superficial gas and liquid velocities. (ii) As Figure 5.8 indicates, higher particle loading implies lower sand velocity. This arises from the particle-particle and particle-wall interactions and liquid phase turbulence intensity reduction with increase in particle loading.

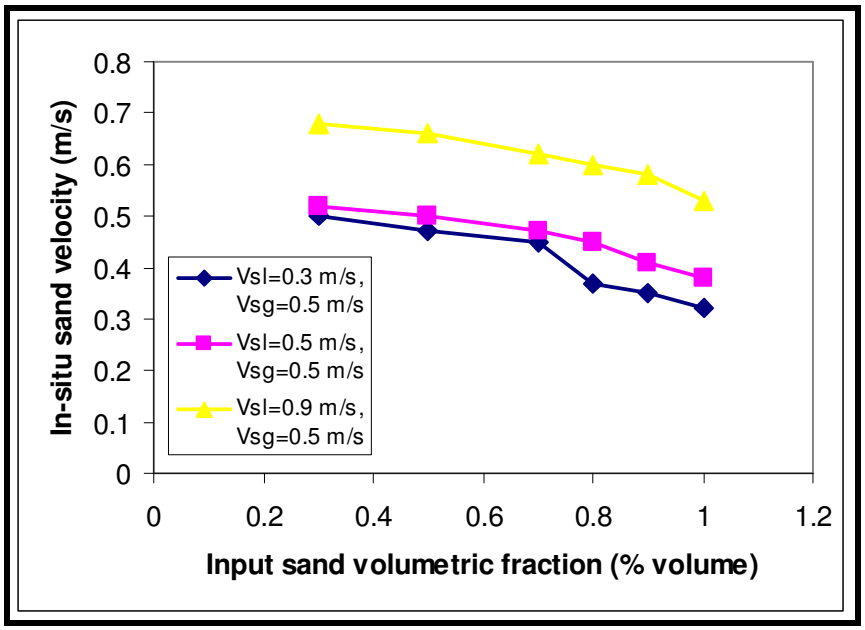

Figure 5-8: In-situ velocity of sand particle as a function of sand loading for different liquid velocities and fixed gas velocity (d_P = 0.0006m and L= 5.3m)

5.3 Sand particle holdup

5.3.1 Axial distribution of solid phase holdup

Figure 5.9 shows the effect of superficial liquid velocity on the axial distribution of sand holdup determined according to section 4.6. Five superficial liquid velocities were compared at a fixed superficial gas velocity and percent sand loading. The smaller superficial liquid velocity gave slightly higher sand holdup. Figure 5.10 shows the axial distribution of sand holdup in the three-phase air-water-sand pipe flow for different superficial gas velocities at a constant superficial liquid velocity and sand loading values. Figure 5.11 shows the effect of sand loading on axial profile of sand holdup. For Figures 5.9 to 5.11, the sand particle holdup decreases with increasing axial distance in the test section as well as as increasing liquid and gas velocities. This trend illustrates the complex interaction between the sand loading and all other parameters which is not well reproduced by existing models.

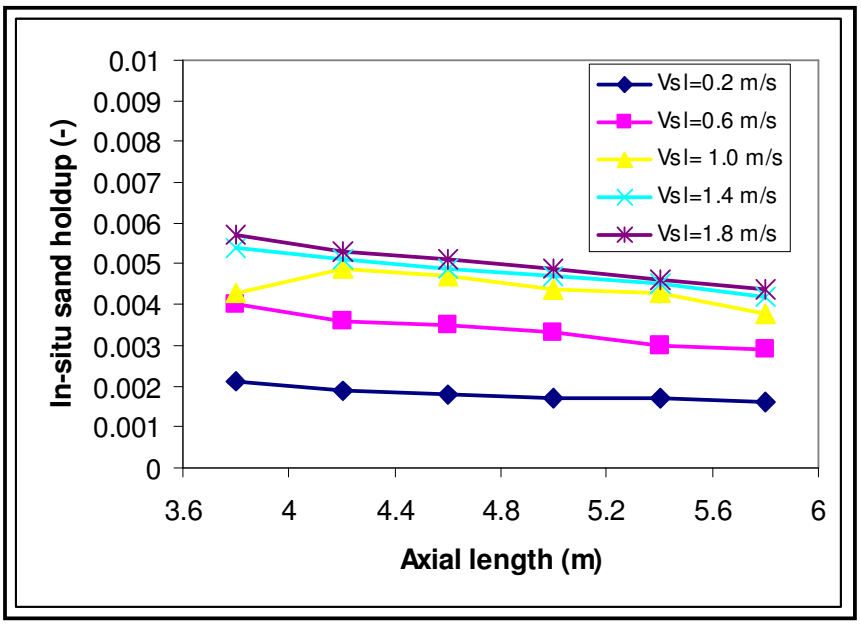

Figure 5-9: Particle holdup profiles for d_P = 0.0003m, V_{SG} = 0.4m/s and ¢ = 0.4%

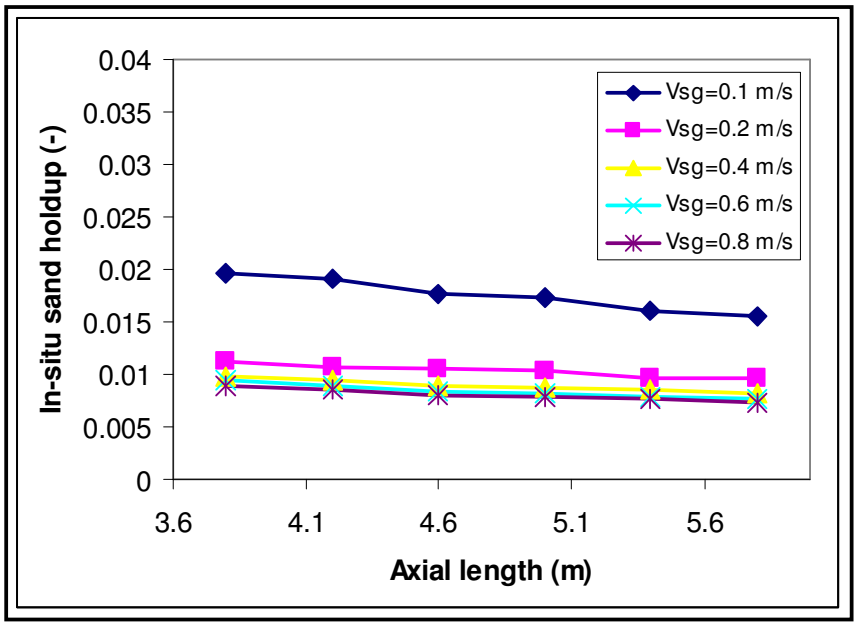

Figure 5-10: Particle holdup profiles for d_P = 0.0003m, V_{SL} = 1.2m/s and ¢ = 0.6%

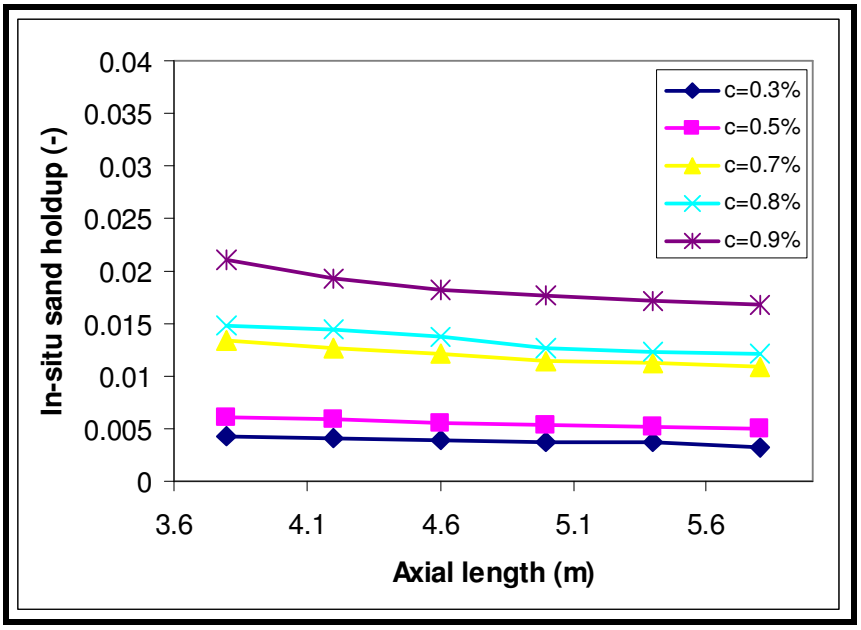

Figure 5-11: Particle holdup profiles for d_P= 0.0003m, V_{SL} = 0.6m/s and V_{SG} = 0.5m/s

5.3.2 Axial distribution of solid phase holdup in different flow regimes

Results of the local in-situ sand holdup profiles for the slug, bubble and stratified flow regimes are shown in Figure 5.12. The sand holdup profiles decrease for all the three flow regimes. The decline of sand holdup profiles is highest for slug flow, followed by bubble and stratified flow regimes, respectively. The decrease is due to the increase in the actual velocity of the liquid phase. It is known that in-situ liquid velocity in gas-liquid two-phase flows (Kvernvold, Vindoy, Sutredt and Soasen, 1984; Gopal and Jepson, 1997) and bubble (Serizawa, Kataoka and Michiyoshi, 1975; Brenn, Braeske, Zivkovic and Durst, 2003) flows is usually higher than the input values because of the momentum transfer between gas bubbles and the liquid phase. In order to determine the main mechanism to enhance the sand transport performance in gas-liquid multiphase flow systems, the gas and liquid superficial velocities were adjusted to impose the same mean velocity in the pipeline. As seen in Figure 5.12, the results of the comparisons indicate that the sand holdup profile obtained from the slug flow regime transport mode is low than those obtained for the bubble and stratified flow regimes.

5.3.3 Axial distribution of solid phase holdup for different flow direction

Figure 5.13 shows the effect of flow direction on the local average in-situ particle holdup. It can be seen that the local average in-situ particle holdup profile is slightly different for vertical, inclined and horizontal pipes. The trend can be explained based on the amount and energy level of gas bubbles that further increases in vertical pipe. The turbulent energy only slightly increases for the inclined pipe compared to the horizontal pipe. The low performance of the horizontal

flow can be attributable to the hydrodynamic at the boundary layer of the pipe. At increase superficial mixture velocity, the sand particle is transported to the boundary layer and held up in the low speed region of the turbulent fluid flow. Many authors have presented evidence of existence of large scale persistent structures of high and low speed regions, sometimes described as ejections and sweeps, near the wall of pipe when fluids flow in turbulent regime (Kaftori, et. al., 1995a; Kaftori, et. al., 1995b; Robinson, 1991).

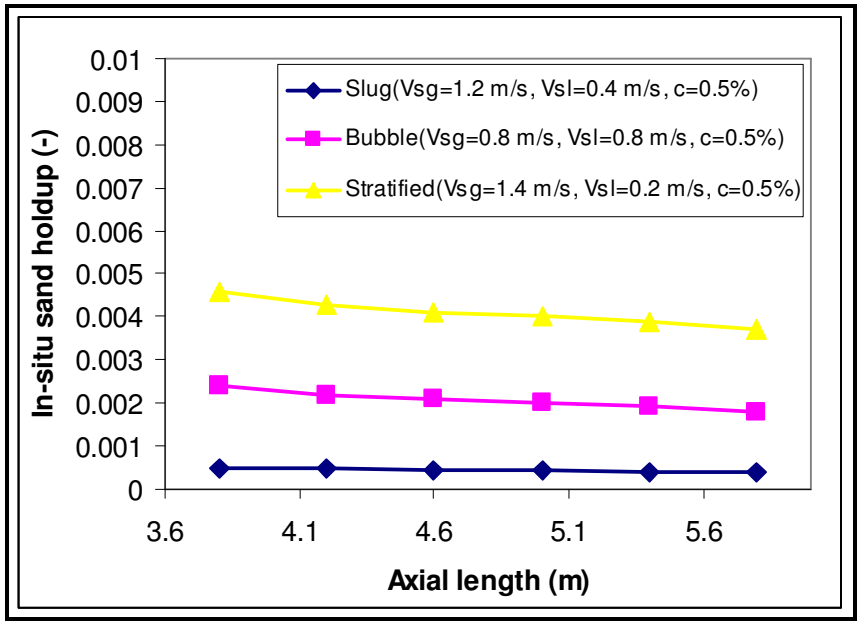

Figure 5-12: Particle holdup profiles for d_P = 0.0007m and varied flow regimes

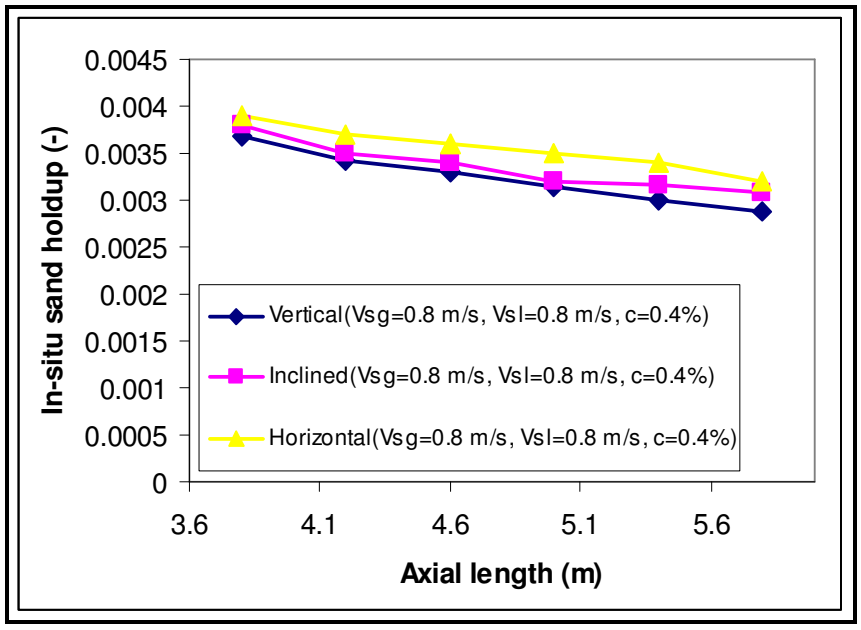

Figure 5-13: Particle holdup profiles for d_P = 0.0007m and varied flow geometries

5.3.4 Effect of liquid velocity on measured global solid holdup

Figure 5.14 shows the variation of the mean sand holdup in the horizontal air-water-sand multiphase flow with increasing superficial liquid velocity for different superficial gas velocities at a fixed particle loading. The sand holdup decreased with increasing superficial liquid velocity irrespective of the increase in the superficial gas velocity. This is due to the increase of the gas drag forces that resulted in a large increase of the sand velocity. Increasing the secondary liquid velocity will reduce the resistance to the movement of particles, hence, the decrease in the mean sand holdup

.

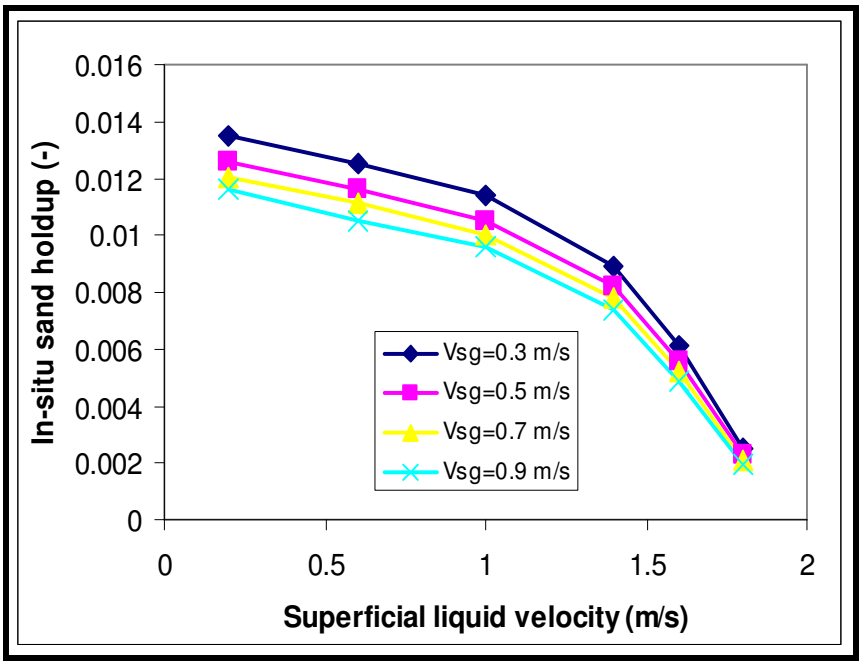

Figure 5-14: Effect of superficial gas velocity and superficial liquid velocity on in-situ particle holdup for d_P = 0.0006m, ¢ = 0.4% and L= 5.3m

5.3.5 Effect of gas velocity on measured global solid holdup

The effect of superficial gas velocity at a varied superficial liquid velocities and constant particle loading on in-situ sand particle holdup is shown in Figure 5.15. Generally, the increase in superficial gas velocity led to higher sand transport rates for the four superficial liquid velocities reported. However, at high superficial liquid velocity, the effect of the gas phase on the mean sand holdup is not well pronounced since the turbulence level of the gas phase is already high.

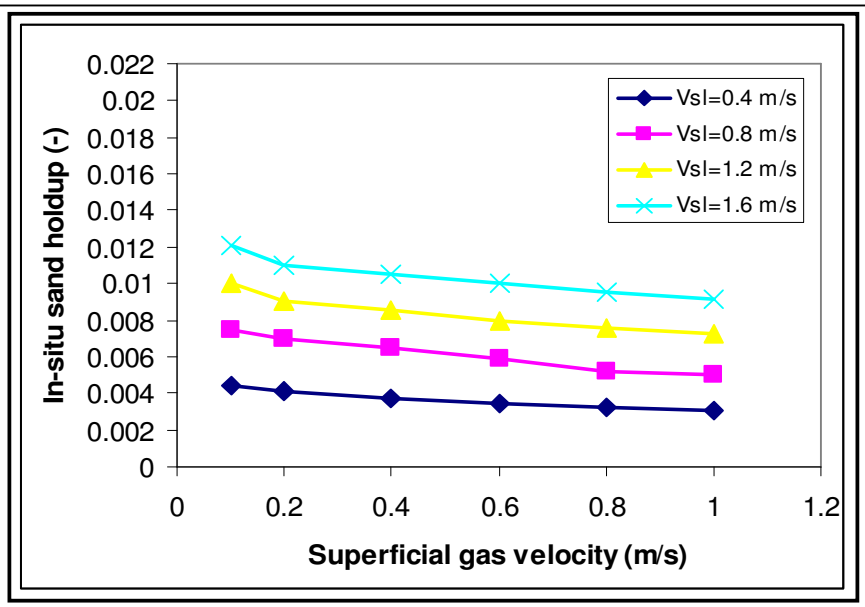

Figure 5-15: Effect of superficial liquid velocity and superficial gas velocity on in-situ particle holdup for d_P= 0.0006m, ¢ = 0.6% and L= 5.3m

5.3.6 Effect of solid concentration on measured global solid holdup

Figure 5.16 reveals that the increase of particle loading lead to increase in global sand particle holdup. The effect of particle loading on the mean sand holdup can be interpreted from the following aspects: (i) the increases of particle loading cause decrease of liquid velocity which invariably decreases the mean sand velocity and ultimately increases the mean sand particle holdup. The effect increases with the increase of the particle loading, which arises from the particle-particle, particle-wall interactions and liquid phase turbulence intensity reduction.

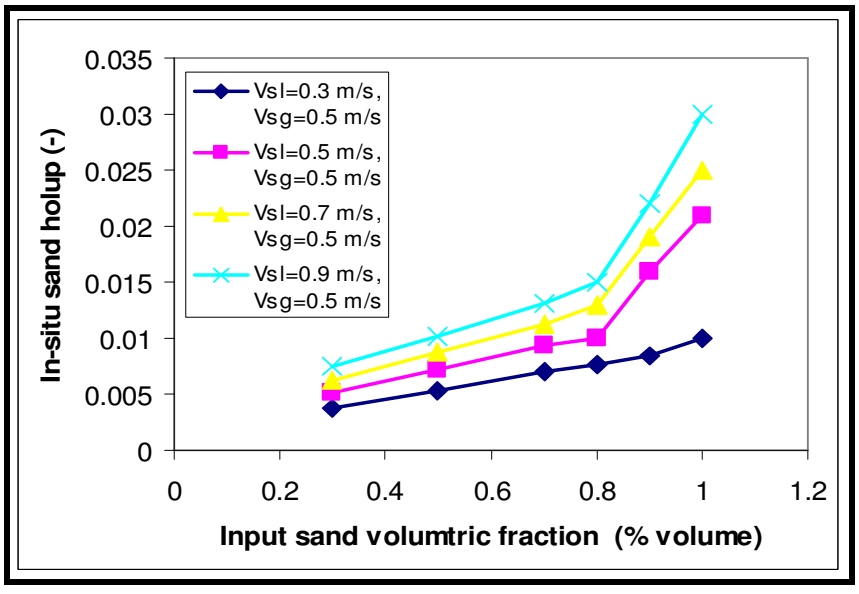

Figure 5-16: Effect of sand particle concentration (volume) on in-situ particle holdup for d_P= 0.0006m and L= 5.3m

5.4 Model validation and comparison

The methods for calculating the average percentage relative error, the root mean square and the standard deviation between the produced and experimental value of the sand transport parameters (particle velocity or particle holdup) are given in Appendix A.

Figure 5.17 presents the proposed model with the predicted results for solid particle velocity in vertical air-water-sand three-phase pipe flow system and the measured experimental data of Sato et. al. (1991) obtained from a vertical pipe for different superficial gas-liquid mixture velocities [equation 2.56]. The calculated and measured results show good agreement. A simple scatter plot of the measured versus calculated solid particle velocity in vertical air-water-sand three-phase pipe flow system for the proposed model within the 10% error index is presented in Figure 5.18. It is observed that the prediction of the proposed model also show good agreement with the experimental dataset of Sato et. al. (1991) originally obtained based on experimental simulation of air-lift pump for manganese nodules production from ocean floor. The Institute of Petroleum Engineering, Clausthal University of Technology has a long history of studies on the design of systems for deep ocean mining of manganese nodules. An experimental facility that mimics the deep ocean mining system was built in the late seventies for a doctoral study to measure the hydraulic gradient due to mixture upward flow and velocity of liquid fluidized manganese nodules in a 35m vertical pipe located in a shaft. An empirical model to compute the system performance under different flow and solid conditions was also developed (Engelmann, 1978). Table 5.1 gives the statistical results of the comparison between the proposed model calculation and measured results for predicting the sand particles velocity in three-phase pipe flow systems.

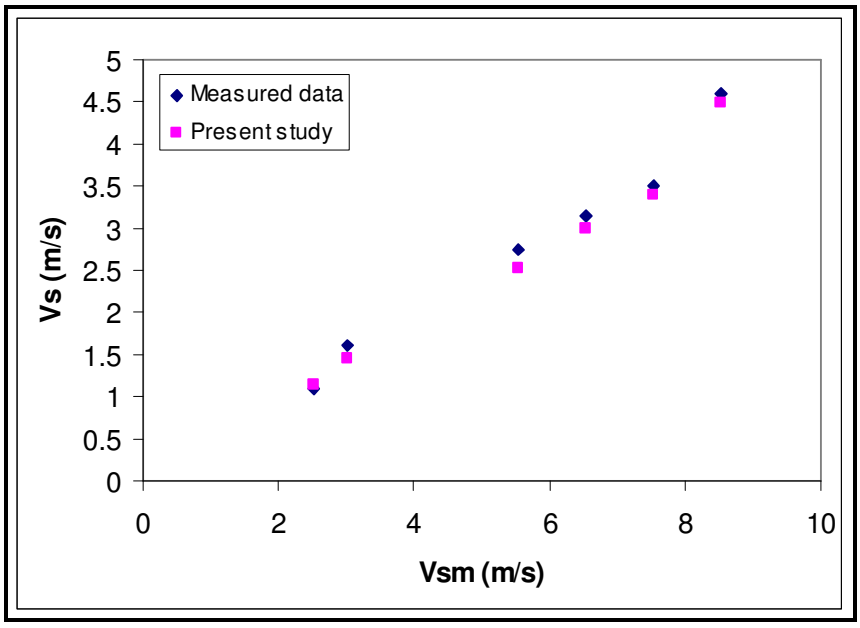

Figure 5-17: Predicted and measured Vs (vertical data of Sato et. al., 1991)

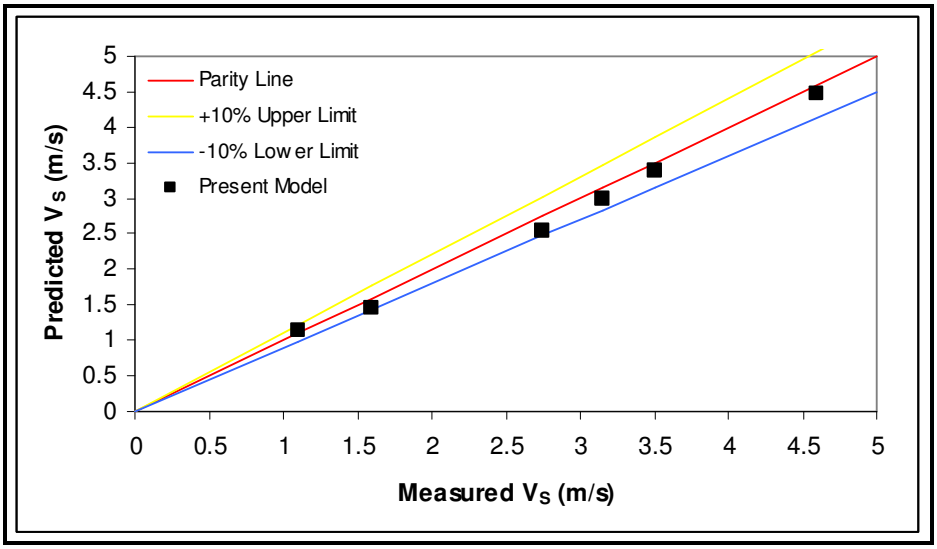

Figure 5-18: Comparison of present model with measured data of Sato et. al., 1991

Table 5-1: Statistical Parameters for the V_S Present Model

	Present Study
Average Percent Error (%)	5.3
Root Mean Square Error (%)	5.8
Percent Standard Deviation (SD)	4.2

The convergent agreement between the proposal model predictions and the measured data may be due to the fact that the proposed model is based on the physical behaviour of the solid particle in the three-phase flow and therefore it is more reliable under any operating, system and geometric conditions.

Figures 5.19 to 5.20 compare the sand particle holdup predicted by proposed model and that of Danielson (2007) using the measured global experimental data obtained from the present study for horizontal three-phase air-water-sand pipe flow system. The predictions of the proposed model show good agreements with this data set. Table 5.2 gives the statistical results of the comparison between the two methods.

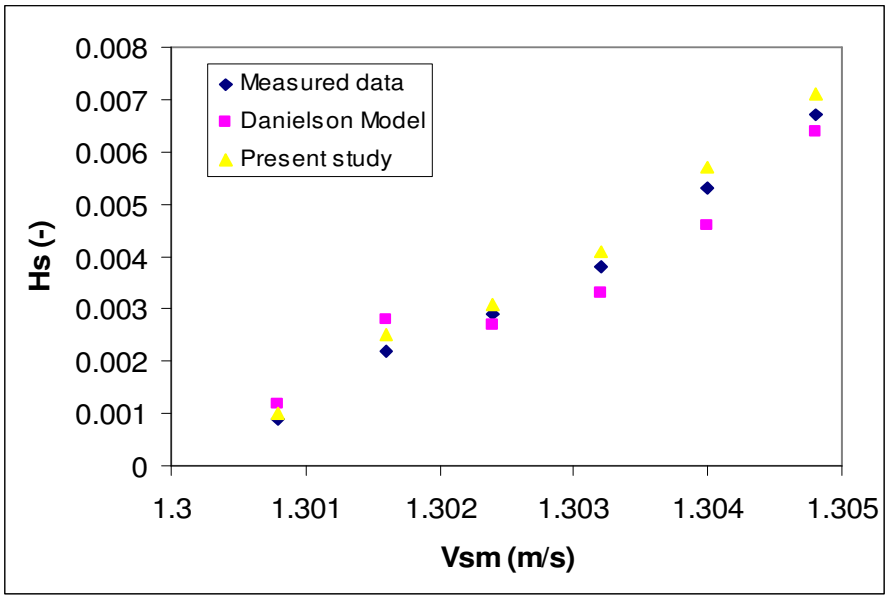

Figure 5-19: Predicted and measured Hs (horizontal data of present study)

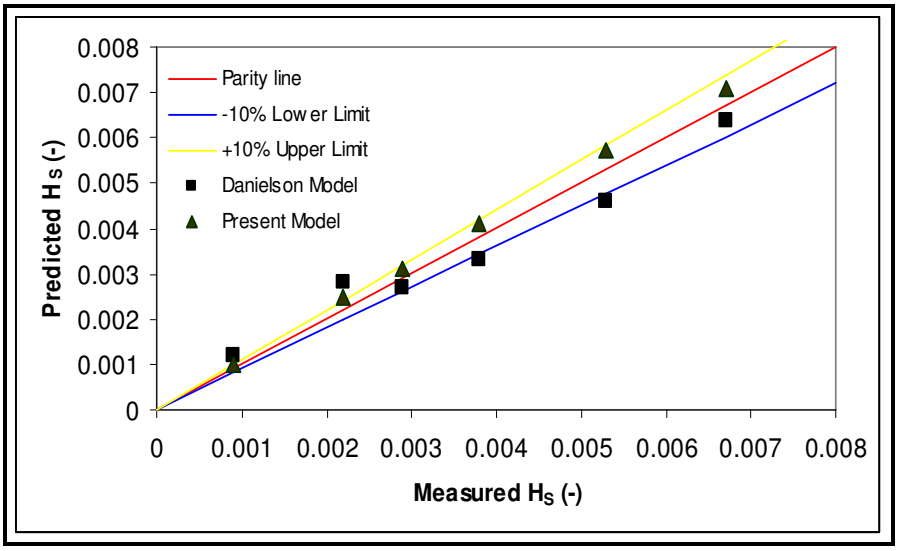

Figure 5-20: Comparison of present model with measured data of present study

Table 5-2: Statistical Parameters for the H_S Models

	Danielson Model (2007)	Present Study
Average Percent Error (%)	11.2	7.6
Root Mean Square Error (%)	13.9	8.2
Percent Standard Deviation (SD)	10.8	5.4

Figures 5.21 to 5.26 show the comparison of the predicted sand particle velocities by present model and existing. The performance assessment was carried out using horizontal measured global sand particle by present study, Stevenson (2001) and Scott and Rao (1971), respectively. Comparison of the existing sand present model predictions with experimental results demonstrates that the proposed model predicts solid particle velocity much better than any of the existing models for the experimental datasets used. The difference between actual particle velocities and model predictions can be anywhere from 6% to 40% as shown in Tables 5.3 to 5.5. The good performance of the proposed model is attributable to the fact that it takes into account the hydrodynamic processes controlling the particle transport in three-phase flow systems. As a matter of fact, the present model shows no dependencies with regard to particular experimental data sets.

The next accurate model among all of the models considered in this analysis is the Danielson model (2007), which is developed based on the drift flux modeling concept that was originally developed for gas-liquid two-phase flows in pipes. In the Stevenson model (2001), the physics of the particle transport in the three-phase pipe flow system is not taken into account. It can be seen in Tables 5.3 to 5.5 that the predictions of particle velocities by the Stevenson model are not satisfactory when they are compared with experimental results different from the data set used for development of this model. A point worth mentioning here is that the correlation developed from the Stevenson model (2001) could only capture roughly 65% of his own data sets within the 10% error index. The reason for the significant improvement of the proposed approach might be that the present model is based on a formulation derived form the fundamental macroscopic balance laws as well as a physical description of various interactions phenomena in a three-phase well and pipeline

The distinct difference between the Stevenson model (2001) and the present model is given in Table 5.6. It is our conclusion that the poor performance of the correlations within the narrow error index 10% may not be due to the weakness of the method alone but the accuracy of the datasets in the context of measurement errors.

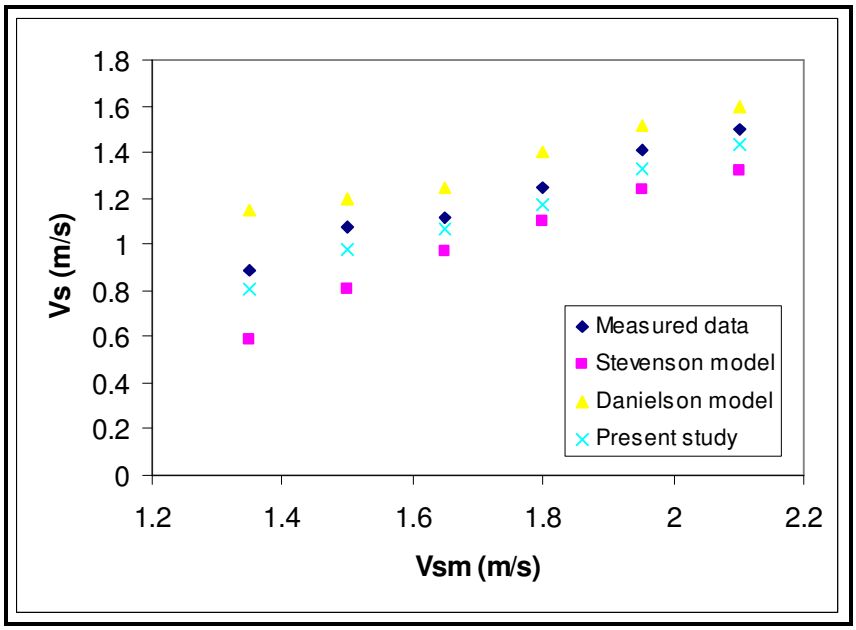

Figure 5-21: Predicted and measured Vs (horizontal data of present study)

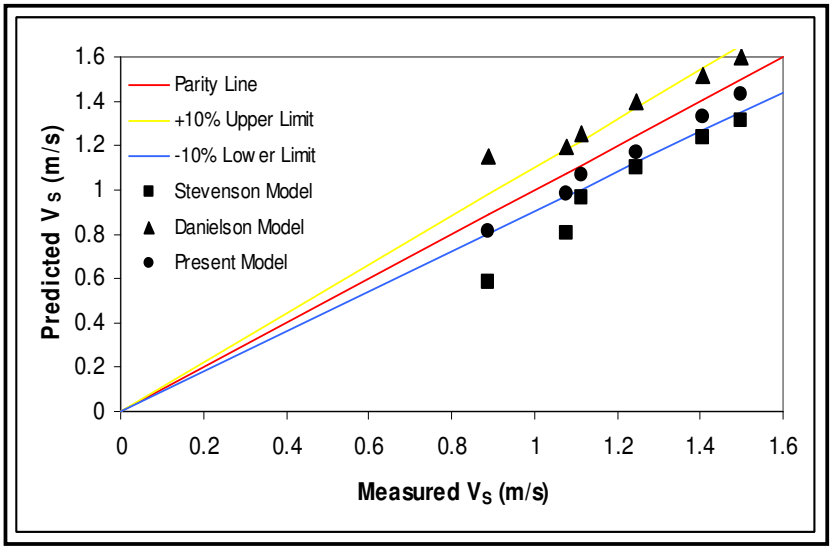

Figure 5-22: Comparison of present model with measured data of present study

Table 5-3: Statistical Parameters for the V_S Model

	Stevenson et. al. (2002)	Danielson Model (2007)	Present Study
Average Percent Error (%)	18.1	13.1	6.4
Root Mean Square Error (%)	20.0	15.1	6.7
Percent Standard Deviation (SD)	14.8	11.7	4.5

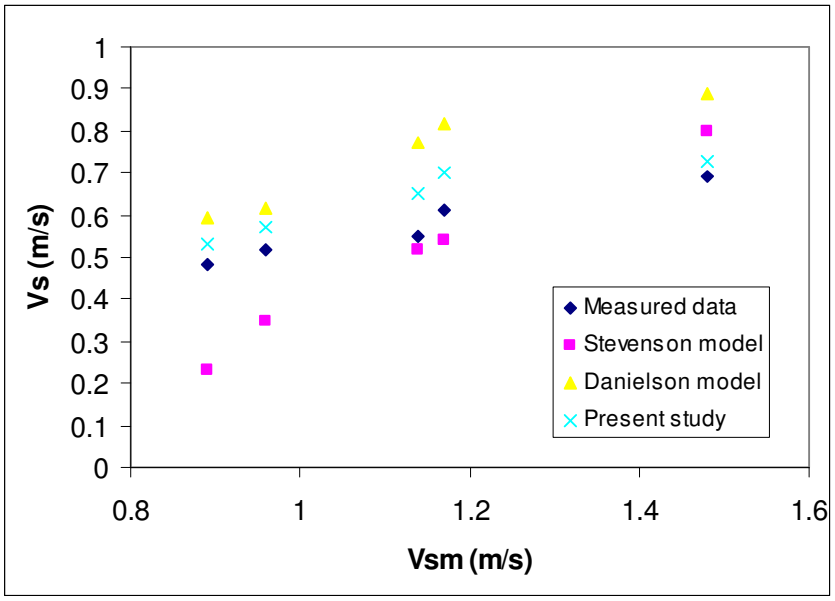

Figure 5-23: Predicted and measured Vs (horizontal data of Stevenson, 2001)

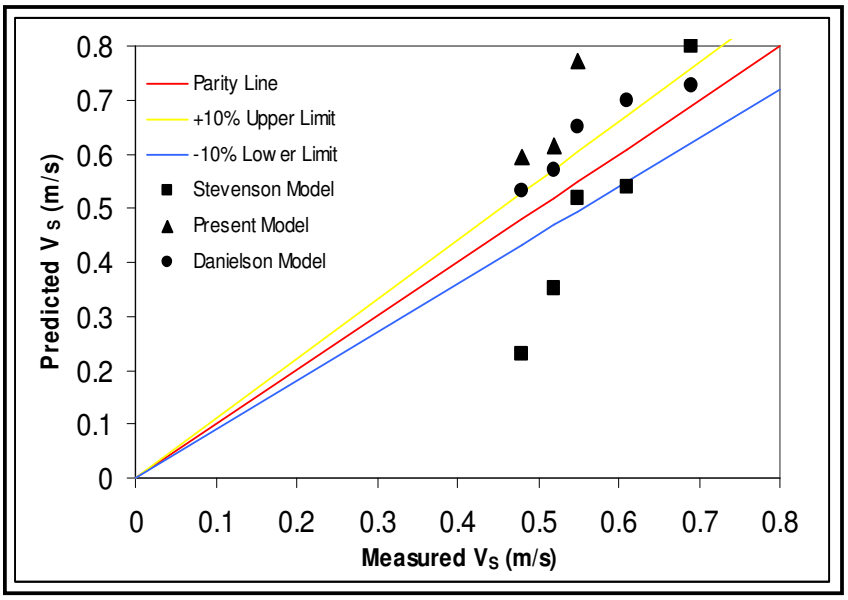

Figure 5-24: Comparison of present model with measured data of Stevenson, 2001

Table 5-4: Statistical Parameters for the V_S Models

	Stevenson et. al. (2002)	Danielson Model (2007)	Present Study
Average Percent Error (%)	23.5	29.0	11.9
Root Mean Square Error (%)	28.9	30.1	12.7
Percent Standard Deviation (SD)	23.9	16.9	8.4

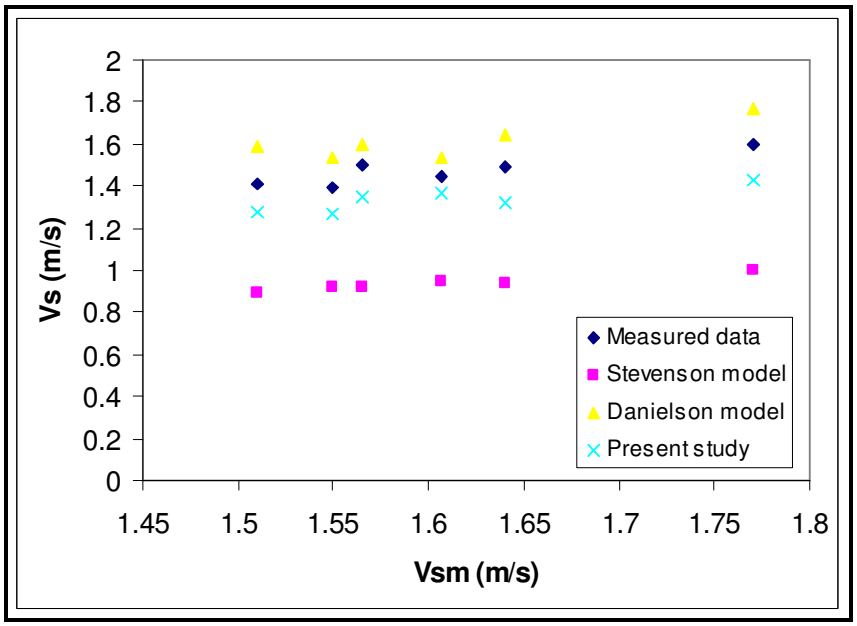

Figure 5-25: Predicted and measured Vs (horizontal data of Scott and Rao, 1971)

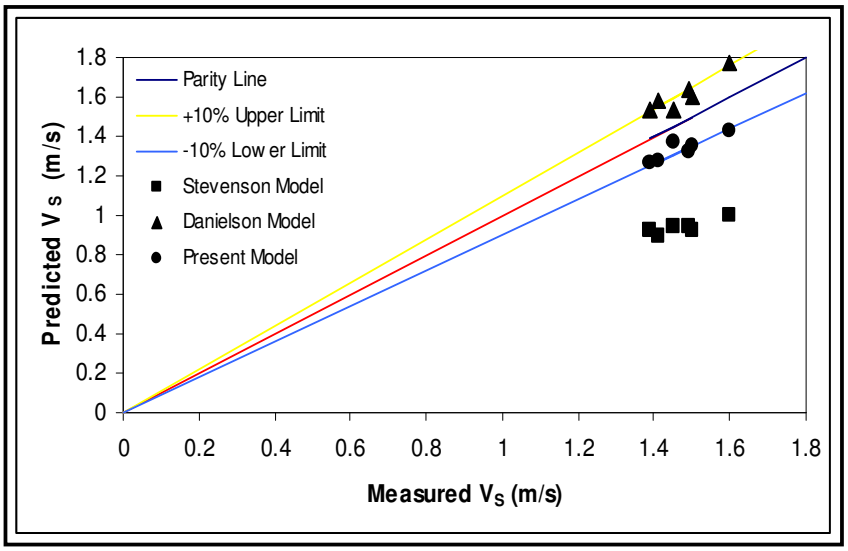

Figure 5-26: Comparison of present model with measured data of Scott and Rao, 1971

Table 5-5: Statistical Parameters for the V_S Models

	Stevenson et. al. (2002)	Danielson Model (2007)	Present Study
Average Percent Error (%)	36.3	6.7	9.3
Root Mean Square Error (%)	36.3	9.6	9.5
Percent Standard Deviation (SD)	20.2	5.6	5.3

5.5 Results and discussion of flow visualization

Typical examples of raw images of air-water-sand three-phase pipe flow obtained from PIV technique are shown in Figures 5.27 to 5.29 The swinging motion of the fast bubble stream and the vertical structures are evident in the figures. At low gas velocity (figure 5.27), no apparent circulation can be obtained in the three-phase air-water-sand pipe flow systems. As the superficial gas velocity reaches a certain value (figure 5.28), a noticeable amount of vortices (local circulation cells) start to form in the multiphase flow stream. With a further increase in the superficial gas velocity (figure 5.29), the size of the vortices increases. From this observation, it could be conjectured that the non-uniformity of the sand particle velocities is due to appreciable liquid velocity gradients caused by large-scale eddy (vortex) formations and high mixing processes.

The averaged profiles of the air-water-sand velocity field were obtained by analyzing 100 grabbed pairs of frames that yield vector fields shown in Figure 5.30. For such a set of vector fields, the velocity averaging was computed in both vertical field of view and a horizontal width (70 x 55 mm^2). It should be noted that the profile are the results of averaging the swinging motion of the sand particle stream and the related flow structures present instantaneously in the flow.

Although the preliminary interest of particle image velocimetry (PIV) in the current investigation is the observation of the flow motion and measurement of the velocity fields, it also allows the calculation of statistical quantities. Root mean square (RMS) is a frequently used measure of the difference (variance) between the instantaneous and ensemble average velocities. The lower the RMS velocities, the higher the accuracy of the PIV measurements used. Figure 5.31 shows the trend for some of the RMS velocities obtained from the present study. The plots in Figures 5.38 to 5.40 show the comparison of the mean velocity profile for water, air-water and air-water-sand pipe flow systems. It can be observed that the addition of sand particles produce a shift of the mean velocity profile that is less than the initial water or air-water velocity profiles. The observed trends could be explained on the basis of momentum transfer effects due to sand particle interactions between the water or air-water systems.

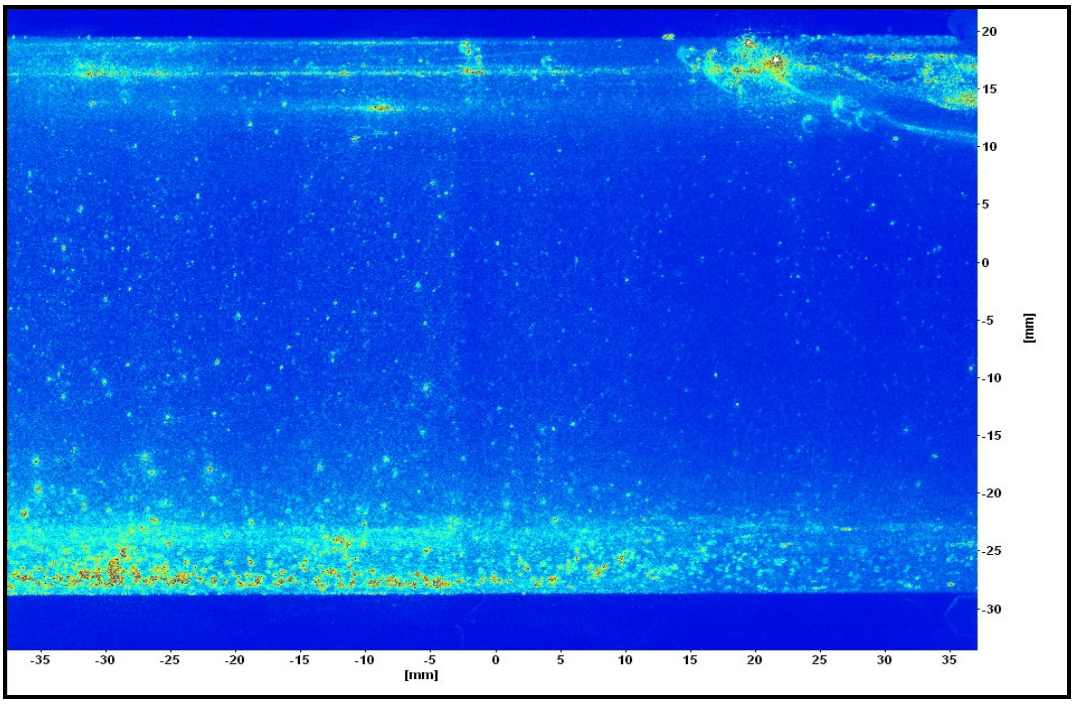

Figure 5-27: Sample raw flow field images of the three-phase horizontal air-water-sand pipe flow systems (d_P= 0.0003m, V_{SL} = 0.4m/s, V_{SG} = 0. 4m/s, ¢ = 0. 4%, plug flow)

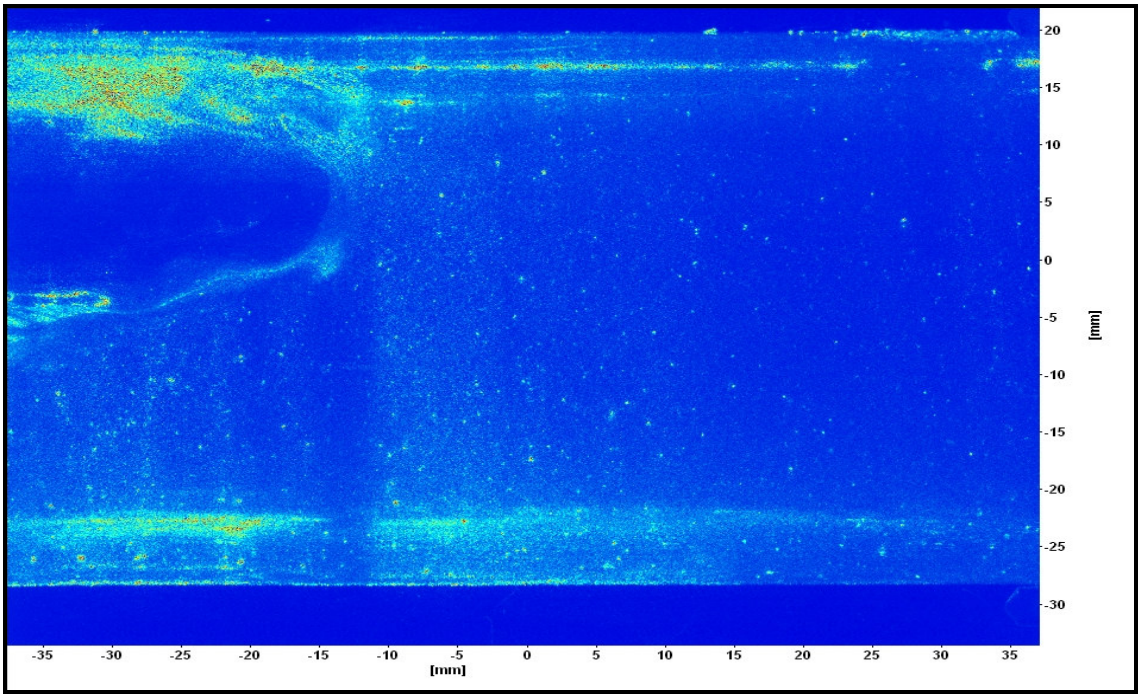

Figure 5-28: Sample raw flow field images of the horizontal three-phase air-water-sand pipe flow systems (d_P= 0.0003m, V_{SL} = 0.4m/s, V_{SG} = 0.6m/s, ¢ = 0. 4%, elongated bubble flow)

5.6 Conclusions

The objective of this chapter was to analyze the experimental results and evaluate the predictive capability of the proposed model.

In the following, we summarize the specific conclusions reached:

- The distribution of sand particle velocity and holdup are not uniform along the axial direction in the three-phase air-water-sand pipe flow systems
- The sand particle velocity in slug flow is significantly higher than that in bubble, dispersed and liquid pipe flows
- For sand particle with an equivalent particle diameter of the order of 0.0006m and pipe diameter of 0.04m, the ratio of particle velocity to gas-liquid mixture velocity is roughly 0.58. the ratio increases with decreasing particle diameter
- Sand particle velocity and holdup can be predicted by the proposed mechanistic model for the majority of the experimental data obtained from the open literature and present study
- Generally speaking, the present model appears superior to the existing methods

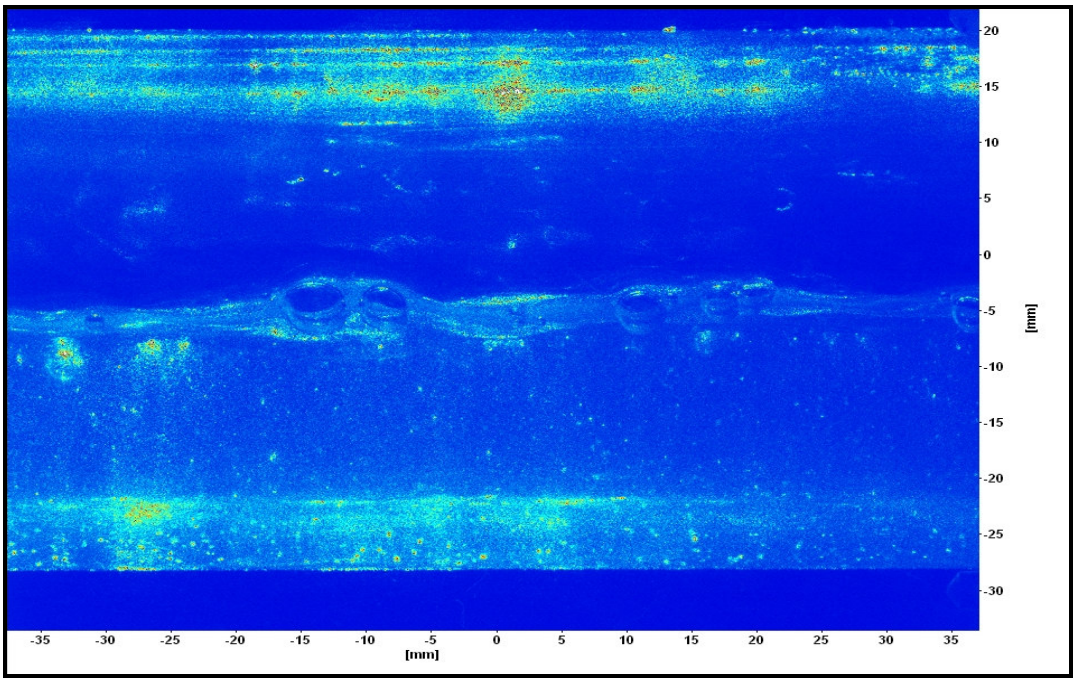

Figure 5-29: Sample raw flow field images of the horizontal three-phase air-water-sand pipe flow systems (d_P= 0.0003m, V_{SL} = 0.4m/s, V_{SG} = 0.8m/s, ¢ = 0. 4%, slug flow)

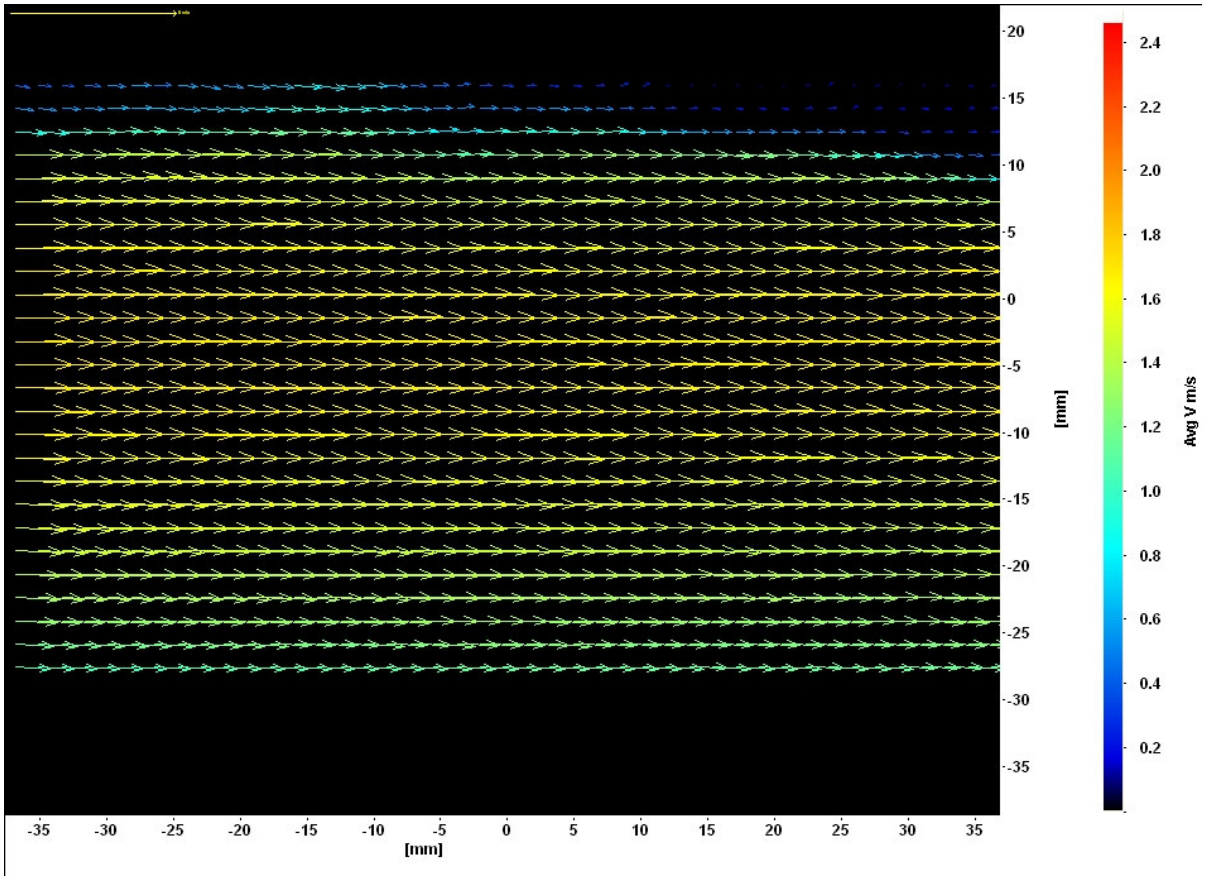

Figure 5-30: Averaged velocity field of the horizontal three-phase air-water-sand pipe flow obtained by PIV systems (d_P= 0.0003m, V_{SL} = 0.8m/s, V_{SG} = 0.6m/s, ¢ = 0. 3%, slug flow)

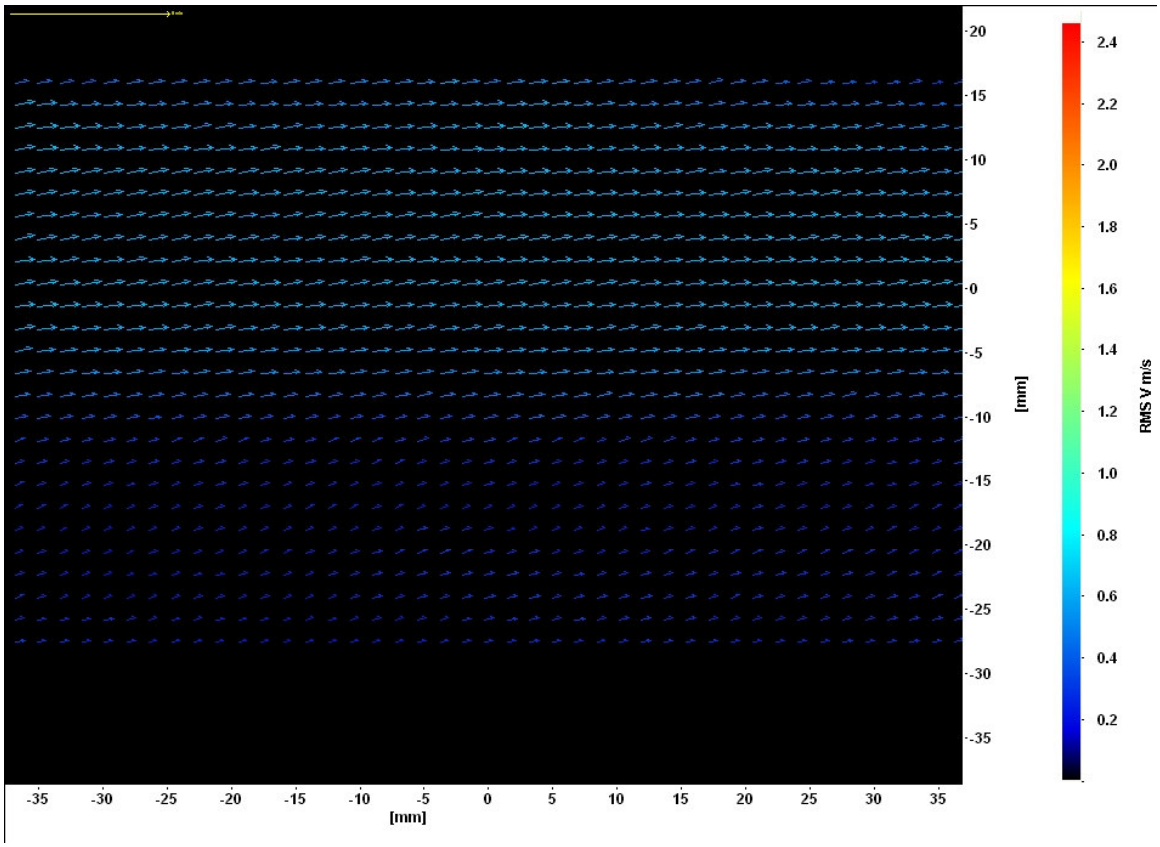

Figure 5-31: RMS velocity field for the horizontal three-phase air-water-sand pipe flow obtained by PIV systems (d_P= 0.0003m, V_{SL} = 0.8m/s, V_{SG} = 0.6m/s, ¢ = 0. 3%, slug flow)

Table 5. 6: Summary of major differences between Stevenson model (2001) and proposed model for sand particle velocity, V_S, predictions

S/N	ITEMS TREATED DIFFERENTLY	PROPOSED MODEL (2008)	STEVENSON MODEL (2001)
1	Constitutive relationship	Newtonian being liquid and solid being incompressible and gas phase exhibiting a real gas behaviour	Newtonian with gas, liquid and solid phases considered as incompressible
2	Hydrodynamic interaction forces between particle-particle, particle-liquid turbulent and particle-pipe wall	Considered	Not considered
3	Pressure effect on gas phase hydrodynamic behaviour	Considered	Not considered
4	Axial slip distribution in three-phase gas-oil-sand pipe flow systems	Considered	Not considered
5	Sand transport characteristics	Phenomenological modeling approach and numerical solution	Empirical and semi-empirical modeling approach based on experimental data
6	Need for empirical adjustable parameters are needed	No	Yes
7	Sand particle velocity model to P-V-T models	Yes	No

8	**Determination of drag coefficient**	**Sand particle size distributions and Corey particle shape factors**	**Sand particle size and sphericity**
9	**Calculation of settling velocity**	**Iterative process**	**Empirical process**
10	**Optimal relationship between sand influx rate and controllable (operating and geometric) variables for improving sand clean-out time, maximizing oil production rate, minimizing pressure loss and reducing sand deposition and erosion risk is**	**Considered**	**Not considered**
11	**Predictions can be made for**	• **Preventive and corrective measures** • **Dispersed bubble, bubbly, stratified, intermittent and annular flow patterns** • **Horizontal, inclined and vertical flow geometries** • **Straight pipe and annuli flow systems** • **Ultra low and moderately high sand loading**	• **Corrective measures** • **Intermittent and stratified flow patterns** • **Horizontal and near-horizontal flow geometries** • **Straight pipes** • **Ultra low sand loading** • **Average or overall sand particle transport characteristics (particle velocity, holdup, flux and mass rate)** • **Overall critical transport velocity** • **Cannot predict optimal transport velocity** • **Cannot predict pressure drop nor carry out system performance optimization for gas-oil-sand multiphase production and systems**

		• **Local sand particle transport characteristics and their distributions (particle velocity, holdup, flux and mass rate)** • **Local critical transport velocity and its distribution** • **Optimal transport velocity** • **Pressure drop and system performance optimization for varied gas-oil-sand multiphase production and system design options**	

6 FIELD APPLICATION EXAMPLES

6.1 Introduction

Although there have been many previous studies on hydraulic and particle transport behaviour in three-phase gas-oil-sand production and well systems, no single model capable of describing sand transport behaviour and system performance in vertical, inclined, and horizontal geometries has been developed. The purpose of this work is to develop a general mechanistic model that is robust enough to fit this need.

In this chapter, the field applicability of the proposed model to two major problems of engineering importance in gas-oil-sand multiphase production and well systems are presented. The simulated well depth was put at 100m due to excessive demand for discretization and computational cells. The case studies enable the calculation of the particle velocity, particle holdup and critical velocity. The sand particle holdup is an important parameter in the calculation of three-phase gas-oil-sand mixture density. The mixture density is needed in estimating changes in the profile along a pipe. The information on sand particle velocity is very important for sand erosion rate prediction and the sizing of the sand management topside equipment. The critical velocity is needed to define the design velocity and to prevent sand deposition and bed development.

6.2 Case study one (vertical flow)

The first case study is presented to illustrate the use of the proposed model and computational algorithm to determine pressure drop, critical transport velocity, particle velocity and holdup in a three-phase flow through a vertical well. The example has been taken from the paper published by Guo (2001).

Table 6.1 lists the relevant well operating and system data. In the calculation using the mechanistic model and the input data, we have assumed an equivalent sand particle size of 0.00025m, which is a typical grain size of unconsolidated reservoirs in the Niger Delta. The output of the simulation performed with the base value is shown in Table 6.2.

Many design and operational conditions influence the calculated pressure drop, critical transport velocity, sand particle velocity and holdup, therefore sensitivity tests are made for the oil production rate while others are taken by their base values listed in Table 6.1. .

Figures 6.1 to 6.4 show the calculated parameters as a function of in-situ gas-oil mixture velocity. The flowing tubing head pressure and average system temperature of 15MPa and 334K were used, respectively for thermodynamic and multiphase flow properties calculations. All the parameters plotted in Figures 6.1 to 6.4 show gradual increase as the in-situ gas-oil mixture velocity increases. Exception to this trend is Figure 6.2 which shows a decreasing trend with increasing in-situ mixture velocity.

Table 6-1: **Parameters used in the case study 1**

S/N	VARIABLES	BASE VALUE
1	Superficial oil rate, m^3/s	0.0184
2	Superficial gas rate, m^3/s	0.0112
3	Sand influx (loading) rate, m^3/s	5.18×10^{-7}
4	Water cut	0
5	Type of production well	Vertical
6	Tubing internal diameter, m	0.097
7	Tubing internal area, m^2	0.0074
8	Tubing shoe depth, m	3467
9	Tubing wall roughness, m	0.00055
10	Surface temperature, K	300
11	Bottomhole temperature, K	368
12	Average system temperature, K	334
13	Static bottomhole pressure, MPa	47
15	Flowing tubing head pressure, MPa	15
16	Oil bubble point pressure, MPa	34
17	Gas-Oil Ratio (GOR), SCF/STB	1375
18	Oil API gravity, Degree	45.7
19	Oil density, kg/m^3	802
20	Oil viscosity, Pa.s	0.0005
21	Gas-Oil surface tension, N/m	0.0187
22	Gas specific gravity	0.69
23	Sand grain size, m	0.00025
24	Sand grain size distribution	100% Fine Sand
25	Sand grain density, kg/m^3	2500
26	Sand grain shape factor	0.910

VARIABLE RANGE

1	Oil rate, m^3/s	0.0132 – 0.0240
2	Gas rate, m^3/s	0.0080 – 0.0133
3	Oil viscosity, Pa.s	0.0003 – 0.060

Table 6-2: Simulated output results for case study 1

S/N	Vsl (m/s)	Vs (m/s)	Hs (-) x 10^{-5}	Vm (m/s)	Vc (m/s)	ΔP (MPa)
1	1.78	1.72	4.10	4.20	2.48	1.18
2	1.90	1.80	3.89	4.36	2.56	1.27
3	2.07	1.84	3.80	4.52	2.68	1.36
4	2.21	1.90	3.68	4.70	2.80	1.42
5	2.36	1.97	3.55	4.87	2.90	1.51
6	2.50	2.01	3.50	5.04	3.03	1.61
7	2.60	2.10	3.33	5.21	3.11	1.70
8	2.78	2.13	3.29	5.39	3.26	1.82
9	2.90	2.20	3.18	5.56	3.36	1.90
10	3.07	2.27	3.09	5.73	3.46	2.00
11	3.21	2.30	3.04	5.90	3.60	2.12

Vsl = In-situ oil velocity
Vs = Calculated in-situ sand particle velocity
Hs = Calculated in-situ sand particle holdup
Vm = Calculated in-situ gas-liquid gas-oil mixture velocity
Vc = Calculated critical velocity
ΔP_i = Calculated pressure drop

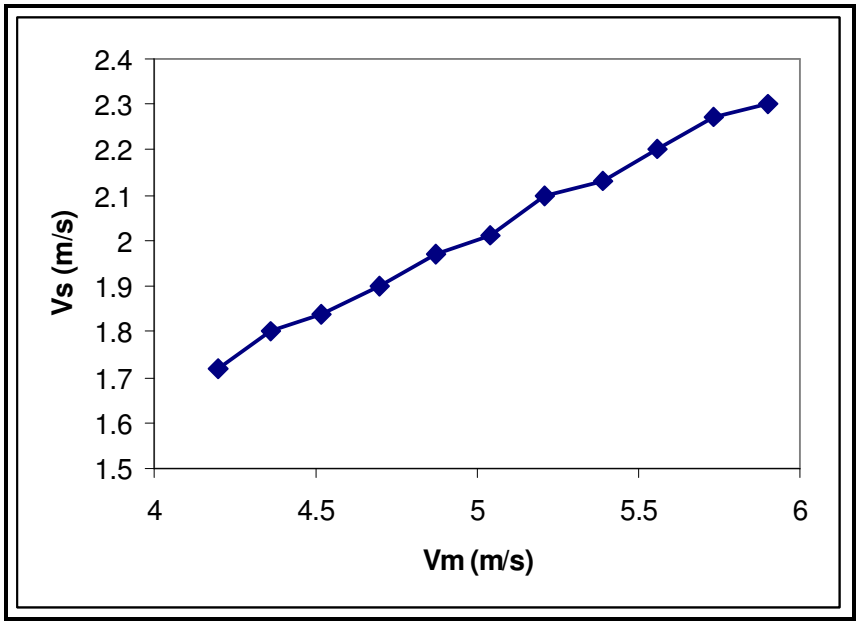

Figure 6-1: Predicted Vs as a function of calculated in-situ Vm

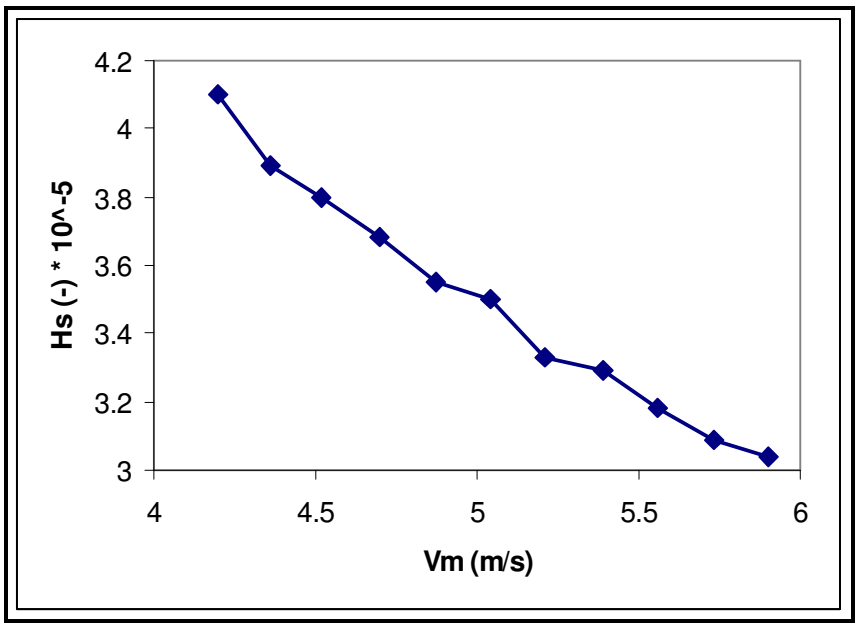

Figure 6-2: Predicted Hs as a function of calculated in-situ Vm

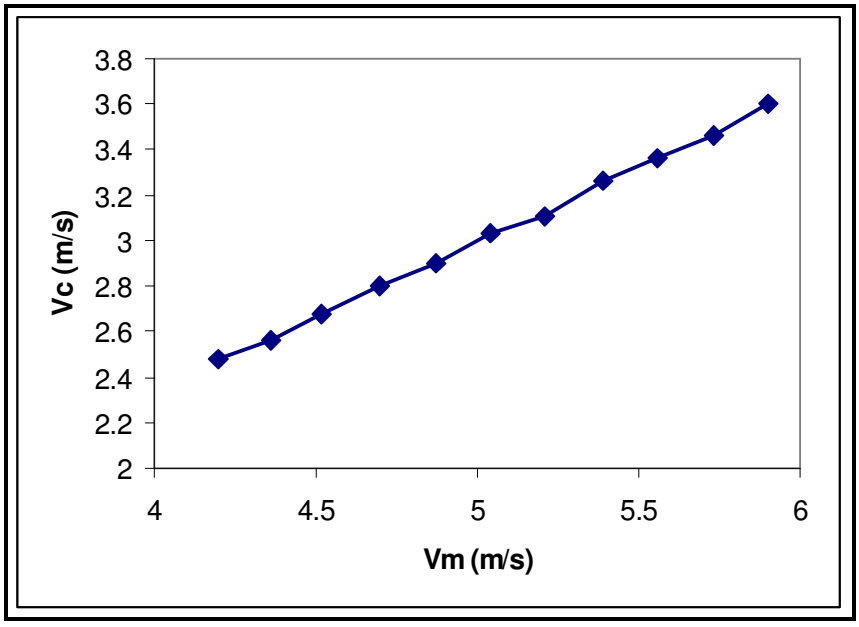

Figure 6-3: Predicted Vc as a function of calculated in-situ Vm

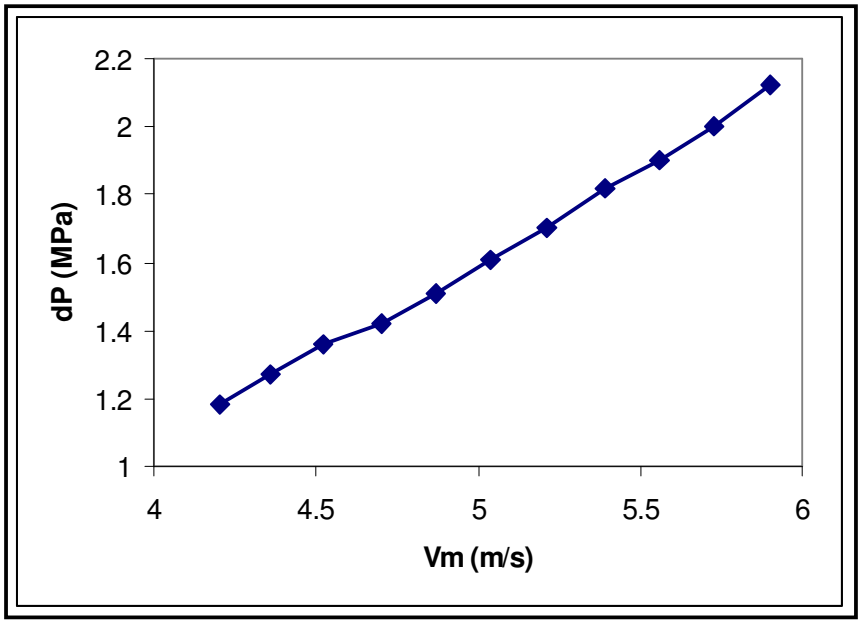

Figure 6-4: Predicted ΔP as a function of calculated in-situ Vm

6.3 Case study two (horizontal flow)

The example two is a slight modification of the case problem reported in the published work by Oudeman (1993) concerning the development of a small offshore field using subsea trunklines. The purpose of this field application example is to apply the present model to predict the behaviour of the particle transported in the three-phase gas-oil-sand pipe flow system.

The prediction of the optimal superficial gas velocity for safe operation (prevention of the sand deposition and bed formation) is also required. The sensitivity analysis of the output of the mechanistic model to changes in oil rate input parameter is investigated so that asset managers can make decisions with greater confidence. All necessary data for the case study two is given in Table 6.3. In-situ flow rates were used. The values of 2540kg/m^3 and 0.913 typical of typical North Sea reservoir sand have been used for the density and shape factor, respectively.

Table 6.4 gives result of the sand particle velocity (carrying capacity), sand particle holdup (concentration), pressure drop and critical transport velocity that is required to prevent sand bed formation for the given base values. The effects of the high, medium and low oil production rates on sand particle velocity, sand particle holdup, pressure drop and critical transport velocity is shown in Figures 6.5 to 6.8. As the in-situ gas-oil mixture velocity increases, the predicted sand transport parameters also increase, which is favourable for sand removal to the topside facilities. On the other hand, the sand particle holdup decreases with increasing in-situ gas-oil mixture velocity. The predicted parameters are significantly affected by oil production rates.

In the absence of measured field data on the predicted sand transport parameters for this case study two, it was decided that the bench-mark to verify the results of the proposed model outputs would be the results from the simplified mechanistic model by Danielson (2007). Figures 6.9 to 6.11 show the comparison between the proposed model and simplified mechanistic model previously developed by Danielson (2007) at a very tight 10% error index. The plots show reasonable agreement since both have been developed based on the physics of the sand particle transport in the three-phase gas-oil-sand pipelines. The Danielson model (2007) has been extensively validated with experimental data obtained from SINTEF petroleum research multiphase flow loop. Tables 6.5 to 6.7 show the statistical parameter between the two methods.

The proposed model was also used to estimate the optimal superficial gas velocity for sand removal at specified range of oil flow rates and given base values. Figures 6.12 to 6.14 show the effect of superficial oil velocity on pressure loss in the subsea trunklines and the optimal gas velocity. The right legs of the pressure loss profiles are dominated by frictional drag forces since the system is dilute. The drag force is inversely proportional to the particle diameter and directly proportional to the slip (critical) velocity. With the left leg of the curve, the gravitational force dominates the system.

In the multiphase transport of gas-oil-sand in pipes, it is important to choose an optimal gas velocity as low as possible to save power consumption and reduce ware and sand particle deposition. By a numerical simulation, the optimal velocity is the one at which the total pressure drop per unit length along a pipe becomes a minimum for a given mass flow rate of sand particles.

The optimal superficial gas velocities were predicted as the inflection point on the plot of the pressure drop due to the three-phase pipe flow as a function of the superficial gas velocity. By an iterative simulation, the optimal gas velocity at which this total pressure drop per unit length along the horizontal trunklines becomes a minimum is predicted for a given system, operating and geometric variables. The gas-oil flow regimes are associated with a different morphological character which has a substantial influence on the sand transport behaviour. The gas phase provides energy for generating intense turbulent flow in the oil phase. The oil motion impacts energy to the sand phase by which they can remain in suspended condition.

Table 6-3: **Parameters used in the case study 2**

S/N	VARIABLES	BASE VALUE
1	In-situ oil rate, m^3/s	0.028
2	Sand loading rate, m^3/s	0.0002% of oil flow rate
3	In-situ gas rate, m^3/s	0.0014 (5% of oil flow rate)
4	Type of pipeline transport system	Horizontal
5	Tubing internal diameter, m	0.190
6	Tubing internal area, m^2	0.028
7	Pipeline length, m	7000
8	Typical value of commercial steel pipe wall roughness, m	0.000046
9	Average system temperature, K	318
10	Oil bubble point pressure, MPa	33.8
11	Oil density, kg/m^3	802
12	Oil viscosity, Pa.s	0.001
13	Gas-Oil surface tension, N/m	0.020
14	Gas specific gravity	0.70
15	Sand grain size, m	0.0003, 0.0007
16	Sand grain density, kg/m^3	2500
17	Sand grain shape factor	0.910

VARIABLE RANGE

In-situ oil rate, m^3/s = 0.010 – 0.040
Sand rate, m^3/s = 0.002% - 2.0% of oil flow rate

Table 6-4: Simulated output results for case study 2

S/N	Vsl (m/s)	Vs (m/s)	Hs (-) x 10^{-6}	Vm (m/s)	Vc (m/s)	ΔP (kPa)
1	0.40	0.34	5.88	0.65	0.31	3.40
2	0.50	0.36	5.56	0.70	0.34	3.90
3	0.60	0.38	5.26	0.76	0.38	4.80
4	0.70	0.40	5.00	0.81	0.41	5.05
5	0.80	0.43	4.65	0.87	0.44	6.30
6	0.90	0.45	4.44	0.92	0.47	7.70
7	1.00	0.47	4.26	0.98	0.51	8.05
8	1.10	0.49	4.10	1.03	0.54	9.90
9	1.20	0.53	3.77	1.10	0.58	10.70
10	1.30	0.54	3.70	1.14	0.60	11.56
11	1.40	0.57	3.51	1.19	0.62	12.20

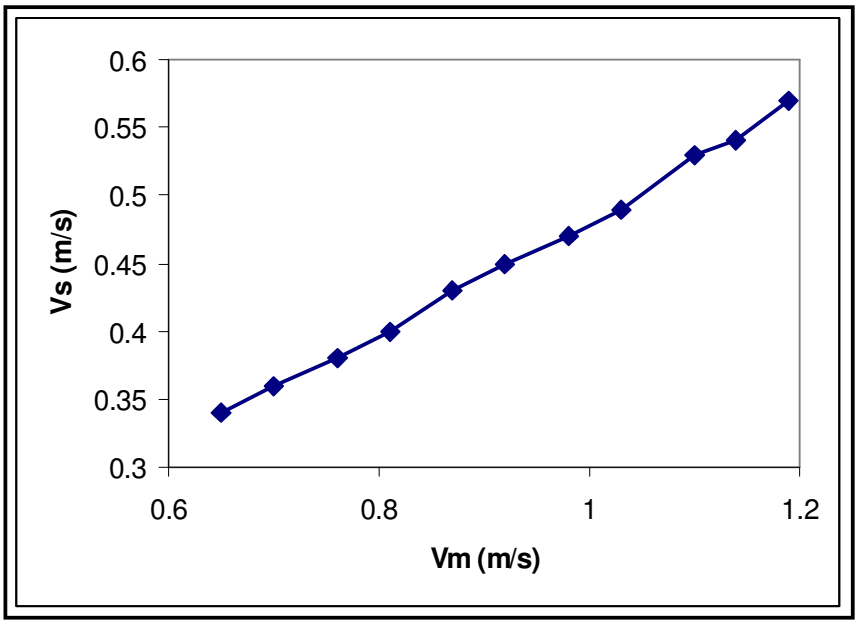

Figure 6-5: Predicted Vs as a function of calculated in-situ Vm (case study 2)

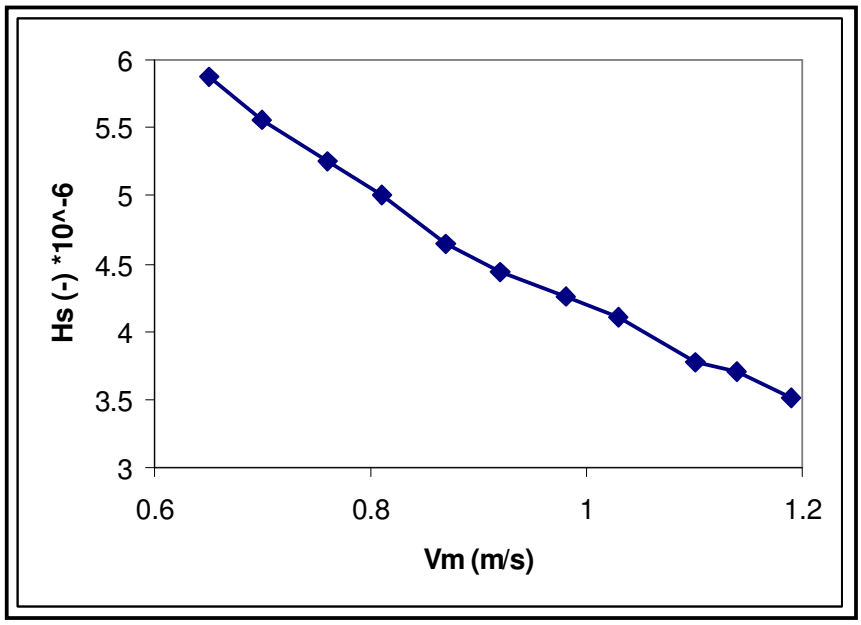

Figure 6-6: Predicted Hs as a function of calculated in-situ Vm (case study 2)

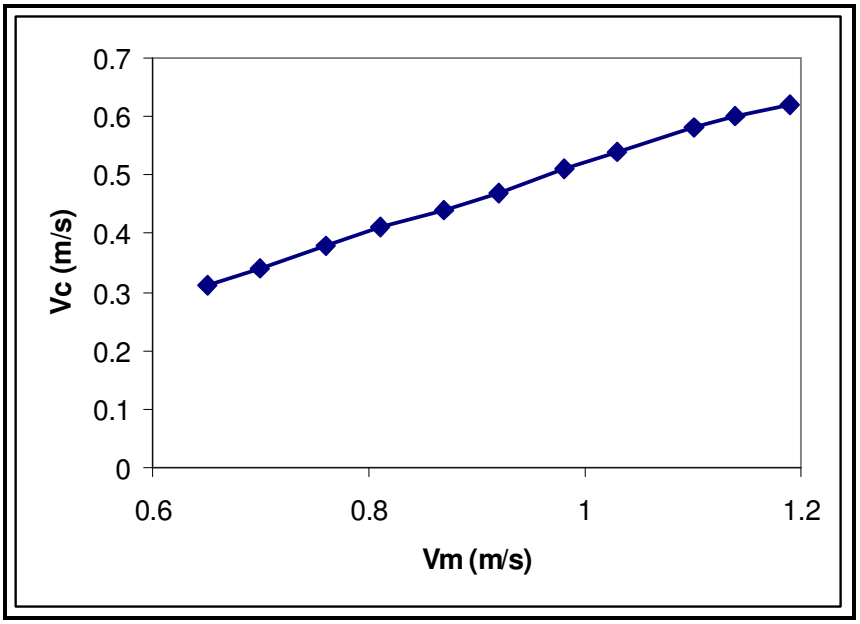

Figure 6-7: Predicted Hs as a function of calculated in-situ Vm (case study 2)

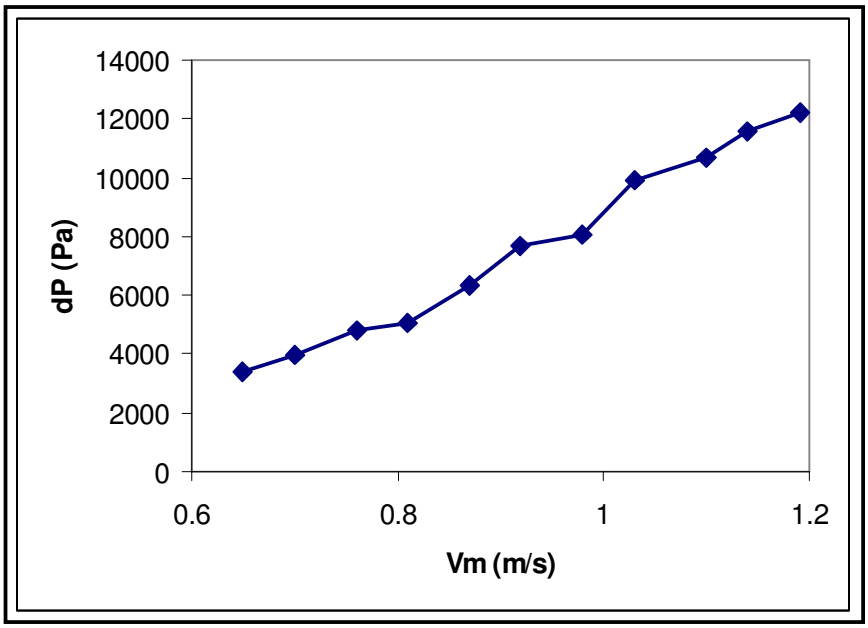

Figure 6-8: Predicted ΔP as a function of calculated in-situ Vm (case study 2)

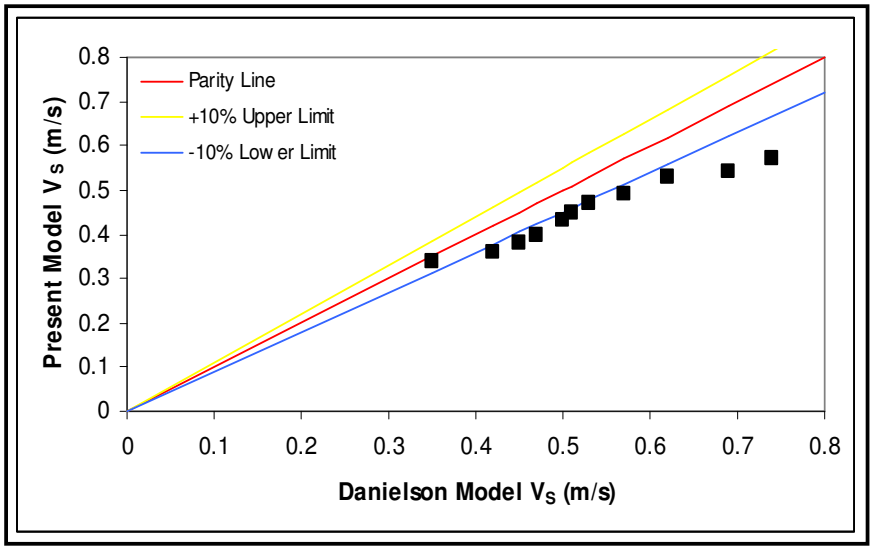

Figure 6-9: Comparison of present model with Danielson model, Vs (2007)

Table 6-5: Statistical Parameters for the V_S Models

	Present Study
Average Percent Error (APE)	14.360
Root Mean Square (RMS) Error	15.220
Percent Standard Deviation (SD)	8.690

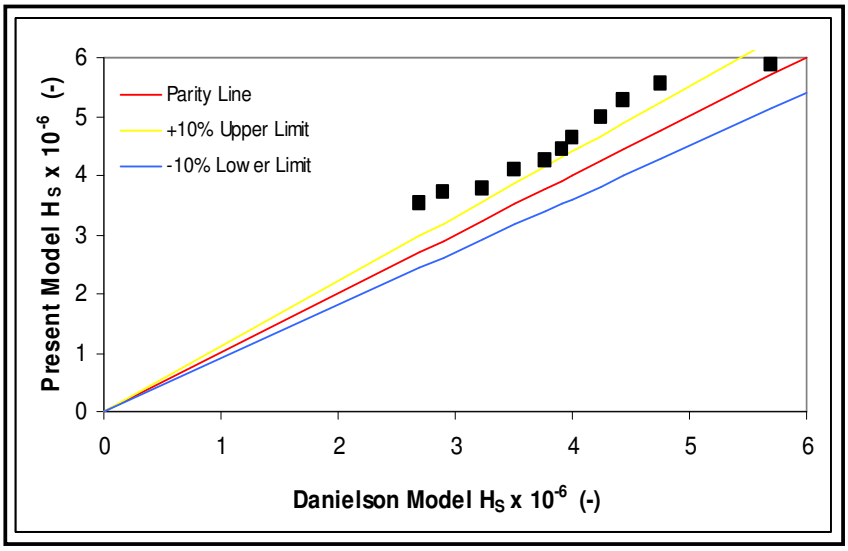

Figure 6-10: Comparison of present model with Danielson model, Hs (2007)

Table 6-6: Statistical Parameters for the H_S Models

	Present Study
Average Percent Error (APE)	17.250
Root Mean Square (RMS) Error	18.530
Percent Standard Deviation (SD)	10.730

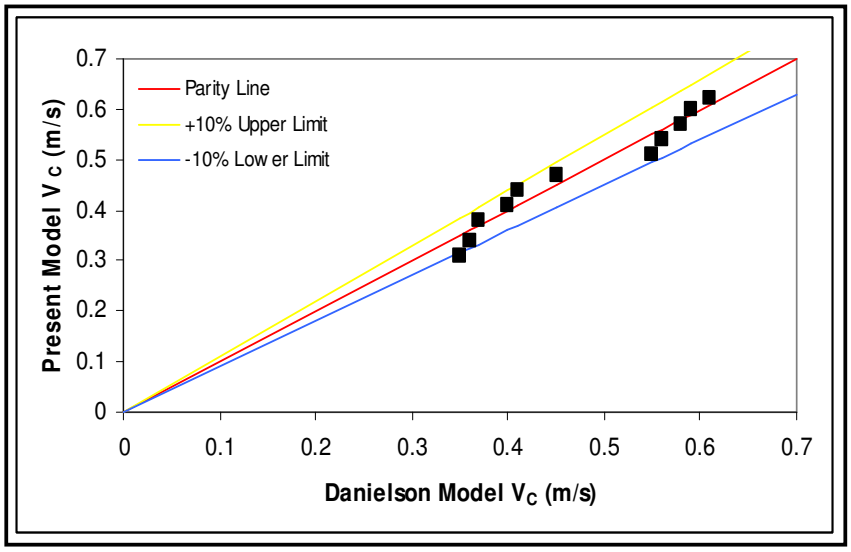

Figure 6-11: Comparison of present model with Danielson model, Vc (2007

Table 6-7: Statistical Parameters for the V_C Model

	Present Study
Average Percent Error (APE)	4.530
Root Mean Square (RMS) Error	5.420
Percent Standard Deviation (SD)	4.280

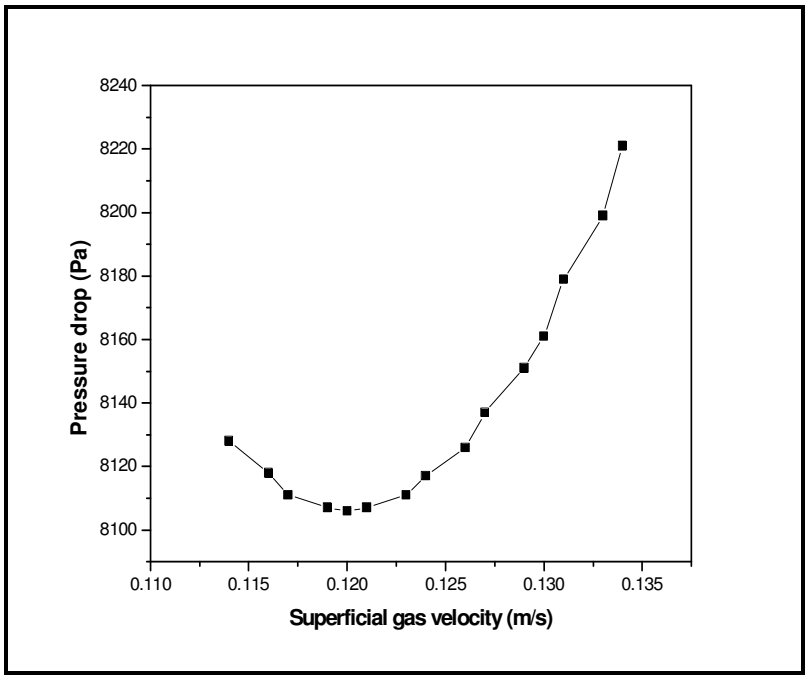

Figure 6-12: Determination of optimal gas velocity for V_{SL} = 1.00 m/s, V_{SS} = 0.00007 m/s and d_S = 0.00030m

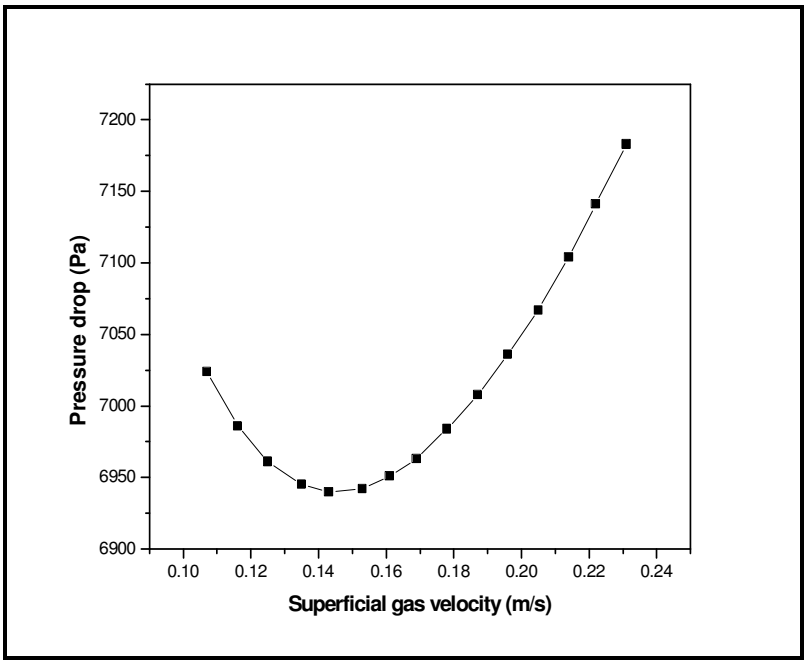

Figure 6-13: Determination of optimal gas velocity for V_{SL}= 1.00 m/s, V_{SS}= 0.00007 m/s and d_S = 0.00030m

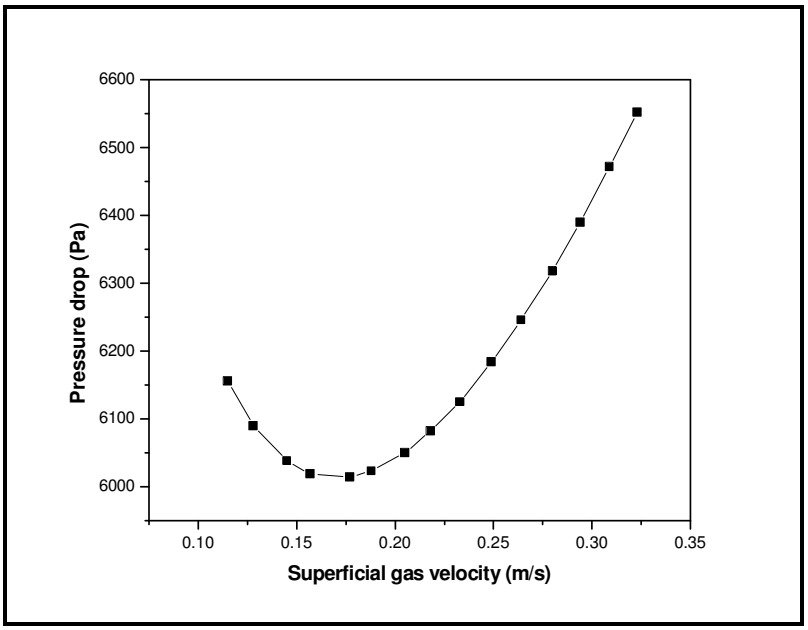

Figure 6-14: Determination of optimal gas velocity for V_{SL}= 1.00 m/s, V_{SS}= 0.00007 m/s and d_S= 0.00030m

6.4 Conclusion

Three-phase gas-oil-sand production and well system design and performance analysis can be made more effective by using the proposed model in this study. The uniqueness of the present model lies in the use of mechanistic model specific to the flow regime encountered and the way the mass and momentum conservation equations are numerically solved to estimate the sand transport and hydraulic parameters at each computational cell. A relatively simple optimization algorithm is used to determine the optimal gas velocity which yield this minimum pressure loss during the transportation of oil-sand two-phase flows through wells and production systems

The proposed predictive model shows a good agreement with a well validated state-of-the-art. The proposed model may be used to lower the costs of sand deposition problems in horizontal multiphase production and well systems. The research findings may also be used to help regulatory agencies to improve guidelines for three-phase gas-oil-sandpipe flow systems.

7 CONCLUSIONS AND RECOMMENDATIONS

7.1 Conclusions

The particle transport problems in three-phase gas-oil-sand production and well systems have been studied using both experimental and theoretical approaches.

The following conclusions are drawn from this study:

- This study reports a first attempt to apply light sheet charged couple device (particle tracking and image velocimetry) techniques in unison to the visualization and fundamental investigation of particle behaviour in the specific case of simulated three-phase gas-oil-sand production operations

- The charged couple device technique proved to be a sufficiently accurate tool to measure the local and global particle velocity and holdup in the three-phase air-water-sand pipe flow system. Visualization of the internal flow structure and video analysis provided a better understanding of the transport processes influencing the particle motion. It also revealed that variation of key operating and geometric parameters could be used to control solid phase hydrodynamics during three-phase gas-oil-sand production operations

- Particle transport characteristics in steady state gas-oil-sand multiphase production and well systems can be described using one-dimensional phenomenological modelling approach with closure equations. The proposed model is general and unified, which can be applied to three-phase gas-liquid-solid flows as applied to production, gas-lift and aerated fluid sand unloading problems

- The numerical solutions can be used to predict in-situ local and global sand particle velocity, holdup, flux and rate in gas-oil-sand multiphase pipelines and wells under various system, operating and geometric conditions

- The numerical solution can also be used to predict critical and optimal transport velocities during three-phase production and sand unloading operations

- The proposed model shows better performance over a broader range of system, operating and geometric conditions compared with the existing state-of-the-art methods

- The proposed model was used to predict particle transport parameters and critical velocities during gas-oil-sand multiphase field production operations. Actual data from a Nigerian oil well and a subsea flowline in the North Sea were used as input data to simulate field conditions

- Implementing the research finding will lower the costs of sand deposition problems in multiphase production operations, thereby encouraging operators to keep sand management wells and to initiate new three-phase gas-oil-sand pipeline projects despite sand transport issues

- The research findings may also help regulatory agencies to improve guidelines for design and operation of three-phase gas-oil-sand flowline and well systems

7.2 Recommendations for future research

There are many interesting directions for continued research in this field of study. A few of the more promising directions, organized by topics are listed in the following subsections:

- Development of a real-time monitoring instrument to quantitatively estimate 1-D and/or 2-D particle transport parameters distributions in intelligent three-phase gas-oil-sand and oil-water-sand production and well systems

- Investigation of the impact of high pressure and/or high temperature on bubble and particle transport characteristics in a large-scale three-phase gas-oil-sand flow test facility

- Two-dimensional steady and dynamic modelling of volumetric fractions, phase velocities and pressure drop distributions in gas-oil-sand and oil-water-sand multiphase flows in complex geometries using multi-fluid modelling and numerical simulation approach

- Investigation of entrainment behaviour for sand bed subjected to gas-oil, oil-water and gas-oil-water multiphase steady and unsteady flows in production and well systems

- Development of integrated simulator of sand influx, transport and erosion as an evaluation tool for SMT

REFERENCES

Almedeij, J. H. and Algharaib, M. K. 2005 Influence of sand production on pressure drawdown in horizontal wells: theoretical evidence. Journal of Petroleum Science and Engineering, Vol. 47, pp. 137-145.

Angelson, S., Kvernvold, O., Linglem, M. and Oslen, S. 1989 Long Distance Transport of Unprocessed Hydrocarbon: Sand Settling in Multiphase Flowlines, Proc. 4th Int. Conf. on Multiphase Flow, Paper D2, BHRA, Nice, 1989. France.

API Recommended Practice for the Design and Installation of Offshore Production Platform Piping Systems. API RP 14E, 1991, American Petroleum Institute, Fifth Edition, Washington DC, October.

Appah, D. and Ichara, M. 1994 Empirical model determines energy required to clean Sand from wellbores, Oil and Gas Journal, Feb., 36-38.

Appah, D. and Ichara, M. and Bouhroun, A. 1997 Aerated wash over technique in sand producing wells, Oil and Gas European Magazine, Vol. 4, 29-33.

Azzorpardi, B. J. 2006 Gas-liquid Flows. Begell House Inc., Connecticut, USA.

Bratli, R.K., Dusseault, M.B., Santarelli, F.J. and Tronvoll, J., 2000 Sand management protocol increases production rate, reduces completion costs. Proc. Trinidad and Tobago Biennial SPE Conf., Port-of-Spain.

Chen, N. H. 1979 An explicit equation for friction factor in pipes. Ind. Eng. Chem. Fund. 18, pp. 296.

Chein, S. F., 1994 Settling Velocity of Irregularly Shaped Sand Particles. SPE Paper 26121, Proceedings of SPE Drilling and General Petroleum Engineering

Colebrook, C. 1939. Turbulent flow in pipes, with particular reference to the transition region between smooth and rough pipe laws. Journal of Institution of Civil Engineering, 11, pp. 133-156.

Danielson, T. J., 2007, Sand transport in multiphase pipelines. Proceedings of the Offshore Technology Conference, Houston, USA, OTC 18691.

Davies, J. T. 1987 Calculation of Critical Velocities to Maintain Solids in Suspension in Horizontal Pipes. Chem. Eng. Science, 42 (7), 1667 – 1670.

Doron, P. and Barnea, D. 1993 A Three Layer Model for Solid – Liquid flow in Horizontal Pipes. Int. J. of Multiphase Flow, 19 (6), 1029 – 1043.

Doron, P. and Barnea, D. 1995 Pressure Drop and Limit Deposit Velocity for Solid – Liquid Flow in Pipes. Chem. Eng. Science, 50 (10), 1595 – 1604.

Doron, P. and Barnea, D. 1996 Flow Pattern Maps for Solid – Liquid Flow in Pipes. Int. J. of Multiphase Flow (1996), **22** (2), 273 – 283.

Doron, P., Garnica, D. and Barnea, D. 1987 Slurry Flow in Horizontal Pipes: Experimental and Modeling. Int. J. of Multiphase Flow, 13 (4), 535 – 547.

Dusseault, M.B., Chun, X.L., Yiqiu, M. and Wu, G., 2002, CHOPS in Jilin Province, China. Proceeding of SPE International Horizontal Well Technology Conf., Calgary, Alberta, Canada, 4-7 November 2002.

Dusseault, M. B., and El-Sayed, S., 2001. Heavy oil production enhancement by encouraging sand production. Proceedings 2000 SPE/DOE Improved Oil Recovery Symposium, Tulsa, Oklahoma, 3-5 April.

Dusseault, M. B., Geilikman, M.B., and Spanos, T.J.T. 1998. Mechanism of Massive Sand Production in Heavy Oils, Proc. 7th UNITAR Int. Conf. Heavy Oils and Tar Sands, Beijing.

Dusseault, M. B., Tronvolli, J., Santilippo, F and Santarelli, F.J., 2000: Sand-self cleaning in high rate oil wells using sand management. Int. Conf. on Formation Damage, SPE 58786, 2000.

Engelmann, H. E. 1978. Vertical hydraulic lifting of large-size particles: a contribution to marine mining. Proceedings of Offshore Technology Conference, Houston, pp. 731-740.

Geilikman, M.B. and Dusseault, M.B., 1997, Fluid-rate enhancement from massive sand production in heavy oil reservoirs", J. of Petroleum Science and Engineering, 17, 5-18. Special Issue: Near Wellbore Formation Damage and Remediation, 1997.

Gillies, R. G., Hill, K. B., Mckibben, M. J. and Shook, C. 1999 Solids transport by laminar Newtonian flows, Powder Technology, Vol. 104, 269-277

Gillies, R. G., Mckibben, M. J. and Shook, C. 1997 Pipeline flow of gas, liquid and sand mixture at low velocity, J. Canadian. Petroleum Technology, 36, 36-42.

Gillies, R. G., Mckibben, M. J. and Shook, C. 1995 Oil, water and sand flow experiments in a model horizontal well, J. Canadian. Petroleum Technology, 34, No. 9, 56-63.

Gopal, M. and Jepson, W.P. 1997 Development of digital image analysis techniques for the study of velocity and void profiles in slug flow, International Journal of Multiphase Flow, Vol. 23, No. 5, 945-965.

Govier, G. W. and Aziz, K.1972 The Flow of Complex Mixtures in Pipes. R. E. Krieger Pub. Co, Florida.

Holte, S., Angelson, S., Kvernvold, O., and Raeder, J. H., 1987. Sand Bed Formation In Horizontal and Near Horizontal Gas-Liquid-Sand. The European Two- Phase Flow Group Meeting, Trondheim, Norway.

Ishii, M. and Mishima, K. 1984 Two fluid model and hydrodynamic constitutive relations. Nuclear Engineering and Design, Vol. 82, pp. 107-126.

Jepson, W. P. 1987 The flow characteristics in horizontal slug flow, Proc. 3rd Int. Conf. on Multiphase Flow, B.H.R. Group, The Hague, Netherlands 18-20 May.

Kaftori, D., Hetstroni, G. and Banerjee, S. 1995a Particle behaviour in the turbulent layer: motion, deposition and entrainment, Physics of Fluid, Vol. 7, No. 5, 1095-1106.

Kaftori, D., Hetstroni, G. and Banerjee, S. 1995b Particle behaviour in the turbulent layer: velocity, flux and concentration distribution, Physics of Fluid, Vol. 7, No. 5, 1107-1121.

King, M. J. J., Fairhurst, C. P. and Hill, T. J. 2001 Solids transport in multiphase flows: applications to high viscosity systems, Journal of Energy Resources, 123, 200-204, September

Liu, M-Y, Wang, H. and Lin, R-t 2006 Visual Investigations on Radial Solid Holdup in Vapour-Liquid-Solid Boiling Fluidized Bed Evaporator with a CCD Measuring System. Chemical Engineering Science, 51, No. 2, 802-813.

Matousek, V. 1997 Flow mechanism of sand-water mixtures in pipelines, Ph.D. Thesis, Technical University of Delft, Delft, Netherlands.

Minagawa, H. and Sakaguchi, T. 1998 Explanation of flow mechanism of gas-liquid-solid Three-phase slug flow in vertical pipes using a three-phase slug flow model, Proceedings of the 3rd International Conference on Multiphase Flow, ICMF ´98, Lyon, France, 8-12 June.

Oudeman, P. 1993 Sand Transport and Deposition in Horizontal Multiphase Trunklines of Sub-sea Satellite Developments, SPE 25142.

Oroskar, A. R., and Turian, R. M., 1980 The Critical Velocity in Pipeline Flow of Slurries. AIChE. J., Vol. 26, No. 4, pp. 550–558.

Papamichos, E., and Malmanger, E.M., 1999. Sand Erosion Model for Volumetric Sand Predictions in a North Sea Reservoir, Paper SPE 64007, 1999.

Perry, R. H., Green, D. W. and Maloney, J. O. 1998 Chemical Engineers Handbook. 7th Edition, McGraw Hill, New York, USA.

Sakaguchi, T., Minagawa, H. and Tomiyama, A. 1997 Slug characteristics and slug modelling of the gas-liquid-solid three-phase slug flow in vertical pipes, Proceedings of the Experimental Heat Transfer, Fluid mechanics and Thermodynamics, Giot, M., Mayinger, F. and Celata, G. P. (editors), 1137- 1144.

Sakaguchi, T., Minagawa, H., Sahara, K., Kato, Y., Kuroda, N. and Matsumoto, T. 1987 Estimation of volumetric fraction of each phase in gas-liquid-solid three-phase flow. Proceedings of the JSME/ASME Thermal Engineering Joint International Conference, Honolulu, Hawaii, March.

Sakaguchi, T., Minagawa, H., Saibe, T. and Sahara, K. 1988 Estimation of volumetric fraction of each phase in gas-liquid-solid three-phase slug flow. Proceedings of the Japan-US Seminar on Two-phase Flow Dynamics, Ohtsu, Japan, July.

Sakaguchi, T., Minagawa, H., Tomiyama, A. and Shakutshi, H. 1992 Gas-liquid-solid three-phase flow in a vertical pipe. International Video Journal of Engineering Research, Vol. 2, 37-45.

Sakaguchi, T., Shakutsui, H., Tomiyama, A., Minagawa, H., and Takahashi, H. 1991 Flow characteristics of gas-liquid-solid three-phase bubbly flow in vertical pipes, Proceedings of the Int. Conf. on Multiphase Flows, ´91-Tsukuba, 24-27 September, 1991, pp. 357-361, Tsukuba, Japan.

Sakaguchi, T., Shakutsui, H., Tomiyama, A., Minagawa, H., and Kitani, S. 1991 Microscopic characteristics of multiphase flow using digital imaging processing, Proceedings of the 1st JSME/ASME Joint International Conference on Nuclear Engineering, Tokyo, Japan, November.

Salama, M.M., 2000, Sand Production Management, Journal of Energy Resources, Vol. 122, 29-33, March.

Sanfilippo, F., Brignoli, M., Giacca, U. and Santarelli, F. J., 1997. Sand Production: From Production to Management, European Formation Damage Conf. Proc., The Hague, SPE # 38185, 1997.

Sato, Y., Yoshinaga, T. and Sadatomi, M., 1991. Data and empirical correlation for the mean velocity of coarse particles in a vertical three-phase air-water-solid particle flow. Proceedings of the international conference on multiphase flows ´91-Tsukuba, September 24-27, 1991, Tsukuba, Japan.

Scott, D.S. and Rao, P. K. 1971 Transport of Solids by Gas-Liquid Mixtures in Horizontal Pipes. The Canadian Journal of Chemical Engineering, 49, pp. 302-309, June.

Shook, C. A., Gillies, R. G., Kristoff, B. J. and Small, M. H. 1991 Sand transport mechanism in horizontal wells, Proc. 4th Petroleum Conference of the South Saskatchewan Section, The Petroleum Society of CIM, Canmet, Regina, Canada, 7-9 October.

Stevenson, P. 2001 Particle transport in pipes by two-phase flows, Ph.D. Thesis, University of Cambridge, Cambridge, United Kingdom.

Stevenson, P., Thorpe, R. B., Kennedy, J.E. and McDermott, C. 2001a The transport of particles at low loading in near-horizontal pipes by intermittent flow, Chemical Engineering Science, 56, 2149-2159.

Stevenson, P. and Thorpe, R. B. 2002a Method calculates sand velocity, hold-up in flowlines, Oil and Gas Journal, 100 (30), 47-50.

Stevenson, P. and Thorpe, R. B. 2003 Energy dissipation at the slug nose and the modeling of solids transport in intermittent flow, Can. J. Chem. Engineering, 81, 271-278.

Stevenson, P., Thorpe, R.B. and Davidson, J.F., 2002b. Incipient motion of a small particle in the viscous boundary-layer at a pipe wall. Chemical Engineering Science, 57, 4505-4520.

Stevenson, P. and Thorpe, R.B., 2002c. The velocity of isolated particles along a pipe in smooth stratified gas – liquid flow. AIChE. Journal, 48, 963-969.

Tippetts, J. R. and Priestman, G.H. 1997 Mobility of solids in multiphase undulating pipeflow, Proc. 8rd Int. Conf. on Multiphase Flow, B.H.R. Group, Cannes, France.

Tronvoll, J., Dusseault, M. Sanfilippo, F. and Santarelli, F.J., 2001 The Tools of Sand Management" 2001 Annual Tech. Conf. and Exhibition, New Orleans, Louisiana, 30 Sept. -3 Oct. 2001.

Weingarten, J.S. and Perkins, T.K., 1992, Prediction of Sand Production in Gas Wells: Methods and Gulf of Mexico Case Studies", SPE 24797, Washington, 4-7 October 1992.

Wicks, M., 1971, "Transport of Solids at Low Concentration in Horizontal Pipes," Advances in Solid-Liquid Flow in Pipes & Its Application, I. Zandi, ed., Pergamon Press, pp. 101–124.

Woldesemayat, M. A. and Ghajar, C. 2004. Comparison of void fraction correlations for different flow patterns in horizontal and upward inclined pipes. International Journal of Multiphase Flow, Volume 33, pp. 347-370.

Xia, J. X., Ni, J. R. and Mendoza, A. J. 2007. Hydraulic lifting of manganese nodules through a riser. ASME Journal of Offshore Mechanics and Arctic Engineering, Vol. 126, pp. 72-77.

Yang, Z. L., Ladam, Y., Laux, H., Danielson, T. J., Goldszal, A., Martins, A. L., 2007, Simulation of Sand Transport in a Stratified Gas-Liquid Two-Phase Pipe Flow. Proceedings of the BHR Multiphase Production Technology Conference, Edinburgh, UK.

APPENDIX A METHODS OF MODEL COMPARISON

Various statistical methods may be used to determine the relative accuracy of the newly developed particle transport and hydraulic models. This can be shown in terms of: (A1) the percentage relative error (PE); (A2) the average percentage relative error (APE); (A3) the roots mean square (RMS); (A4) the standard deviations (SD) and (A5) the correlation coefficient (to measure the quality of fit)

Equations for this statistical analysis are given as follows:

a. **The percentage relative error between the predicted and experimental values**

$$PE_i = \left| 1 - \frac{\text{Estimated(i)}}{\text{Measured (i)}} \right| 100 \qquad [A1]$$

b. **The average percentage relative error between the predicted and experimental values**

$$APE = \frac{1}{N} \sum_{i=1}^{N} \left| PE_i \right| \qquad [A2]$$

c. **The root mean square (RMS) error between the predicted and experimental values**

$$RMS = \sqrt{\frac{I}{N} \sum_{i=1}^{N} \left(\left| PE_i \right| \right)^2} \qquad [A3]$$

d. **The deviation of the relative error around the average percentage relative error**

$$SD = 100 \sqrt{\frac{1}{N-1} \sum_{i=1}^{N} \left[\left(\left| 1 - \frac{\text{Estimated(i)}}{\text{Measured (i)}} \right| \right) - \left(\frac{1}{N} \sum_{i=1}^{N} \left| 1 - \frac{\text{Estimated(i)}}{\text{Measured (i)}} \right| \right) \right]^2} \qquad [A4]$$

APPENDIX B COMPUTATIONAL ALGORITHM

Based on the particle transport, hydraulic, numerical and optimization models discussed in Chapter 3, a computer program is developed using Microsoft Visual Basic version 7.0. Figure B-1 shows summarized schematics of the computational algorithm.

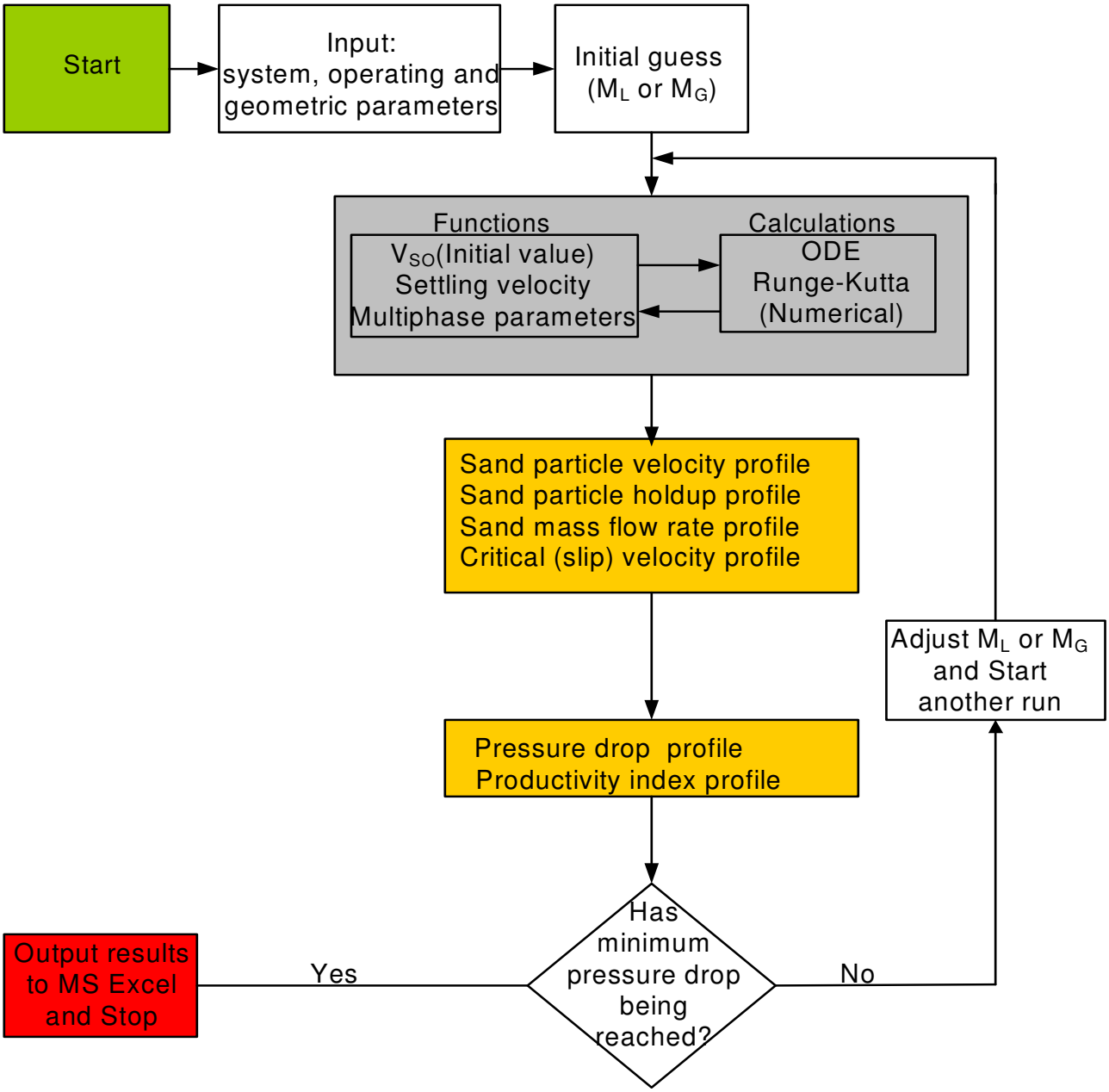

Figure B-1: Schematics of the computational algorithm

APPENDIX C COMPUTER PROGRAM

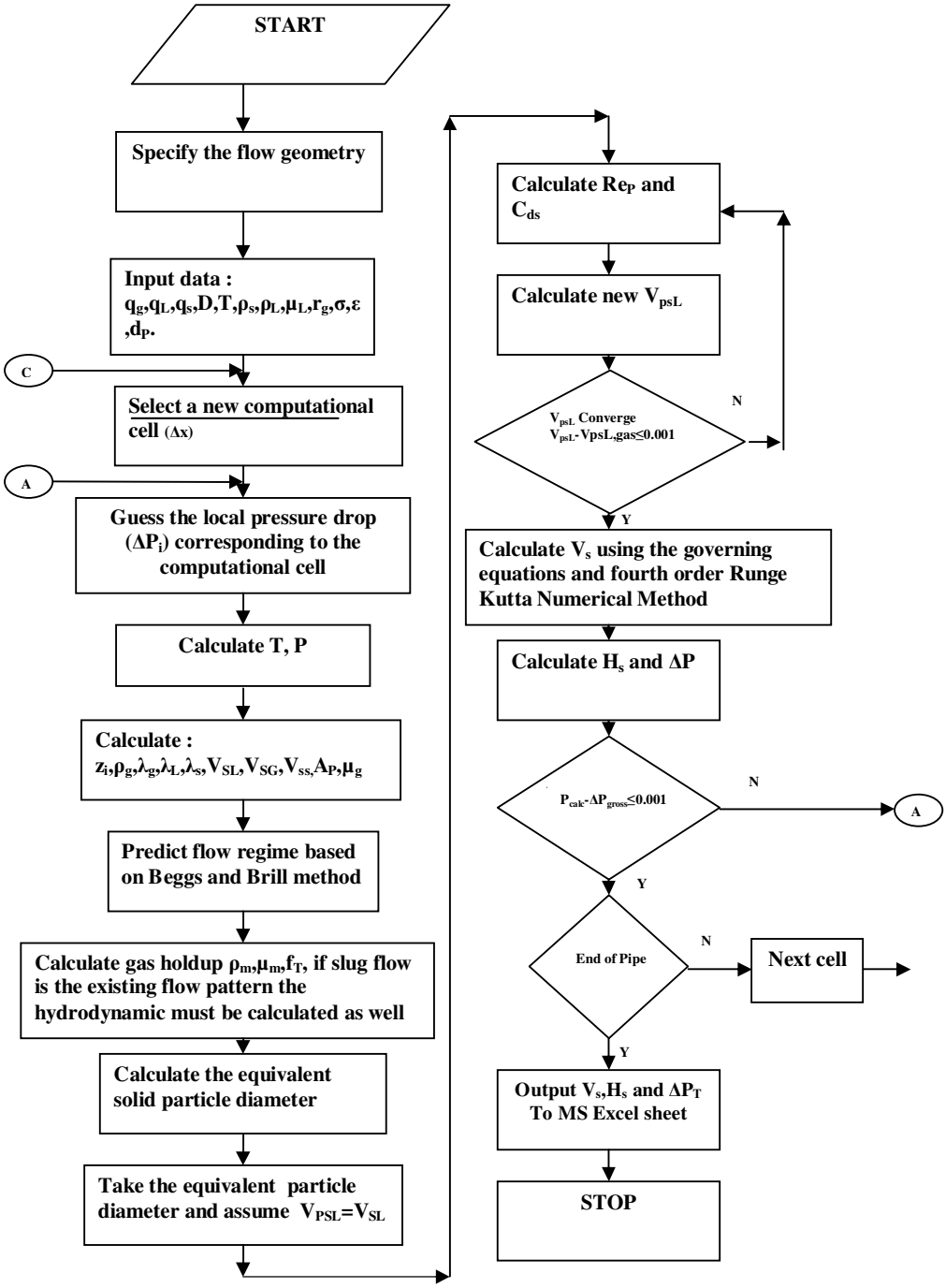

APPENDIX D OPTIMZATION PROGRAM

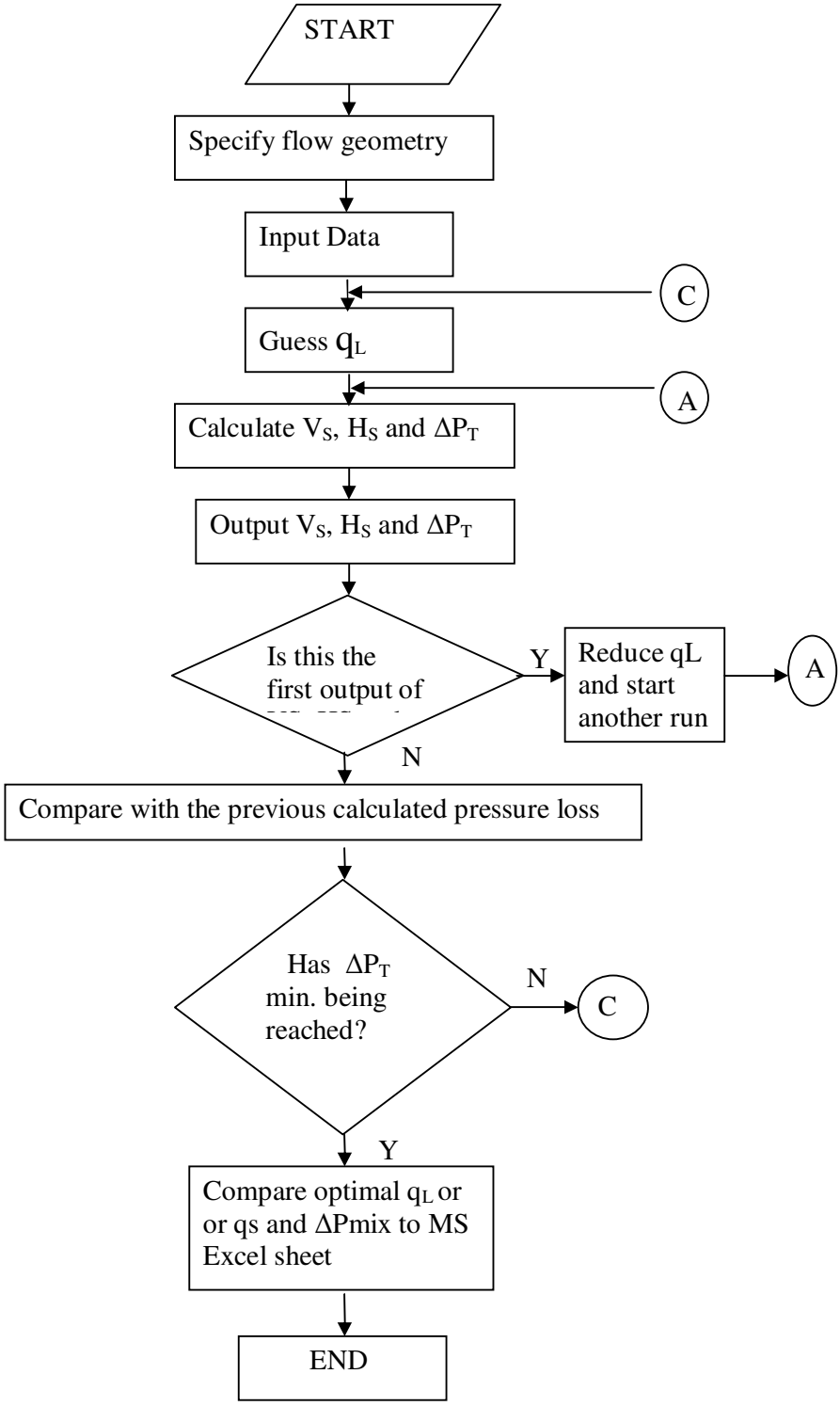

APPENDIX E FLOW PATTERN PROGRAM

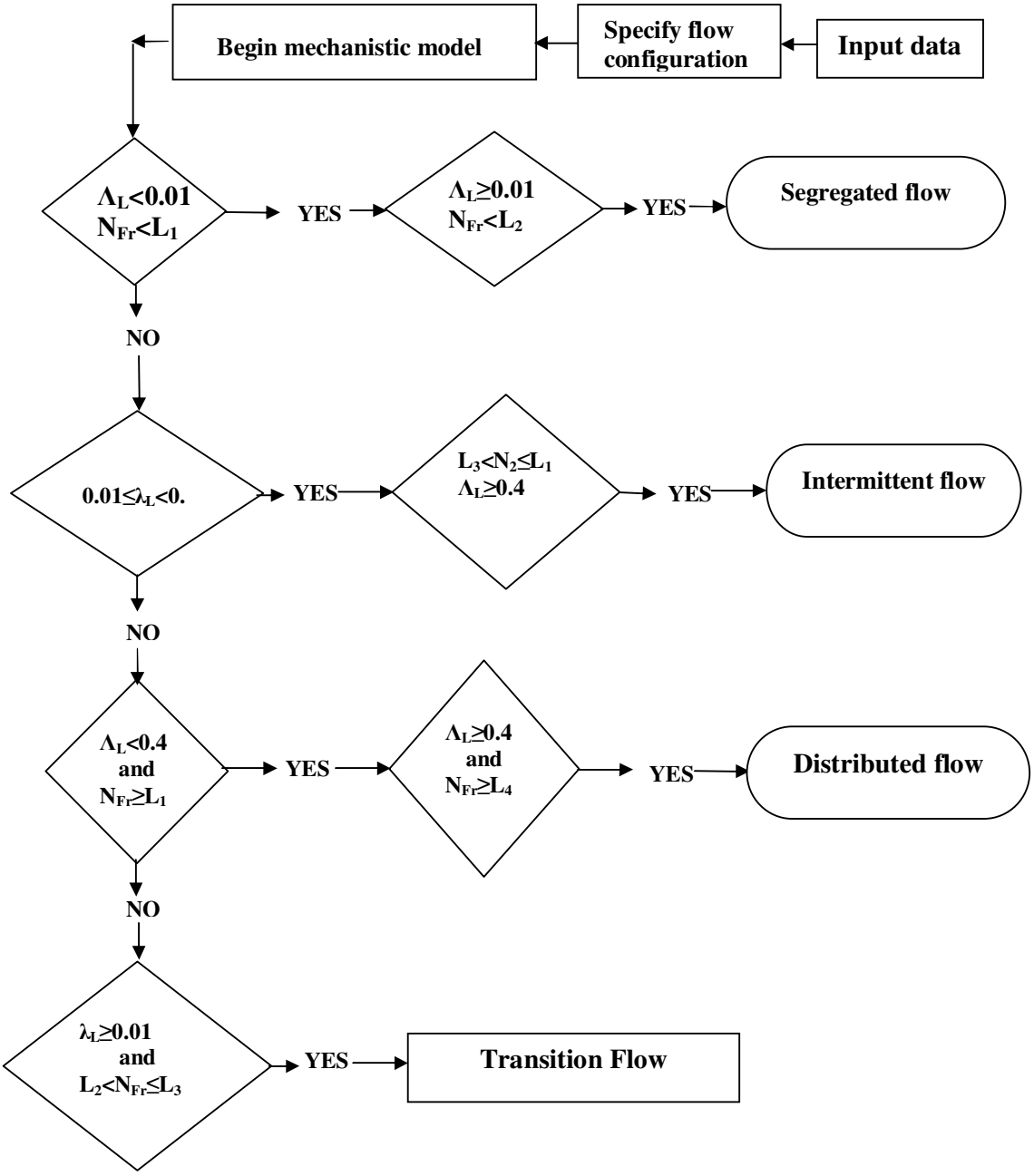

CURRICULUM VITAE

Oladele Bello was born in Ibadan, Nigeria on April 30, 1974. His parents are Tade Olayinka Bello and Agnes Adenike Bello. He completed a Master of Science degree program in chemical engineering at Obafemi Awolowo University, Ile-Ife, Nigeria in 1999. He joined the Department of Chemical Engineering of Ladoke Akintola University of Technology, Ogbomoso, Nigeria as a faculty staff in the research and teaching of petroleum technology in 2000. In October 2004, he enrolled for a PhD petroleum engineering degree program in the Institute of Petroleum Engineering, Clausthal University of Technology. He has presented exercises to masters' petroleum engineering degree students and coordinated the masters' petroleum engineering (Drilling, Production and Gas Supply Specialization Option) seminar course for two sessions (SS 2007 and SS 2008). He also participated in many other departmental activities. He has contributed to six journals, and a number of national and international conferences.